CANADIAN THESES ON MICROFICHE

I.S.B.N.

THESES CANADIENNES SUR MICROFICHE

National Library of Canada
Collections Development Branch

Canadian Theses on
Microfiche Service

Ottawa, Canada
K1A 0N4

Bibliothèque nationale du Canada
Direction du développement des collections

Service des thèses canadiennes
sur microfiche

NOTICE

The quality of this microfiche is heavily dependent upon the quality of the original thesis submitted for microfilming. Every effort has been made to ensure the highest quality of reproduction possible.

If pages are missing, contact the university which granted the degree.

Some pages may have indistinct print especially if the original pages were typed with a poor typewriter ribbon or if the university sent us a poor photocopy.

Previously copyrighted materials (journal articles, published tests, etc.) are not filmed.

Reproduction in full or in part of this film is governed by the Canadian Copyright Act, R.S.C. 1970, c. C-30. Please read the authorization forms which accompany this thesis.

THIS DISSERTATION
HAS BEEN MICROFILMED
EXACTLY AS RECEIVED

AVIS

La qualité de cette microfiche dépend grandement de la qualité de la thèse soumise au microfilmage. Nous avons tout fait pour assurer une qualité supérieure de reproduction.

S'il manque des pages, veuillez communiquer avec l'université qui a conféré le grade.

La qualité d'impression de certaines pages peut laisser à désirer, surtout si les pages originales ont été dactylographiées à l'aide d'un ruban usé ou si l'université nous a fait parvenir une photocopie de mauvaise qualité.

Les documents qui font déjà l'objet d'un droit d'auteur (articles de revue, examens publiés, etc.) ne sont pas microfilmés.

La reproduction, même partielle, de ce microfilm est soumise à la Loi canadienne sur le droit d'auteur, SRC 1970, c. C-30. Veuillez prendre connaissance des formules d'autorisation qui accompagnent cette thèse.

LA THÈSE A ÉTÉ
MICROFILMÉE TELLE QUE
NOUS L'AVONS REÇUE

NL-339 (r. 82/08)

Canada

EMULSION POLYMERIZATION OF BUTADIENE

BY

BHUPENDER S MINHAS

Thesis Submitted to the School of Graduate Studies
as Partial Fulfillment of the Requirements For the
Degree of Ph.D in Chemical Engineering

UNIVERSITY OF OTTAWA
OTTAWA, CANADA, 1983

UNIVERSITÉ D'OTTAWA
UNIVERSITY OF OTTAWA

ABSTRACT

The research work involved the experimental study of the effects of the addition of nonreactive liquid additives, heptane and cyclohexane, on the emulsion polymerization of butadiene. Based on the experimental results, a theoretical model was developed for emulsion polymerization in the presence of a nonreactive diluent. The study also involved the measurement of associated physical, solution and transport properties of butadiene.

The measured properties included the solubility of butadiene in heptane in the temperature range from 4 to 50 °C at atmospheric pressure. Butadiene was found to be highly soluble in heptane. The solubility of butadiene in water at 4 °C and atmospheric pressure was found to be low; however, it increased with an increase in surfactant concentration in water. The diffusivity of butadiene was also measured in heptane in the temperature range from 4 to 50 °C. The critical micelle concentration of the surfactant was determined by means of viscosity and density measurements. It was found to be 2.5 g dm^{-3}.

A polymerization reactor which had the essential features of a commercial reactor, was designed for the butadiene emulsion polymerization studies. It was constructed of glass,

teflon, aluminum and stainless steel, and was suitable for operation at pressure of up to 690 kPa. It was essentially a small batch reactor, for processing less than 200 cm^3 of emulsion at a time, while the auxiliary equipment was designed to use the reactor as a calorimeter to obtain polymerization rate data utilizing the heat of polymerization.

The emulsion polymerization of butadiene was performed at 10 °C. The addition of both of the nonreactive solvents caused a reduction in the rate of polymerization as well as a reduction in the molecular weight of the polymer formed. The reduction in the rate was more than expected on the basis of mere monomer dilution with the additive. For heptane the rate of polymerization was approximately second order in initial concentration of monomer in the oil phase. Cyclohexane was less effective as a retarder for the polymerization, the order of reaction was 1.5 to monomer concentration in the oil phase. The addition of the additives had no measurable effect on the relative proportion of cis-1,4, vinyl, and trans-1,4 structures of polybutadiene. It was found that the rate of polymerization and the average molecular weights of the polymer increased with an increase of surfactant concentration. However, the change in the rate of polymerization and molecular weight with surfactant concentration was greater in the presence of heptane. It was observed that the rate of polymerization remained essentially constant with the variation of initiator concentration, irrespective of the addition of heptane. Finally it was noted that the in-

crease of initiator concentration caused a reduction in the polymer molecular weight. This reduction was found to be greater in the presence of heptane.

A theoretical model was developed to explain the experimental results for the emulsion polymerization of butadiene in the presence of nonreactive additives. The model takes into account the monomer concentration in the particle and the viscosity of the additives to explain the reduction in the rate of polymerization. It is suggested that the water insoluble additives depress the activity of the monomer in the latex particles, which results in a decrease in the rate of polymerization below that expected on the basis of mere monomer dilution. It is postulated that the increase in the number of particles in the emulsion, when the surfactant concentration is increased, is greater in the presence of a solvent. This postulation is used to explain the higher dependence of the rate and the molecular weight on the surfactant concentration, in the presence of nonreactive solvent. Mathematical equations were developed for the model. The rate of polymerization and the molecular weight equations are given below:

$$\frac{dP}{dt} = 0.369 \left[\frac{k_p \cdot d_m \phi_m \cdot A}{N_{Avc}\, d_p}\right]^{0.6} (R(1 - \phi_m - \phi_a))^{0.4}\, \bar{q}$$

$$\bar{M}_n = 0.369 \left[\frac{k_p d_m \phi_m A}{R}\right]^{0.6} [N_{Avo} d_p (1 - \phi_m - \phi_a)]^{0.4}$$

A separate research study for the development of diffusivity correlations was also performed. New correlations for the prediction of diffusion coefficients for normal paraffin solvents and solutes, for aqueous solutions, for nonpolar solutions and a general correlation were developed. The molar volume, parachor and radius of gyration for both solute and solvent were used as correlating parameters. The new correlations represent a significant improvement in accuracy for the prediction of diffusivities.

ACKNOWLEDGEMENTS

The author wishes to thank Professor W. Hayduk for his kind assistance and invaluable guidance throughout the course of this investigation.

The author is also indebted to Professor V. Hornof for the use of an analytical instrument, the Gel Permeation Chromatograph, to Mr. G. Gasperetti and his staff for their technical aid in constructing the equipment used in this work and to Miss S. Ekka for her fine typing job.

For financial aid the author wishes to express his gratitude to the Department of Chemical Engineering, Professor W. Hayduk and the Graduate School of the University of Ottawa.

CONTENTS

LIST OF TABLES

LIST OF FIGURES

NOMENCLATURE

A	surface area of surfactant molecules present in 1 dm^3 of aqueous phase
[A]	surfactant concentration, $mol.dm^{-3}$ of water
A	Margules constant
[a]	additive concentration, $mol.dm^{-3}$
B	densitometer apparatus constant
C	constant in Equation 3.14
C_3	constant in Equation 6.1
C_4	constant in Equation 6.8
C_5	constant in Equation 6.13
c	molar concentration, $mol.cm^{-3}$
cmc	critical micelle concentration
D	diffusivity, $cm^2.s^{-1}$
D_{AB}	diffusivity of component A in B, $cm^2.s^{-1}$
D_{AB}	diffusivity of component A in infinitely dilute solution of A in B, $cm^2.s^{-1}$
d	density, $kg.dm^{-3}$
d_p	polymer density, $kg.dm^{-3}$
F	mole fraction in Equations 3.3 and 3.4
f_i	fugacity of component i in Equation 2.17
H_{AB}	Henry's constant of component A in B

H_{AM} Henry's constant of component A in mixture

h Planck's constant

[I] initiator concentration, $mol.dm^{-3}$

J molar flux (no bulk flow), $mol.cm^{-2}.s^{-1}$

j mass flux (no bulk flow), $g.cm^{-2}.s^{-1}$

K volume growth rate constant, defined by Equation 3.32

k Boltzman constant

k_d initiator-decomposition rate constant, $dm^3.mol^{-1}.h^{-1}$

k_i polymerization initiation rate constant, $dm^3.mol^{-1}.h^{-1}$

k_p propagation rate constant, $dm^3.mol^{-1}.h^{-1}$

k_t termination rate constant, $dm^3.mol^{-1}.h^{-1}$

k_{tc} termination by combination rate constant, $dm^3.mol^{-1}.h^{-1}$

k_{td} termination by disproportionation rate constant, $dm^3.mol^{-1}.h^{-1}$

L Ostwald coefficient

[M] monomer concentration, $mol.dm^{-3}$

[M·] total concentration of all chain radicals

M molar mass, $g.mol^{-1}$ ($kg.kmol^{-1}$)

$\bar{M}_n$ number average molar mass, $g.mol^{-1}$ ($kg.kmol^{-1}$)

$\bar{M}_w$ weight average molar mass, $g.mol^{-1}$ ($kg.kmol^{-1}$)

N total number of particles in 1 dm^3 of aqueous phase

N_t total number of particles in 1 dm^3 of aqueous phase at time t

N_{Avc} Avogadro's number

n_i number of particles of radius r_i in Equation 3.19

P polymer volume in 1 dm^3 of aqueous phase

P_t total pressure, kPa

$\mathbb{P}$ parachor $g^{0.25}.cm^3.mol^{-1}.s^{-0.5}$

p_i partial pressure of component i, kPa

p_i^o vapour pressure of component i, kPa

q number of free radicals in a particle

$\bar{q}$ average number of free radicals in a particle

R radius of gyration

$\mathbb{R}$ gas constant

R_i rate of initiation

R_p rate of polymerization, %conversion.h^{-1}

R_t rate of termination

R number of radicals formed per dm^3 of water per second

$[R\cdot]$ radical concentration, mol.dm^{-3}

r radius of a particle

$\bar{r}_p$ average rate of polymerization, g polybutadiene.s^{-1}

S solubilization in surfactant solution, mol.dm^{-3} of aqueous phase

$\sum S_i^o$ summation of solubilization of pure components

T absolute temperature

τ vibration frequency, cycles.s^{-1}

t time, s

t_p particle age, s

$\bar{t}_p$ average time needed for a single radical to enter a particle, s

V molar volume, dm^3.mol^{-1}

$\bar{V}$ partial molar volume

V_S volume of the system in Equation 3.22

W_R heat evolved due to reaction, watts, in Equation 5.1

ΔW latent heat of vaporization at normal boiling point

ΔW_p heat of polymerization, kJ.mol^{-1}

w_{Ai} mass fraction of solute A at gas-liquid interface

w_{Al} mass fraction of solute A in the bulk of liquid

x	mole fraction

Greek Letters:

α	hydrogen-bonding factor
β	collision radius in Equation 3.14
Γ	Wilke-Chang association parameter
γ	activity
δ	solubility parameter, $(cal.cm^{-3})^{1/2}$
ϵ	initiator efficiency in Equation 2.4
η	viscosity, mPa.s
$[\eta]$	intrinsic viscosity
θ_3	index in Equation 6.1
θ_4	index in Equation 6.2
θ_5	index in Equation 6.3
θ_6	index in Equation 6.4
θ_7	index in Equation 6.5
θ_8	index in Equation 6.6
θ_9	index in Equation 6.7
Λ	number of converted mole of monomer in the system
λ	number of free radicals captured by a particle
μ	chemical potential
σ	interfacial tension, $dynes.cm^{-1}$
τ	binary interaction parameter, defined by Equation 2.26
ϕ	volume fraction in the particle
Ω	Mark-Houwink coefficient defined by Equation 2.16
ω	Mark-Houwink coefficient defined by Equation 2.16

Subscripts:

A	component A
a	additive
B	component B
D	component D
G	gas
L	liquid
m	monomer
x	degree of polymerization
y	degree of polymerization
1	droplet
2	micelle

Superscripts:

g	gas
i	ideal
l	liquid
o	pure component
v	vapour

Chapter I

INTRODUCTION

Emulsion polymerization is a process for conducting a polymerization reaction for a monomer in the micelles which are formed by dissolving a surfactant in a dispersing medium (usually water). These micelles act as tiny reactors independent of each other, and lead to the formation of polymer dispersion. The kinetics of emulsion polymerization in the presence of nonreactive liquid additives have been studied by several investigators (1-4). It was reported that additives generally caused a reduction in the polymerization rate and also a reduction in the molecular weight of the polymer formed. The explanations given by the investigators for their experimental results suggest that further experimentation is required to elucidate the results obtained.

The aim of this investigation was to engage in a systematic study of the effects of the addition of nonreactive solvents on the kinetics of emulsion polymerization of butadiene, and to develop a theoretical model to explain the experimental results. The effect of the additives on the average molecular weight and the molecular structure of the butadiene polymer obtained, was also investigated. The additives utilized were heptane and cyclohexane. These are

good solvents for butadiene so that the polymerization experiments could be performed at atmospheric pressure by initially dissolving the monomer in the solvent. These solvents were chosen because they were of different viscosity; therefore, the effect of a difference in solvent viscosity on emulsion polymerization of butadiene could be studied.

The investigation was commenced with the measurement of the physical properties of aqueous potassium laurate solutions. The measurements of the solution density and viscosity were used to determine the critical micelle concentration.

The next phase of the investigation was the determination of solution and transport properties of butadiene, in particular its solubility and diffusivity in heptane, water and surfactant solutions. These properties were considered useful in elucidating the mechanism of emulsion polymerization in the presence of nonreactive solvents.

The study culminated with the design and operation of a batch polymerization reactor. Emulsion polymerization of butadiene is generally conducted in the laboratory by means of bottle reactors. But in the present investigation a batch reactor was designed in order to include the essential features of an industrial reactor. The reactor was kept small, having a total volume of 400 cm^3 , for safety reasons. The auxiliary equipment for the reactor was designed to measure the quantity of heat evolved from the polymerization reac-

tion. This latter measurement was useful for determining the rate of polymerization. Different polymerization experiments were conducted to study the effect of various parameters including temperature, solvent, surfactant and initiator concentrations. In each experiment, the polymerization rate, the molecular weight and molecular structure of the resulting polybutadiene was obtained. The polybutadiene samples were analyzed by Gel Permeation Chromatography, and Infrared Spectrophotometry, for the determination of the molecular weight and molecular structure, respectively.

A theoretical model was proposed to explain the experimental results obtained in this investigation. The proposed model divides the reaction time into two intervals the demarcation between which depends on the disappearance of inactive micelles. As the reaction proceeded surfactant from the inactive micelles was used to stabilize growing polymer particles. In the model, consideration is given to the solvent viscosity and its effect on monomer activity. Chapter 3 has been devoted to the theoretical development of the model for emulsion polymerization in the presence of a non-reactive solvent.

Part of this investigation also involved the development of correlations for diffusivity in liquids. Because the mechanism of diffusion in liquids is only partly understood, semi-empirical correlations based on known physical properties of the substance are commonly used to predict the dif-

fusion coefficients in liquid systems. A number of correlations were tested and new ones were developed, using the diffusivity data available in the literature.

The complete study is presented in seven chapters, the first being the introduction itself. The second chapter gives a brief review of the literature which is relevant to this investigation. As mentioned above, the theoretical development is discussed in Chapter 3. The details of the experimental equipment and the operating techniques involved are described in Chapter 4. The properties of the chemicals used in this investigation are presented in Chapter 5. The results and discussion of this study are presented in Chapter 6, and the conclusions drawn therefrom are given in Chapter 7.

Chapter II

THEORY AND LITERATURE SURVEY

The purpose of this chapter is to give a brief review of the literature which is relevant to this investigation, for example, initiation and mechanism of free radical polymerization, emulsion polymerization and its mechanism, and a critical review of the effects of nonreactive liquid additives on emulsion polymerization. The analysis and molecular structure of polybutadiene are also discussed in this chapter. The literature concerned with the properties of dissolved butadiene, such as its solubility and diffusivity in certain solvents and soap solutions, is also reviewed.

2.1 INITIATION

Emulsion polymerization is initiated by the generation of free radicals in the reaction medium. Free radicals can be generated in a number of ways from various initiators. Two most commonly used methods are the thermal decomposition of relatively unstable substances, and the chemical reaction of an unstable oxidizing agent with a suitable reducing agent. A free radical is a substance with an unpaired electron. Two free radicals are usually formed when a covalent bond of an initiator is broken. Free radicals are extremely reactive,

and the two radicals deactivate themselves when they come in contact with each other. They occur in extremely low concentrations when utilized for polymerization initiation and have a very short average life span of less than one-tenth of a second before they decompose further or react with another substance. They initiate polymerization by opening the double bond of vinyl monomers and transferring their unpaired electrons to the monomer molecules, forming radical chains (5). Polymerization then proceeds by successive addition of further monomer molecules to the radical end of the growing chain. It is usually postulated that the radical chains are as reactive as the initial free radical. Therefore, the deactivation of a radical chain with a free radical or another radical chain is as probable as the mutual deactivation of free radicals. All the free radicals generated are not able to initiate polymerization reactions because of the mutual deactivation of some of them. The efficiency with which radicals initiate chains can be estimated by comparing the number of radicals generated with the number of polymer chains formed. Most initiators in typical vinyl polymerization reactions have efficiencies between 60 and 100%.

The initiators used in emulsion polymerization are water soluble and are capable of providing a continuous supply of free radicals. The initiator, potassium persulfate, at a concentration of 0.02 $mol.dm^{-3}$ and at 60 °C is able to provide radicals for more than 33 hours (6). Certain initiators

can be successfully used only above certain temperatures, below which they do not thermally decompose. At low temperatures (less than 20 °C) free radicals are usually generated by the chemical reaction of an oxidizing agent with a reducing agent. This process is known as redox initiation. The numerous redox initiation systems, which have been successfully used to initiate polymerization, have been reviewed by Bacon (7). Whitby et al. (8) studied a large number of amine-peroxide redox systems for emulsion polymerization of styrene. Cumenehydroperoxide was found to be particularly effective when reacted with alkyl amines. Ethylene amines, from diethylenetriamine to nonaethylenedecamine, were investigated. The results showed that the tetraethylenepentamine and the pentaethylenehexamine were most reactive with cumenehydroperoxide to form the free radicals which initiate polymerization reactions. The mechanism of the hydroperoxide-amine initiation system has not been studied in detail. Blackley (9) postulated the radical generating reaction for this initiation system as follows:

$$ROOH + R'NH_2 \rightarrow RO\cdot + R'NH\cdot + H_2O \qquad (2.1)$$

It has also been postulated that minute traces of iron present as an impurity in the emulsion form complexes with the amine which react with the hydroperoxide to produce free radicals. It has been claimed that rigorous purification of all recipe components to make them iron-free resulted in a

reduction of the effectiveness of the hydroperoxide-amine system. In the present investigation the cumenehydroperoxide-tetraethylenepentamine redox system was used, which had been found by Whitby et al. (8) to give a satisfactory rate of polymerization and molecular weight of the polymer formed.

2.2 FREE RADICAL POLYMERIZATION

Free radical polymerization is the most commonly used method for the preparation of polymer from vinyl or diene monomers. It involves a chain reaction, in which monomer molecules are successively added to an activated site at the end of a growing polymer chain. The activated site is an unpaired electron. The mechanism of free radical polymerization can be explained by a description of the various steps involved.

The process of chain initiation involves two steps: the first is the decomposition of the initiator to yield a pair of free radicals, and the second is the addition of a monomer molecule to the free radical. The second step involves the transfer of an unpaired electron from the free radical to the monomer molecule forming a chain radical.

$$I \xrightarrow{k_d} 2R\cdot \qquad (2.2)$$

$$R\cdot + M \xrightarrow{k_i} RM\cdot \qquad (2.3)$$

The rate of decomposition of the initiator to free radicals is considerably slower than the rate of addition of monomer to free radicals. Thus, initiator decomposition is the rate determining step in the chain initiation sequence. The rate of initiation of chain radicals can be written as:

$$R_i = \frac{d[R\cdot]}{dt} = -2\,\frac{d[I]}{dt} = 2\,\epsilon\,k_d[I] \qquad (2.4)$$

The factor ϵ, the initiator efficiency in the rate expression, takes into account the fact that not all free radicals generated initiate a chain; some of the radicals are lost by mutual deactivation. The factor 2 in the rate expression arises from the fact that two radicals are formed by the decomposition of one initiator molecule.

The process of chain propagation involves the successive addition of monomer molecules to the chain radicals and it can be represented by the following equations:

$$RM\cdot + M \xrightarrow{k_p} RM\cdot_2 \qquad (2.5)$$

$$RM\cdot_x + M \xrightarrow{k_p} RM\cdot_{x+1} \qquad (2.6)$$

It is usually postulated that the chain radical reactivity expressed by k_p is independent of the molecular weight or number of monomer molecules in the growing chain. Based on this assumption the rate of chain propagation can be written as:

$$R_p = -\frac{d[M]}{dt} = k_p[M]\sum[M_x^{\cdot}] = k_p[M][M^{\cdot}] \qquad (2.7)$$

The last step in the chain process is the termination of the growing chain radicals, which results in the formation of polymer. The termination of chain radicals can occur either by combination or by disproportionation:

i) Combination

$$RM_x^{\cdot} + RM_y^{\cdot} \xrightarrow{k_{tc}} P_{x+y} \qquad (2.8)$$

$$R_t = -\frac{d[R^{\cdot}]}{dt} = 2k_{tc}[M^{\cdot}]^2 \qquad (2.9)$$

ii) Disproportionation

$$RM_x^{\cdot} + RM_y^{\cdot} \xrightarrow{k_{td}} P_x + P_y \qquad (2.10)$$

$$R_t = -\frac{d[R^{\cdot}]}{dt} = 2k_{td}[M^{\cdot}]^2 \qquad (2.11)$$

Both types of termination may occur at all temperatures of polymerization. At high temperatures however, the rate of termination by disproportionation is higher than that by combination. On the other hand at low temperatures combination is the dominant termination reaction.

2.3 MICELLES

The function of a surfactant in emulsion polymerization is to increase the solubility of monomer in the aqueous phase. A large part of the surfactant usually exists in the form of micelles, which act as the loci for reacting polymer molecules. Micelles are formed when the concentration of the surfactant in the aqueous solution exceeds the critical micelle concentration (cmc). The size and shape of the micelles depend on the surfactant used. The size of micelles is usually expressed as an aggregation number, which expresses the average number of surfactant molecules present in each micelle. The aggregation number is usually within the range of 50 to 100 (10). It is considered that micelles are spherical or rod-like in shape with the hydrophobic ends of the surfactant molecules oriented inward and the hydrophilic ends outward as shown in Figure 1. The addition of a small amount of electrolyte such as potassium chloride causes a marked reduction in the cmc of a surfactant, but the effect becomes progressively less as larger quantities are added. In an emulsion system the surfactant concentration is generally in the range of 25-30 $g.dm^{-3}$ of aqueous phase which is greatly in excess of the cmc, so that most of the surfactant is present in micellar form (11). The total number of micelles in an emulsion system is extremely large. In 1 cm^3 of aqueous phase of a typical emlusion there are approximately $5x10^{19}$ molecules of surfactant. If the aggregation number is assumed to be between 50 and 100, the

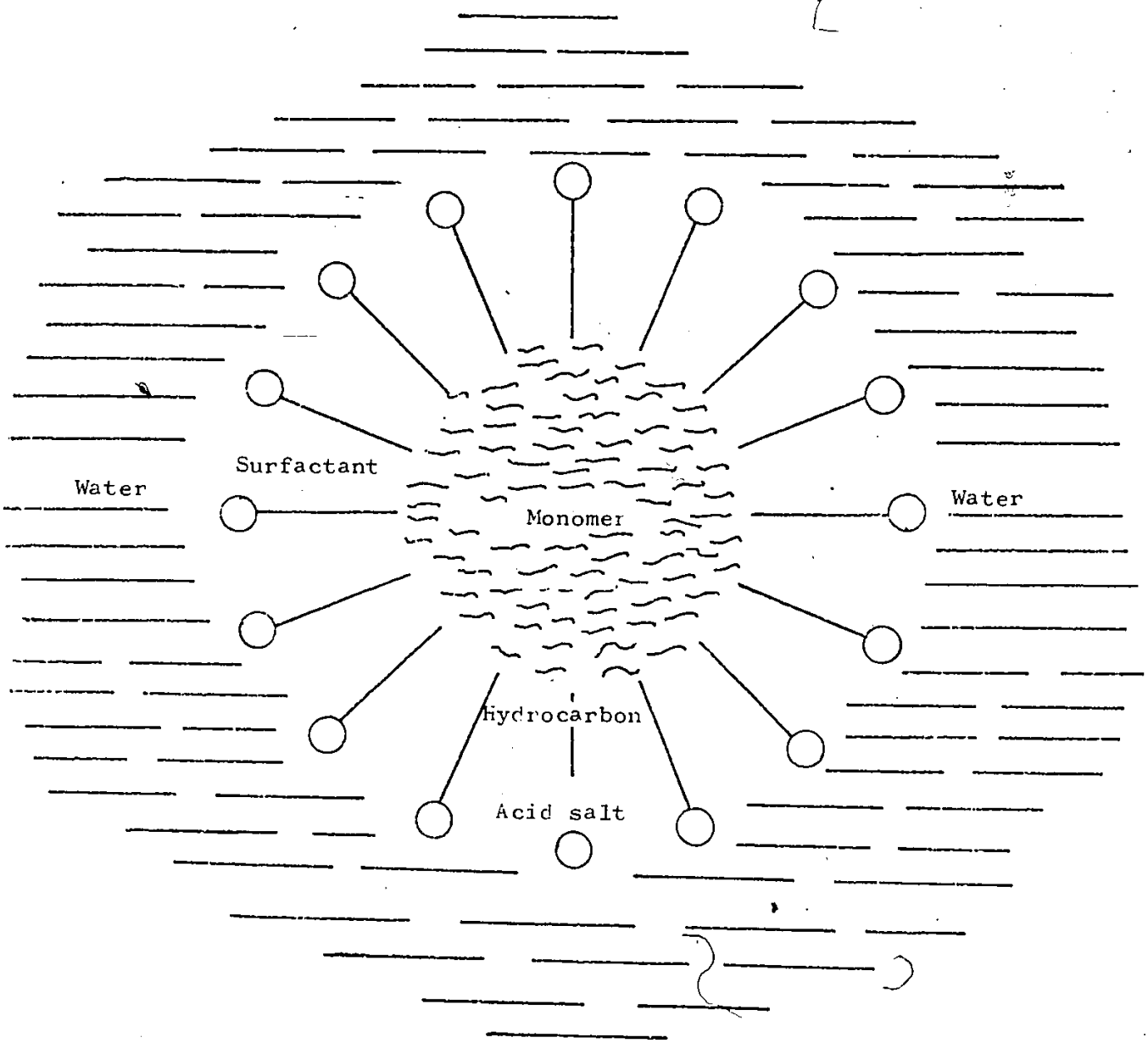

Figure 1 - Diagram of micelle with solubilized monomer

equivalent number of micelles lies between 5×10^{17} and 1×10^{18} per cm^3 of aqueous solution. The extremely high combined surface area of the micelles is characteristic of emulsion polymerization and constitute a major difference from other polymerization techniques. A comprehensive review of the phenomenon of micelle formation in aqueous solution has been published by Shinoda (12) and is used as a reference in the above presentation.

The solubility of monomer in micellar solutions is generally higher than that in water. When dissolved in a micellar solution, monomer tends to diffuse into the central region of the micelles. This results in an increased or enhanced solubility of the monomer and is known as solubilization.

2.4 EMULSION POLYMERIZATION

Emulsion polymerization is a complex and industrially important method for producing polymeric materials especially elastomers. There are some inherent advantages of emulsion polymerization. One advantage is that heat removal during polymerization presents no difficulty since the viscosity of the latex remains low, even at high monomer conversions. The combination of surfactant, mild agitation of emulsion and small size of polymer particles minimizes the coalescence of particles. This characteristic of emulsion polymerization makes it suitable for the production of elastomers. One of the principal advantages of emulsion polymerization is the

possibility of forming polymer of high molecular weight at a very high rate of polymerization. In this respect emulsion polymerization stands alone among other techniques of polymerization (13). Commercially, emulsion polymerization is used in the production of synthetic rubber such as polybutadiene and styrene-butadiene rubber. Also, the polymer latex product of emulsion polymerization has been employed in coating and glue industries.

A number of theories have been proposed to describe the mechanism of emulsion polymerization. Among these, Harkins theory (14,15) was the first. It is also the basis of two other important theories: those of Smith-Ewart (16) and Gardon (17-22).

The mechanism of emulsion polymerization according to Gardon will now be described. When a relatively water insoluble monomer is added to an aqueous surfactant solution, three phases result: an aqueous phase in which small amounts of monomer and surfactant are dissolved, a dispersed phase in which emulsified monomer droplets of diameter 0.5 to 1.0 μm, are found and a micellar phase saturated with monomer. In emulsion systems the number of monomer droplets and micelles are extremely large. The number of monomer droplets is approximately 10^{12} per cm^3 and the number of micelles 10^{18} per cm^3 of emulsion. The polymerization is initiated by the addition of a water soluble initiator which is capable of producing free radicals. The free radicals react with the dis-

solved monomer molecules present in the aqueous phase forming chain radicals (radicals). Gardon believes that these radicals diffuse into micelles or monomer droplets before becoming long enough to precipitate. Micelles and monomer droplets capture the radicals at a rate proportional to their surface areas. Because it is estimated that initially the combined surface areas of micelles is approximately sixty times that of the emulsified monomer droplets, it is considered that the majority of the radicals are captured by the micelles. Hence, the portion of polymerization which takes place in the monomer droplets can be ignored.

Gardon divides emulsion polymerization into three intervals depending on the time of the disappearance of the micellar phase and the emulsified monomer droplets. During interval I, radicals are considered to diffuse into the micelles to initiate polymerization. The micelles then contain both monomer and polymer particles. As the polymerization reaction proceeds, the micelles, now called latex particles, continue to grow by absorbing dissolved monomer from the aqueous phase, which in turn is replenished from the monomer droplets. The monomer droplets, therefore, serve as a monomer reservoir for the continued polymerization in the particle during interval I.

Gardon explains the above mechanism for monomer absorption using thermodynamic concepts. Gardon postulates that the free energy of mixing favours the entry of monomer mol-

ecules from the aqueous phase to the latex particles. The free energy of mixing is counteracted by the interfacial free energy change due to the increase in the surface area of the latex particles as they swell by absorbing monomer molecules. Therefore the latex particles can absorb monomer until the interfacial free energy change and free energy of mixing reach an equilibriuim. It follows that the monomer concentration in the latex particles remains constant during polymerization as long as the aqueous phase is saturated with monomer.

As the size of the latex particles increases, more surfactant molecules are required on the surface of the particles for stabilization. Surfactant molecules are absorbed from the aqueous phase on the latex particles until the concentration of surfactant in the aqueous phase becomes less than the cmc. At concentrations below the cmc the inactive micelles (those in which polymerization has not yet been initiated) collapse and supply the necessary surfactant to the growing particles for stabilization; thus, no new latex particles can be formed. This situation is considered to occur at a conversion of between 2 and 15% and correspond to the end of interval I.

During interval II the latex particles formed during interval I continue to grow. Since the number of particles and the concentration of monomer in each particle are constant, the rate of polymerization remains constant during interval II. The continuous diffusion of monomer from the

droplets to the latex particles results in the disappearance of the droplets at a conversion of between 50 and 80%. Thereafter unreacted monomer is left only in the latex particles. The absence of monomer as a separate phase corresponds to the commencement of interval III. During this final interval the rate of polymerization decreases continuously as the monomer in the latex particles is consumed. It is considered that conversions approaching 100% are usually achieved and that the final polymer particles have diameters of the order of 0.05 to 0.2 μm, that is, intermediate in size between the initial micelles and the monomer droplets.

Gardon developed a mathematical model for his proposed mechanism. The model was developed for a persulfate initiator which produces two identical free radicals for initiation, and for reactions carried out under isothermal conditions. Calculations led to the following expressions for the rate of polymerization, the constant total number of particles which remain after interval I, and the number average molecular weight:

$$\frac{dP}{dt} = 0.369[R(1-\phi_m)]^{0.4}\left[\frac{k_p d_m \phi_m A}{N_{Avo} d_p}\right]^{0.6} \bar{q} \qquad (2.12)$$

$$N = 0.369\ A^{0.6}\left[\frac{R(1-\phi_m)N_{Avo} d_p}{\phi_m k_p d_m}\right]^{0.4} \qquad (2.13)$$

$$\bar{M}_n = 0.369[N_{Avo}\, d_p(1-\phi_m)]^{0.4} \left[\frac{k_p d_m \phi_m A}{R}\right]^{0.6} \qquad (2.14)$$

The average number of free radicals per particle at steady state , $\bar{q}$, is an important parameter in the Smith Ewart theory (16). When the value of this parameter ($\bar{q}$) is equal to a half, the rate of polymerization becomes:

$$\frac{dP}{dt} = 0.185\ [R(1-\phi_m)]^{0.4} \left[\frac{k_p d_m \phi_m A}{N_{Avo} d_p}\right]^{0.6} \qquad (2.15)$$

It corresponds to the physical situation in which radicals diffuse into the particles one at a time and in which transfer of radicals out of particles is negligible. Entry of a second radical into a particle results in instant termination. Thus each particle has a growing polymer molecule or radical in it for half of the time while during the other half of the time there is no polymerization because there is no radical present in it. Since the rate of radical entry into the particles is constant at any time , half of the particles contain one radical and the other half contain none. The Smith-Ewart model is generally found to describe the polymerization mechanism for water insoluble monomers such as styrene. For certain monomers however, it was observed that there is transfer of radicals out of particles particularly for monomers insoluble in their polymer (5).

In such cases $\bar{q}$ is less than a half. At high conversions for certain monomers such as styrene and methylmethacrylate $\bar{q}$ was found to range from 2 to 10 (5). Therefore, $\bar{q}$ may be considered to be different for different monomers and conversions.

Gardon presented an extensive comparison between predictions based on his theory and corresponding experimental results (18). It was claimed that the predicted values were in good agreement with experimentally measured parameters for a wide range of emulsion polymerization systems including those of styrene and butadiene. However, Gardon did not postulate a theory applicable for emulsion polymerization in the presence of nonreactive liquid additives in the nature of that attempted in this work.

2.5 EFFECTS OF NONREACTIVE LIQUID ADDITIVES ON EMULSION POLYMERIZATION

Emulsion polymerization in the presence of nonreactive liquid additives has been studied by various investigators (1-4). It was reported that the effect of these additives was in general to reduce the polymerization rate and the average molecular weight of the polymer. In this section a brief review is made of the literature concerning the influence of a solvent on free radical bulk polymerization. Subsequently a review of the literature dealing with emulsion polymerization in the presence of nonreactive liquid additives is also presented.

Since the original proposal of the free radical polymerization mechanism by Staudinger et al. (23) many investigators studied the effect of using a solvent on free radical polymerization reactions. Norrish et al. (24) discovered that the rate of polymerization of methylmethacrylate increases with time particularly when high conversions are reached. This phenomenon was explained by Trommsdorff et al. (25) by taking into account the viscosity of the polymerization medium. In order to investigate the effects of viscosity of the polymerizing medium on the reaction rates, the elementary rate constants were determined at various conversions in different solvents. The results indicated that the rate of the termination process varied with viscosity to a much greater extent than that for the rate of the propogation process (26,27). Schulz et al. (28,29) estimated the reaction rate constants for the free radical polymerization of methylacrylate in several solvents. Their results indicated that the termination rate constants were inversely proportional to the viscosity of the solvents. Their results also indicated that the propogation rate constants were reduced to a lesser extent than the termination rate constants with an increase in viscosity. Similar results were also obtained in the free radical polymerization of benzylmethacrylate. It was concluded, therefore, that the solvent effect is mainly due to the influence of solvent viscosity on the termination process. The result is that an increase in

the viscosity has the net effect of increasing the polymerization rate for this situation.

Seymour et al. (1,2) studied the effects of several nonreactive liquid additives on emulsion polymerization of styrene at 50 °C. They used Triton X-405 as the surfactant and potassium persulfate as the initiator for their investigations. They divided the used additives into different categories on the basis of their viscosities and solvent powers for dissolving the polystyrene. Benzene, cyclohexane and octane were categorized as nonviscous and good solvents for polystyrene; heptane and hexane were categorized as nonviscous and poor solvents for polystyrene; whereas diisoctylphthalate and Nujol were categorized as viscous and nonsolvents. Their study revealed that the presence of good nonviscous solvents retarded the rate of polymerization, while the presence of poor nonviscous solvents resulted in less of a reduction. The polymerization rate was highest in the presence of viscous nonsolvents. The rate was also influenced by the quantity of the additives. As the quantity of the additive was increased, the rate of polymerization was further reduced. It was observed that the additives which retarded the rate of polymerization also reduced the average molecular weight of the product. They also observed the effect of surfactant concentration on the rate of polymerization in the presence of Nujol at a concentration of 0.025 parts per part of styrene. The reaction rate was found to depend on the surfactant concentration to the 1.8 power.

Seymour et al. (1,2) explained their observations on the basis of two properties of the additives, their viscosity and their solvent power. They contended that a viscous poor solvent increased the viscosity of the reaction mixture within the polymerizing particles resulting in lower diffusion rates especially those of the macro-radicals. This reduced the rate of termination of chain radicals present in the polymerizing particles and in effect, enhanced the rate of propagation. Conversely, a decrease in the viscosity of the reaction mixture in the polymerizing particles as a result of the addition of a good and nonviscous solvent, retarded the rate of polymerization and reduced the molecular weight of the polymer.

Blackley and Haynes (3) conducted similar investigations with aromatic hydrocarbon additives, namely, benzene, toluene and ethylbenzene, as well as with cyclohexane. They also studied the emulsion polymerization of styrene at 50 °C , but using sodium lauryl sulfate as the surfactant and potassium persulfate as the initiator. In the presence of all these additives the rate of polymerization was reduced. The aromatics were found to reduce the rate of polymerization more than cyclohexane. They expected the reduction in the rate of polymerization as a result of monomer dilution by the additives, but the observed reduction was much greater than expected on the basis of mere monomer dilution. They also observed that a greater number of particles was formed

in the presence of the additives. By considering the number of particles present they observed that the rate of polymerization was reduced in each particle in the presence of additives. Their observations indicated that there was a decrease in intrinsic viscosity of the polymer formed in the presence of additives. They explained their results by Trommsdorff 'gel' effect; that is, the addition of nonviscous additives lowers the viscosity of the medium inside the particles. A decrease in viscosity enhances the rate of termination, which results in the reduction of the molecular weight of the polymer and the rate of polymerization. Their explanation raised a question that if the Trommsdorff 'gel' effect is so important in the presence of additives, then in the emulsion polymerization of styrene in the absence of any additive, more than one free radical may be present in at least some of the particles. They were neither able to disprove or substantiate their contention concerning the number of free radicals in the polymer particles at one time.

Azad et al. (4) studied the effect of nonreactive additives on the kinetics of a seeded emulsion polymerization of styrene at 50 °C. The seed latex was initially prepared by an emulsion polymerization at 50 °C using SDS as the surfactant and potassium persulfate as the initiator. They chose the method of seeding the emulsion polymerization to keep the number of particles constant in the emulsion. Therefore the effect of other parameters on the kinetics of emulsion

polymerization was independent of the variation of number of particles. They observed that in the presence of water insoluble additives the rate of polymerization was lower than that calculated on the basis of monomer dilution. Azad et al. (4) proposed another mechanism to explain their observations. They postulated that the water insoluble additive was not transported through the water; instead it remained in the monomer droplets, reducing its activity which in turn lead to a lower activity of monomer in the polymerizing particles. They developed equations for the swelling of the seed latex in the presence of water insoluble additives in the monomer phase. Their observation with water insoluble additives such as octadecane and tetracosane agreed well with theoretical predictions based on equations for equilibrium swelling. On the other hand, it was suggested that when the additives were relatively water-soluble, the reduction in the rate of polymerization was influenced by two things: first, the monomer was diluted by the additives and next, chain transfer probably occurred with the additives. It was postulated that chain transfer to the water soluble additives, sometimes resulted in diffusion of free radicals out of the particles. This resulted ultimately in a lowering of the average number of free radicals in the polymerizing particles, which in turn explained the reduction in the rate of polymerization.

The explanation given by Azad et al. (4) appears to be incomplete. Some inconsistency in explanation may be observed when considering that the addition of the aromatic hydrocarbon additives, benzene, toluene or ethylbenzene retarded the rate of polymerization to the same extent (3). The solubility of these additives in water is of the same order; therefore, in order to explain the same order of reduction in the rates, by the mechanism suggested by Azad et al. (4), the chain transfer constants of these additives would likewise need to be of the same order. The chain transfer constants as tabulated in Table 1 can be seen to be quite different, however. Therefore, the postulation of chain transfer with additive as an explanation for the observed retardation appears to be only partially justified.

TABLE 1

Chain transfer constants and solubility parameters of aromatics

compound	chain transfer constants (30)		solubility parameter (31)
	At 60 °C	At 100 °C	
Benzene	0.018	0.184	9.2
Toluene	0.125	0.65	8.9
Ethylbenzene	0.67	1.62	8.9

The above literature survey suggests that a satisfactory mechanism of emulsion polymerization in the presence of non-reactive additives is not yet fully developed. It is the

purpose of this work to study the kinetics of emulsion polymerization of butadiene in the presence of nonreactive liquid additives, and to develop a theoretical model for the various effects of the additives.

2.6 MOLECULAR STRUCTURE OF POLY (1,3-BUTADIENE)

The structural arrangement of butadiene in its homopolymer depends upon the number of double bonds participating in the polymerization. The molecular structure of butadiene, which has two double bonds, is shown in Figure 2a. If only one double bond participates in the polymerization the vinyl or 1,2 polybutadiene shown in Figure 2b would be formed. In turn, vinyl polymer structures could occur in three different forms, the isotactic form, in which all the unreacted vinyl groups are oriented toward one side of the polymer chain, the syndiotactic, in which the vinyl groups appear alternately on one side and then the other side, and the last one is the atactic form in which the vinyl groups are randomly oriented. These vinyl structures are shown in Figure 2c. The other polymer structures arise when both double bonds participate in polymerization and the four carbons of the butadiene molecules form the backbone of the polymer chain. In this case cis-1,4 and trans-1,4 structures are possible as shown in Figure 2d. Polybutadiene produced in an emulsion system usually contains a mixture of all possible structural arrangements of butadiene. The proportion of the

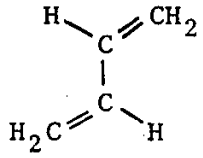

trans

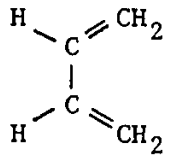

cis

Figure 2a

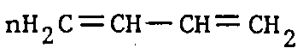

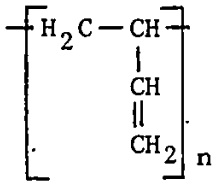

1,2-polybutadiene

Figure 2b

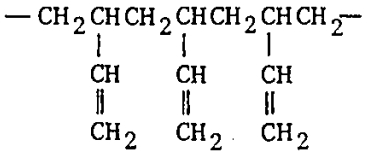

isotactic 1,2-polybutadiene

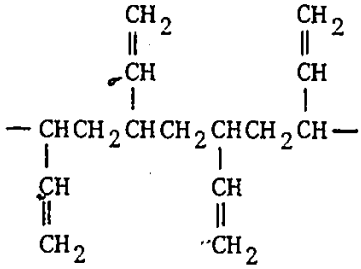

syndiotactic 1,2-polybutadiene

Figure 2c

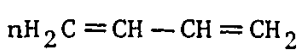

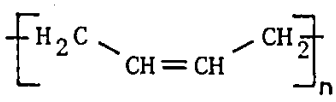

cis-1,4-polybutadiene

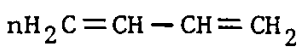

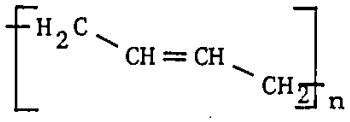

trans-1,4-polybutadiene

Figure 2d

Figure 2 - Structural arrangement of butadiene and polybutadiene

different molecular structures depends on various parameters including the type of initiator, type and concentration of surfactant used and the polymerization temperature. Hampton (32) analysed the proportion of various structures obtained at different polymerization temperatures. The proportion of unreacted vinyl groups was found to vary very little with polymerization temperature. However, the proportion of trans-1,4 decreased and cis-1,4 increased as the polymerization temperature was raised. The polybutadiene, therefore, prepared at low temperature was found to contain a high proportion of trans-1,4 structure. This greater regularity in configuration for butadiene polymer is associated with improved physical properties. On the other hand the polybutadiene prepared at high temperature contains a random sequence of vinyl, cis-1,4 and trans-1,4 structures. This random sequence is considered to be the major reason for the poor physical properties of the polybutadiene product. Thus, the butadiene elastomers are usually synthesized at low temperatures. In the present investigation the polymerization temperature was kept constant at 10 °C.

2.7 ANALYSIS OF POLYBUTADIENE

Polybutadiene prepared by an emulsion polymerization technique has a distribution of molecular weights as well as different configurations. The average molecular weight and the molecular structure of polybutadiene can be determined by several methods. The methods for measuring the average

molecular weight include membrane osmometry, light scattering, viscosity measurement and gel permeation chromatography (GPC). Membrane osmometry yields the number average molecular weights, $\bar{M}_n$. The primary difficulty with this method is that the sample has to be washed thoroughly to remove surfactant and other emulsion ingredients for accurate measurement. From light scattering measurements the weight average molecular weight, $\bar{M}_w$ may be obtained. The major drawback of this technique is that great care is required to eliminate contamination of the dissolved sample with minute particles or dust in the polybutadiene solution which give meaningless results. Viscosity measurements are an indirect method for determining molecular weight, that is, it provides a value which is proportional to but not an actual absolute value of the average molecular weight. Analysis by GPC provides a molecular weight distribution, which can be used to calculate both $\bar{M}_n$ and $\bar{M}_w$. Therefore, GPC was used in the present investigation.

The separation of polybutadiene molecules by GPC is based upon differences in their size, which is closely related to the molecular weight. Separation is accomplished by injecting the polybutadiene solution into a continuously flowing stream of solvent which passes through a GPC column. In the GPC column highly porous, tiny, rigid gel particles, called STYRAGEL are closely packed together. The pore sizes in the gel particles may vary from relatively small to very large

depending on the molecular weight to be analysed. As the solution flows through the gel particles, molecules of small sizes penetrate more pores than molecules of large sizes. Therefore, the small size molecules take longer time to emerge than do the larger molecules. If the pore size of the gel is in the right range, the GPC column can separate the polymer molecules based on their sizes with the largest molecules eluting from the column first.

The GPC is calibrated with monodispersed polystyrene standards. A whole series of polystyrene standards of molecular weight from 600 to 1.8 million are available. One characteristic of these standards that makes them unique is their very narrow molecular weight distribution. For calibration, between 6 and 12 of these standards dissolved in suitable solvents are systematically charged into the GPC and from the curve of polymer concentration versus time it is established at what volume the particular polymer molecular weights are eluted. A calibration plot is then made of the product of intrinsic viscosity of polystyrene standard solutions and respective molecular weight versus elution volume. The product of intrinsic viscosity and molecular weight is considered to be equivalent to a hydrodynamic volume. The theoretical justification for the calibration curve is based on the fact that polymer molecules elute from gel packed column on the basis of their hydrodynamic volume. The usage of this calibration curve requires the Mark-Houwink

coefficients, Ω and ω, of the polymer which is to be analysed. These coefficients relate the intrinsic viscosity with the molecular weight.

$$[\eta] = \Omega M^{\omega} \qquad (2.16)$$

This calibration curve has been shown to be valid for obtaining absolute molecular weight for polystyrene, polyvinyl chloride, polybutadiene and numerous other polymers (33).

Polymer structure is often characterized by infrared spectrophotometry. Infrared spectrophotometry is concerned with the measurement of the absorption spectra which arises when molecules undergo a transition between quantum states corresponding to two different internal energies. The energy difference, ΔE, between the states is related to the frequency of radiation absorbed or emitted by the quantum relation $\Delta E = h\nu$. An infrared spectrophotometer uses a glowing light source to provide light with wavelengths from 2.5 to 15 μm. It has been used by various investigators to determine the relative proportion of cis-1,4, vinyl and trans-1,4 structures in polybutadiene. Hampton (32) assigned the 10.3, 11.0 and 13.8 μm wavelengths to trans-1,4, vinyl and cis-1,4 structures respectively. Binder (34) used the same wave lengths as was used by Hampton for trans-1,4 and vinyl structures but used 14.7 μm for the cis-1,4 structure. Richardson (35) determined trans-1,4 and vinyl structures only and obtained cis-1,4 structure by difference. In the pres-

ent investigation the stereospecific polymer, cis-1,4 polybutadiene obtained from Polysar Limited, Sarnia, was used to find the exact absorbance frequency of the cis-1,4 structure, which matched Hampton's value of 13.8 μm.

2.8 SOLUTION PROPERTIES OF BUTADIENE

The study of the solution properties of butadiene was of only indirect relevance to emulsion polymerization. It involved the measurement of the solubility of butadiene in water and aqueous surfactant solutions. These measurements were useful when dealing with the emulsion polymerization of butadiene. The solubility of butadiene in heptane, styrene and heptane-styrene mixtures was also measured. The study also involved the development of various empirical correlations for the prediction of molecular diffusivities in liquids. The literature concerning the solubility and diffusivity of gases in liquids is reviewed in brief.

2.8.1 Solubility

The solubility of a gas in a liquid is determined by the equation of phase equilibrium; the fugacity of component A will be the same in both the liquid and gas phases at equilibrium (36):

$$f_i^v = f_i^\ell \qquad (2.17)$$

Assuming that the gas phase is ideal and neglecting any non-idealities resulting from solute-solvent interactions, Equation 2.17 becomes Raoult's law after substituting vapor pressure for fugacity:

$$P_i = x_i P_i^\circ \qquad (2.18)$$

The ideal solubilities of gases above their critical temperature can be calculated from Equation 2.18 using a hypothetical vapor pressure, which can be obtained by extending the vapor pressure curve to the solution temperature. The ideal solubility given by Equation 2.18 suffers from two serious defects. First, it is independent of the nature of the solvent; that is, at a fixed temperature and partial pressure it predicts the same solubility in all solvents. This is contrary to observed behaviour. Secondly, Equation 2.18 predicts that at constant partial pressure the solubility of a gas always decreases with rising temperature. This prediction is not always true. Hence, Equation 2.18 is used only for a rough estimate of gas solubility.

Another method for predicting gas solubilities is by Henry's law (36):

$$f_A = H_{AB} x_A \quad \text{for} \quad x_A << 1 \qquad (2.19)$$

Henry's law provides a good approximation when the solubility and the partial pressure of the solute are small and when

the temperature is well below the critical temperature of the solvent.

Many attempts have been made to correlate gas solubilities. The success of these correlations have been limited because of lack of reliable experimental data and at the same time a satisfactory theory for gas liquid solutions has not been established. Hildebrand and Scott (31,37) developed the regular solution theory for nonpolar systems. They defined a regular solution as: one involving no entropy change when a small amount of one of its components is transferred to it from an ideal solution of the same composition, the total volume remaining unchanged. Based on the regular solution theory, two equations have been developed for the prediction of solubilities of gases in liquids. The first, Equation 2.20, is for systems in which solute-solvent molecules do not differ greatly in size and the second, Equation 2.21, is for solutions involving large differences in molecular sizes.

$$-\ell n x_A = -\ell n x_A^i + \frac{V_A^\ell (\delta_B - \delta_A)^2}{RT} \qquad (2.20)$$

$$-\ell n x_A = -\ell n x_A^i + \frac{V_A^\ell (\delta_B - \delta_A)^2}{RT} + \ell n\left(\frac{V_A^\ell}{V_B}\right) + \left(1 - \frac{V_A^\ell}{V_B}\right) \qquad (2.21)$$

These equations are used for the prediction of gas solubilities in nonpolar solvents. Hayduk and Laudie (38) have presented a prediction method based on H-bonding factors for

estimation of gas solubilities in polar solvents. The H-bonding factor was defined as:

$$\alpha = \frac{x_A}{x_A^i} \qquad (2.22)$$

Miyano and Hayduk (39) later on expressed H-bonding factors by a simplified Margules equation and found it more useful to correlate the solubilities of gases in pure solvents as well as in solvent mixtures. The H-bonding factors for a binary system was expressed as:

$$-\ell n\, \alpha = A_{AB} x_B^2 \qquad (2.23)$$

Several correlations have been developed for the prediction of gas solubilities in mixed solvents. The equation provided by Krischevsky (40) was considered valid for ideal solvent solutions:

$$\ell n\ H_{AM} = x_B\, \ell n\, H_{AB} + x_D\, \ell n\, H_{AD} \qquad (2.24)$$

Another equation, provided by O'Connell and Prausnitz (41), which is considered to apply fairly well for nonpolar solvents is presented below:

$$\ell n\ H_{AM} = x_B\, \ell n\, H_{AB} + x_D\, \ell n\, H_{AD} - \tau_{BD} x_B x_D \qquad (2.25)$$

The constant τ_{BD} is the characteristic of the B,D binary pair interaction and can be estimated using the regular solution theory as:

$$\tau_{BD} = \frac{(\delta_B-\delta_D)^2(V_B+V_D)}{2\,\mathbb{R}T} \qquad (2.26)$$

The other correlations for the treatment of solutes in mixed solvents may be found in the literature (36).

In emulsion polymerization of a monomer, the monomer is dissolved in an aqueous surfactant solution. It has been found that the solubility of butadiene in the aqueous surfactant solution is significantly higher than in water. Surfactant is capable of forming micelles in the aqueous phase. These micelles are usually spherical in shape and absorb monomer molecules into their central region as discussed in Section 2.3. Therefore, the presence of micelles increases the solubility of monomer in the aqueous surfactant solution. The enhancement of monomer solubility is known as solubilization. The phenomenon of solubilization has been studied in detail by Klevens (42) and by McBain and Hutchinson (43). The extent of solubilization is affected by surfactant type, surfactant concentration, nature of solubilized substance and concentration of simple electrolytes in the surfactant solution. According to McBain and Richards (44) the solubilizing power of a surfactant increases quite sharply when both its concentration and chain length (molecular weight) are increased. Their results also concluded

that the number of molecules of solubilized substances per molecule of surfactant is constant for a given surfactant at all surfactant concentrations, and the extent of solubilization can be increased by the addition of simple electrolytes. Stearns et al. (45) have provided evidence to suggest that the effect of electrolyte is essentially to make more surfactant available for forming more micelles through the lowering of the cmc. As discussed in Section 2.3 the number of micelles is considered to lie between $5x10^{17}$ and $1x10^{18}$ per cm^3 of aqueous phase. Each micelle contains between 50 and 100 solubilized monomer molecules, depending upon the nature of the surfactant (11). Therefore it is considered that the solubilized material in the surfactant solution is not present as suspended or emulsified droplets, but is incorporated in the colloidal particles (micelles) of the surfactant itself. It is in solution in the same sense that the surfactant itself is in solution. The micelles may be considered to form a separate phase within the emulsion system.

2.8.2 Diffusivity

Molecular diffusion is concerned with the movement of individual molecules through a substance resulting from a concentration differential. The rate of diffusion is commonly described in terms of a molar flux and a diffusion coefficient, as defined by Fick's law:

$$J_A = -D_{AB} \nabla c_A \qquad (2.27)$$

During emulsion polymerization the monomer diffuses from the monomer droplets to the aqueous phase. In the aqueous phase, the monomer concentration is very low. In such cases, where solute A diffuses in an infinitely dilute solution of A in B, the diffusion coefficient is denoted by D°_{AB}. For scientific applications D°_{AB} is considered to be valid for concentrations of 10 mole percent (46).

Several theories have been proposed for the mechanism of diffusion including those involving a hydrodynamic, kinetic, statistical-mechanical or thermodynamic basis or a combination of these. The diffusion theories have been reviewed in detail by Ghai et al. (47,48). Because of our limited knowledge of the liquid state, the theories provide only a partial basis for the prediction of diffusion coefficients. Therefore, to predict the diffusion coefficient a number of empirical correlations have been developed. Some of the important empirical correlations are presented below.

Wilke and Chang (49) introduced a correlation taking into account the molecular weight of the solvent and an empirical association factor. Empirically fitted constants resulted in the following equation:

$$D^{\circ}_{AB} = 7.4(10^{-8}) \frac{(\Gamma M_B)^{0.5} T}{\eta_B V_A^{0.6}} \qquad (2.28)$$

Scheibel (50) developed another correlation by eliminating the association factor from the Wilke-Chang correlation:

$$D^{\circ}_{AB} = \frac{KT}{\eta_B V_A^{1/3}} \qquad (2.29)$$

In the above equation the value of the constant K is:

$$K = 8.2(10^{-8})\left[1 + \left[\frac{3V_B}{V_A}\right]^{2/3}\right] \qquad (2.30)$$

The value of the constant K was determined separately for several solvents as below:

(i) for water, $K = 25.2(10^{-8})$ if $V_A < V_B$

(ii) for benzene, $K = 18.9(10^{-8})$ if $V_A < 2V_B$

(iii) for other solvents, $K = 17.5(10^{-8})$ if $V_A < 2.5V_B$

Reddy and Doraiswamy (51) proposed the following relation:

$$D^{\circ}_{AB} = \frac{K' M_B^{0.5} T}{\eta_B (V_A V_B)^{1/3}} \qquad (2.31)$$

The value of K' in the above equation is:

$$K' = 10(10^{-8}) \text{ when } \frac{V_B}{V_A} \leq 1.5 \qquad (2.32)$$

$$K' = 8.5(10^{-8}) \text{ when } \frac{V_B}{V_A} \geq 1.5 \qquad (2.33)$$

In general, most investigators found that the above three correlations predict a similar value of the diffusion coefficient. However, in the case of water as the solute, the prediction accuracy from the Reddy-Doraiswamy correlation was considered better (46).

Another general correlation developed by King et al. (52) utilizing latent heat of vaporization as a measure of the intermolecular forces involved, is given below:

$$D^{\circ}_{AB} = 4.4(10^{-8}) \frac{T}{\eta_B} \left[\frac{V_B}{V_A}\right]^{1/6} \left[\frac{\Delta W_B}{\Delta W_A}\right]^{0.5} \qquad (2.34)$$

A recently developed general correlation by Tyn and Calus (53) was considered to have a better accuracy for prediction than any other existing correlation. Utilizing the parachor as a measure of molecular interaction, Tyn and Calus developed the following correlation:

$$D^{\circ}_{AB} = 8.93(10^{-8}) \frac{T}{\eta_B} \frac{V_A^{1/6}}{V_B^{1/3}} \left(\frac{\mathbb{P}_B}{\mathbb{P}_A}\right)^{0.6} \qquad (2.35)$$

For the development of their correlation they treated water as a dimer, in that they considered that the value of the molar volume and parachor was doubled. They also considered the organic acid solutes as dimers except when diffusing in water, methanol and butanol; then they were treated as mo-

nomers. For predictions involving non-associating solutes in monohydroxy alcohols, the value of the molar volume and parachor was multiplied by a factor which was related to the solvent viscosity as follows:

$$\psi = 8\eta_B \tag{2.36}$$

With these rules, Tyn and Calus claimed that their general correlation was the best available.

Correlations have also been developed for predicting diffusivities at infinite dilution in water. These correlations are expected to be of greater accuracy than using one of the general correlations. One such correlation for water as solvent developed by Othmer and Thakar (54) is presented below:

$$D^{\circ}_{AB} = \frac{14.0(10^{-5})}{\eta_B^{1.1} V_A^{0.6}} \tag{2.37}$$

The correlation was based on data published prior to 1950. A more recent correlation developed by Hayduk and Laudie (55) using data published after 1950 is shown below:

$$D^{\circ}_{AB} = \frac{13.26\ (10^{-5})}{\eta_B^{1.14}\ V_A^{0.589}} \tag{2.38}$$

Both correlations yield similar, but not identical results. It was found that an average absolute error of 10% could be expected with either correlation.

As part of this work all of the above mentioned correlations were tested for their accuracy and new ones were developed by using the literature data available. For the development of new correlations the nonlinear optimization technique was used. The technique involved the Box-modified Gauss method. This method was selected because of its most rapid convergence after testing all the optimization techniques avialable at the computer center of the University of Ottawa. In this method the sum of squares functions was minimized to obtain the desired parameter values (56).

Chapter III

THEORETICAL DEVELOPMENT

A theoretical model is proposed for emulsion polymerization in the presence of a nonreactive liquid additive. The Gardon model for simple emulsion polymerization, which is presented in Section 2.4 was modified to propose this model. The proposed model will be examined in Chapter 6 to see whether it actually describes the effects of the addition of nonreactive liquid additives, heptane and cyclohexane, on the kinetics of emulsion polymerization of butadiene. The purpose of this chapter is to present the development of the theoretical model.

When a monomer is mixed with a nonreactive miscible liquid solvent and agitated with an aqueous surfactant solution until equilibrium is established, three phases result. First, one will find an aqueous phase saturated with monomer, additive and surfactant, second, a micellar phase saturated with the monomer and with the additive, and third, the emulsified droplets of the monomer-solvent solution. The physical picture of the emulsion is shown in Figure 3. The solubility of monomer and solvent in the aqueous phase is assumed to be extremely low, therefore only a small amount of monomer and solvent is present in the aqueous phase. The

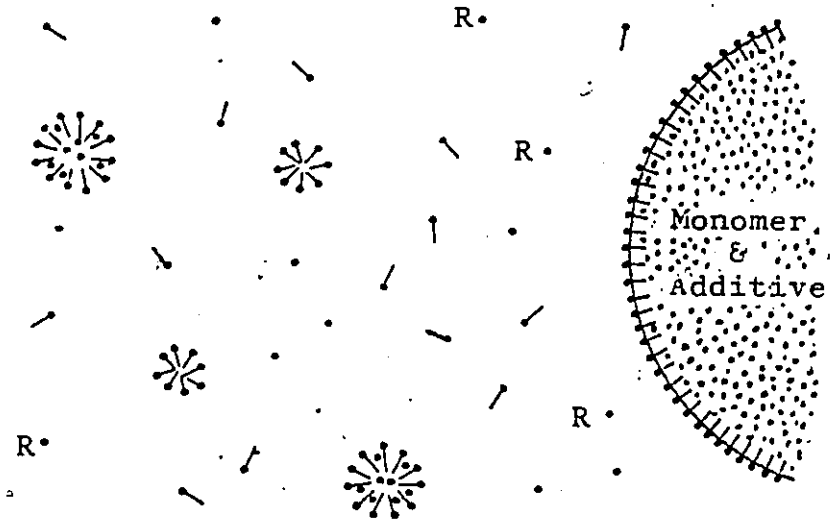

Figure 3 - Diagram of the emulsion before initiation

monomer and solvent concentration in the micelles and in the emulsified droplets is assumed to depend upon the solubilization of monomer and of solvent and upon the monomer to solvent ratio in the feed. The monomer to solvent ratio in the micelles can be found out as follows:

At a certain concentration of the aqueous surfactant solution, let S_m° (mol.dm^{-3} of solution) be the solubilization of pure monomer and S_a° (mol.dm^{-3} of solution) the solubilization of pure additive. The concentration of monomer and solvent in the micelles, in terms of mole fraction, when the equimolar mixture of monomer and solvent is dissolved, will be:

$$S_m = \frac{S_m^\circ}{\sum S_i^\circ} \qquad (3.1)$$

$$S_a = \frac{S_a^\circ}{\sum S_i^\circ} \qquad (3.2)$$

The mole fraction of monomer in the micelles, F_{m_2}, can be calculated from the mole fraction of monomer in the feed, x_m, by using the following relation:

$$F_{m_2} = \frac{S_m x_m}{S_m x_m + S_a (1-x_m)} \qquad (3.3)$$

$$F_{a_2} = 1 - F_{m_2} \qquad (3.4)$$

The polymerization is initiated by the addition of water soluble initiators, which generate free radicals. These radicals are generated randomly throughout the aqueous phase. The free radicals react with the dissolved monomer in the aqueous phase and form chain radicals. It is believed that these radicals, before becoming long enough to precipitate, are absorbed either by the micelles or by the droplets due to high concentration of the micelles and droplets in the aqueous phase. The number of monomer droplets and surfactant micelles are estimated to be approximately 10^{12} /cm^3 and 10^{18} /cm^3 respectively, as discussed in Section 2.4. It has been suggested that the micelles and the droplets absorb the radicals proportional to their surface areas (5,17). The surface area of micelles is approximately sixty times larger than that of emulsified droplets (17). Hence it is hypothesized that the majority of the radicals are absorbed by the micelles and that the extent of polymerization taking place in the droplets is sufficiently small so that it can be ignored.

In the Gardon model the reaction taking place during emulsion polymerization is divided into three intervals. As presented in Section 2.4, the time of disappearance of the micellar phase corresponds to the commencement of interval II and the time of disappearance of emulsified monomer droplets corresponds to the commencement of interval III. However in the proposed model the polymerization reaction is

divided into two intervals. The emulsified droplets do not disappear in the presence of a nonreactive liquid additive. In interval I free micelles (containing no polymer) are present and as the reaction proceeds and the free micelles are consumed, the complete disappearance of free micelles marks the commencement of interval II. During interval I, radicals diffuse into the micelles and initiate polymerization, converting the micelles into latex particles. New latex particles are formed and their number increases as the radicals are absorbed by the micelles. In the latex particles as the monomer molecules are consumed by the reaction, new monomer molecules are absorbed from the aqueous phase. The equilibrium concentration of monomer in the aqueous phase is maintained by the diffusion of monomer from the emulsified droplets. As Gardon (17) described, the driving force for the diffusion of monomer into the latex particles is the free energy of mixing, which is countered by the interfacial free energy change of the system. The interfacial free energy change of the system is caused by the increase in the surface area of the particles, which increases in size during polymerization. As the particles grow in size, more surfactant molecules are absorbed on their surface for the stabilization of the particles. The continuous absorption of the surfactant molecules on the latex particles results in a decrease in surfactant concentration in the aqueous phase. Gradually the surfactant concentration becomes

less than the cmc and as a result, the micelles in which the polymerization has not yet been initiated, collapse and the surfactant dissolves and migrates to the polymer particles. Thus no additional latex particles are formed. This corresponds to the end of interval I. The physical picture after interval I is depicted in Figure 4.

During interval II the number of latex particles remain constant. The polymerization continues in the latex particles and the monomer diffuses from the droplets to the aqueous phase and subsequently from aqueous phase to the particles. It is assumed in the proposed model that the presence of relatively water insoluble additive depresses the activity of monomer, and thus concentrates the monomer in the droplets. Therefore at equilibrium the concentration of monomer in the latex particles is less than that expected from simple dilution. The distribution of monomer between the droplets and the latex particles in the presence of an additive can be explained from thermodynamic considerations. The chemical potential, $\mu_{r_1}^{c_1}$, of the monomer inside a droplet of radius r_1 containing the additive at concentration C_1 is related to the chemical potential, $\mu_p^{c_1}$, of the monomer at the same concentration in contact with a plane surface by (57):

$$\mu_{r_1}^{c_1} - \mu_p^{c_1} = \frac{2\sigma \bar{V}_{m_1}}{r_1} \qquad (3.5)$$

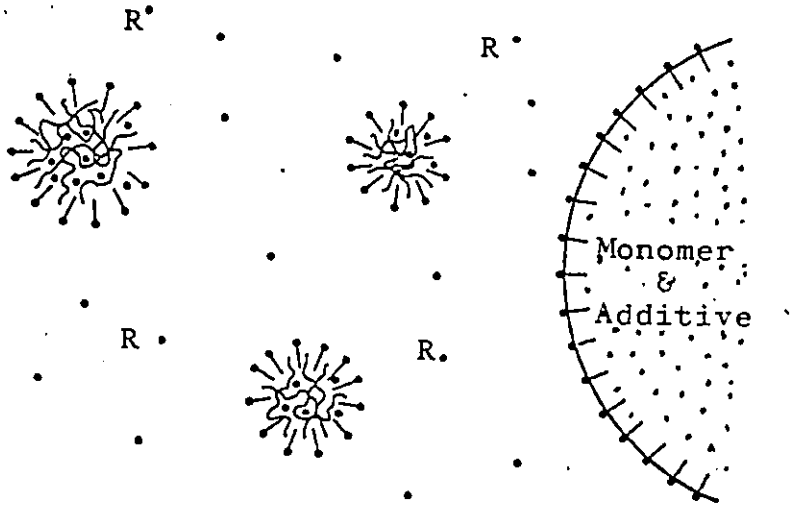

Figure 4 - Diagram of the emulsion in interval II

The presence of an additive has simply reduced the chemical potential of monomer in the droplets. In plane surfaces, the chemical potential of the monomer, $\mu_p^{c_1}$, in a solution of concentration C_1 is related to its chemical potential in the pure state μ_p° by:

$$\mu_p^{c_1} - \mu_p^\circ = IRT \ln \gamma_{m_1} \tag{3.6}$$

Substitution from Equation 3.5 gives:

$$\mu_{r_1}^{c_1} - \mu_p^\circ = \frac{2 \sigma \bar{V}_{m_1}}{r_1} + IRT \ln \gamma_{m_1} \tag{3.7}$$

Similarly for a latex particle of radius r_2 and additive concentration C_2, the following equation can be written:

$$\mu_{r_2}^{c_2} - \mu_p^\circ = \frac{2 \sigma \bar{V}_{m_1}}{r_2} + IRT \ln \gamma_{m_2} \tag{3.8}$$

Substitution from Equation 3.7 gives:

$$\mu_{r_1}^{c_1} - \mu_{r_2}^{c_2} = 2\sigma \left[\frac{\bar{V}_{m_1}}{r_1} - \frac{\bar{V}_{m_2}}{r_2}\right] + IRT \ln \frac{\gamma_{m_1}}{\gamma_{m_2}} \tag{3.9}$$

The difference in chemical potential of the monomer in the droplet and in the latex particle in the presence of an additive, as expressed by Equation 3.9, is the driving force

for the movement of monomer. Physically this imbalance is rectified by the diffusion of the monomer. At equilibrium:

$$\mu_{r_1}^{c_1} = \mu_{r_2}^{c_2} \tag{3.10}$$

$$2\sigma \left[\frac{\bar{V}_{m_1}}{r_1} - \frac{\bar{V}_{m_2}}{r_2}\right] + \mathrm{IRT} \ln \frac{\gamma_{m_1}}{\gamma_{m_2}} = 0 \tag{3.11}$$

Since $r_1 >> r_2$ then:

$$\frac{\bar{V}_{m_1}}{r_1} - \frac{\bar{V}_{m_2}}{r_2} = - \frac{\bar{V}_{m_2}}{r_2} \tag{3.12}$$

Therefore, Equation 3.11 becomes:

$$\ln \gamma_{m_1} = \ln \gamma_{m_2} + \frac{2\sigma \bar{V}_{m_2}}{r_2 \mathrm{IRT}} \tag{3.13}$$

Since $2\sigma V_{m_2}/(r_2 \mathrm{IR}\,T)$ is a positive quantity a γ_{m_1} is larger than a γ_{m_2}. The activity is directly proportional to the concentration. Therefore the concentration of monomer, at equilibrium, in the latex particles is less than expected from simple dilution. Thus, the experimental rate of polymerization in the presence of an additive becomes lower than expected on the basis of monomer dilution. The thermodynamic considerations of the depression in the monomer activity, due to the presence of water insoluble liquid additive has been treated in detail by Ugelstad and coworkers (58-64).

It is assumed in the proposed model that the extent of reduction in the rate of polymerization depends upon the physical properties of the additive including its viscosity and solvent power to dissolve the monomer and polymer. The presence of the additive affects the viscosity of the reaction medium inside the particle. A change in the viscosity influences the diffusivity of monomer, polymer and radicals inside the particles, which results in a change in the elementary rate constants. It has been observed that a change in the viscosity of the reaction medium mainly affects the termination process whereas the influence on the propogation process is significantly less (27,28,65). The relation between termination rate and viscosity is developed by using a model proposed by Allen and Patrick (66). This model relates the rate constant for reaction between species A and B, k_{AB}, with the collision radius for an encounter, β_{AB}, as follows:

$$k_{AB} = C\ D_{AB}\ \beta_{AB} \qquad (3.14)$$

For the termination step in a polymerization reaction, β_{AB}, is related to the size of a freely rotating polymer segment of a polymer molecule and to its molecular weight. The mutual diffusion coefficient, D_{AB}, is dependent upon whether the molecular motion required to cause an encounter is controlled by the segmental or translational diffusivity of the chain, or whether or not that diffusion is influenced by

chain entanglements. The variation in termination rate constant may be conveniently expressed as a ratio of the values at different times during the reaction. Let k_{t_o} refer t time, t_o, then Equation 3.14 becomes:

$$\frac{k_t}{k_{t_0}} = \left[\frac{D_p}{D_{p_0}}\right]\left[\frac{\beta}{\beta_0}\right] \tag{3.15}$$

Neglecting the variation of the collision radii with conversion Equation 3.15 becomes:

$$\frac{k_t}{k_{t_0}} = \left[\frac{D_p}{D_{p_0}}\right] \tag{3.16}$$

Neglecting the collision radii with conversion is equivalent to ignoring changes of molecular weight with conversion. This approximation is quite reasonable for emulsion polymerization because the molecular weight changes little, if any, with conversion (17). Therefore, the termination rate is directly proportional to the diffusivity. From an observation of diffusivity correlations, it is observed that the diffusivity is frequently inversely proportional to the viscosity of the medium (67):

$$D_p \propto \frac{1}{\eta_p} \tag{3.17}$$

Utilizing the relation between viscosity and diffusivity the following equation is obtained:

$$\frac{k_t}{k_{t_0}} = \left[\frac{\eta_{p_0}}{\eta_p}\right] \qquad (3.18)$$

That is, it may be considered that the rate of termination is inversely proportional to the viscosity of the reaction medium. Hence, the addition of an additive, which increases the viscosity of the reaction medium inside the particle, tends to result in a reduction in the termination rate. This may result in the possibilty of more than one radical existing in the latex particles. Thus the rate of polymerization obtained would be expected to increase.

The rate of polymerization in interval II is expected to remain constant as long as the variation of monomer concentration in the latex particles is insignificant due to the diffusion of monomer from the droplets to the particles. However, after certain time the drop of monomer concentration in the droplets may reduce the rate of diffusion of monomer to such an extent that the monomer concentration in the particles decreases. Thus the rate of polymerization no longer remains constant and begins to decrease. As the monomer concentration continues to decrease with the increasing conversion so does the rate of polymerization. Therefore below a certain concentration of monomer in the droplets, the rate of diffusion of monomer from the droplets

to the latex particles becomes the polymerization rate controlling step.

The mathematical expressions for the proposed model will now be developed. The approach followed for this development is similar to that adopted by Gardon (17) although the expressions obtained are different and take into account the presence of additive in the emulsion polymerization. The differential equation for the initial rate of formation of latex particles will now be developed. If n_i is the number of particles of radius r_i per unit volume of aqueous phase, then the surface area of all particles at any given instant is:

$$4\pi \sum n_i r_i^2 \tag{3.19}$$

If N_t is the number of particles per unit volume of aqueous phase at time t, the differential equation for the rate of generation of particles is:

$$\frac{dN_t}{dt} = R\left[1 - \left(\frac{4\pi}{A}\right)\left(\sum n_i r_i^2\right)_t\right] \tag{3.20}$$

The rate of polymerization depends upon the monomer and radical concentration. In homogeneous polymerization it is written as:

$$-\frac{d[M]}{dt} = k_p[M][R] \tag{3.21}$$

In emulsion polymerization, each particle can be considered to be a separate reactor and the above rate equation can be modified accordingly. Considering a particle as a system, the differential equation for the number of converted moles of monomer in the system is written as:

$$\frac{d\Lambda}{dt} = -V_s \frac{d[M]}{dt} \tag{3.22}$$

The equation expressing the number of radicals in the system is:

$$q = N_{Avo} V_s [R\cdot] \tag{3.23}$$

The equation expressing the monomer volume fraction is:

$$\phi_m = V_m [M] \tag{3.24}$$

The addition of a nonreactive liquid additive is expected to affect the rate of conversion. Therefore the effect of the addition of an additive is taken into account by an equation expressing the additive volume fraction as:

$$\phi_a = V_a [a] \tag{3.25}$$

Substitution from the above equations into Equation 3.21 gives the following polymerization rate for emulsion polymerization:

$$\frac{d\Lambda}{dt} = \frac{k_p \phi_m q}{N_{Avo} V_m} \tag{3.26}$$

As discussed above, latex particles grow in size during polymerization. The differential equation describing the increase in particle size is derived by considering the volume of polymer in the particle:

$$\frac{\Lambda V_m d_m}{d_p} = [\frac{4\pi}{3}] r^3 (1 - \phi_m - \phi_a) \qquad (3.27)$$

The derivative of Equation 3.27 when combined with the value of $d\Lambda/dt$ from Equation 3.26 gives:

$$\frac{dr^3}{dt} = [\frac{3}{4\pi}][\frac{k_p}{N_{Avo}}][\frac{d_m}{d_p}][\frac{\phi_m}{1-\phi_m-\phi_a}]q \qquad (3.28)$$

The above equation describes the change of particle size with time. If it is assumed that the number of radicals in a particle during polymerization is always one, the differential equation for the particle size becomes:

$$\frac{dr^3}{dt} = [\frac{3}{4\pi}][\frac{k_p}{N_{Avo}}][\frac{d_m}{d_p}][\frac{\phi_m}{1-\phi_m-\phi_a}] \qquad (3.29)$$

For a particle nucleated at time τ after initiation of polymerization and for an initial radius assumed to be zero at that time, its volumetric, and surface area, growth rate are proportional to the cube and the square of the radius with time, respectively as follows:

$$r^3 = \left[\frac{3}{4\pi}\right]\left[\frac{k_p}{N_{Avo}}\right]\left[\frac{d_m}{d_p}\right](t-\tau)\left[\frac{\phi_m}{1-\phi_m-\phi_a}\right] \qquad (3.30)$$

$$r^2 = \left[\left[\frac{3}{4\pi}\right]\left[\frac{k_p}{N_{Avo}}\right]\left[\frac{d_m}{d_p}\right](t-\tau)\left[\frac{\phi_m}{1-\phi_m-\phi_a}\right]\right]^{2/3} \qquad (3.31)$$

As has been described above, up to a certain conversion the monomer concentration is assumed to remain constant in the particle. It is also assumed for the development of the proposed model that the additive concentration in the particle remains constant. Under these assumptions a new constant K is defined as:

$$K = \left[\frac{3}{4\pi}\right]\left[\frac{k_p}{N_{Avo}}\right]\left[\frac{d_m}{d_p}\right]\frac{\phi_m}{(1-\phi_m-\phi_a)} \qquad (3.32)$$

Using the above assumptions Equation 3.20 can be solved for a final number of particles, N, at the end of interval I, as previously evaluated by Gardon (17).

$$N = 0.208\ A^{0.6}\left[\frac{R}{K}\right]^{0.4} \qquad (3.33)$$

Assuming that the monomer and additive volume fractions remain constant in the particles, the variation of conversion with time can be calculated. This evaluation is based on the fact that the amount of polymer formed is proportional to

the total volume of the particles or to $\sum n_i r_i^3$. A particle formed at time τ has a cubed radius of $K(t-\tau)$ at time t, according to previous assumptions. Hence the number of particles formed in $\Delta\tau$ at time τ is ΔN_τ. When the total volume is divided by $4\pi/3$, the following equation can be written:

$$(\sum n_i r_i^3)_t = \sum_{\tau=0}^{\tau=t} K(t-\tau)\ \Delta N_\tau \qquad (3.34)$$

Substitution from Equation 3:20 results in the following integral equation:

$$(\sum n_i r_i^3)_t = RK \int_0^t (1 - \frac{4\pi}{A} (\sum n_i r_i^2)_\tau)(t-\tau)d\tau \qquad (3.35)$$

The volume of polymer per unit volume of aqueous phase can be written as:

$$P = (1 - \phi_m - \phi_a)(\frac{4\pi}{3})(\sum n_i r_i^3)_t \qquad (3.36)$$

The above equations were solved the same way as Gardon (17) solved a similar sets of equations to obtain the amount of polymer produced during interval I:

$$P = 0.351\ (\frac{k_p}{N_{Avo}})(\frac{d_m}{d_p})\ \phi_m R\ t^2 \qquad (3.37)$$

Equation 3.37 shows that initially the conversion is proportional to initiator concentration and does not depend upon the surfactant concentration.

The expression for the number average molecular weight of the polymer formed during interval I can be derived by considering the average time, $\bar{t}_p$, needed for a single radical to enter a particle. The $\bar{t}_p$ can be found out as follows:

The number of radicals entering a latex particle per second is

$$\frac{d\lambda}{dt_p} = 4\pi r^2 [\frac{R}{A}] \qquad (3.38)$$

For the sake of simplicity, it is assumed that a newly formed particle has zero initial radius and particle age t_p is measured from the time of entrance of a free radical. At time t_p the radius of the particle is $(K\ t_p)^{1/3}$ by Equations 3.29 and 3.32. Thus:

$$\frac{d\lambda}{dt_p} = 4\pi (Kt_p)^{2/3} [\frac{R}{A}] \qquad (3.39)$$

$$\lambda = [\frac{12\pi}{5}]\ K^{2/3} t_p^{5/3}\ [\frac{R}{A}] \qquad (3.40)$$

The average time $\bar{t}_p$ needed for a single radical to enter a particle which contains only one growing polymer chain, is obtained by setting $\lambda=1$.

$$\bar{t}_p = \left[\frac{5}{12\pi}\right]^{0.6} \left[\frac{A}{R}\right]^{0.6} \frac{1}{K^{0.4}} \qquad (3.41)$$

The average volume of a particle with one terminated chain in it is $(4\pi/3).K\bar{t}_p$. The value of $\bar{M}_n$ is obtained by multiplying this volume by the volume fraction of polymer in the particle, $(1-\phi_m-\phi_a)$, by the polymer density, d_p , and by Avogadro's Number N_{Avo}.

$$\bar{M}_n = \left[\frac{4\pi}{3}\right] K\bar{t}_p \ (1 - \phi_m - \phi_a) \ d_p N_{Avo} \qquad (3.42)$$

Substitution from Equations 3.32, 3.33 and 3.41 yields:

$$\bar{M}_n = 1.44 \ k_p \cdot d_m \cdot \phi_m \cdot \left[\frac{N}{R}\right] \qquad (3.43)$$

The average molecular weight, as is clear from Equation 3.43, depends upon the rate of entry of radicals in the latex particles.

The mathematical analysis is now extended to interval II. In interval II, the number of latex particles remains constant. Therefore, the total volume of polymer present in one unit volume of aqueous phase can be calculated as follows:

$$P = \Lambda \ V_m \ N\left[\frac{d_m}{d_p}\right] \qquad (3.44)$$

Differentiating Equation 3.44 gives:

$$\frac{dP}{dt} = V_m \ N\left[\frac{d_m}{d_p}\right] \frac{d\Lambda}{dt} \qquad (3.45)$$

Substitution for $d\bar{v}/dt$ from Equation 3.26 yields:

$$\frac{dP}{dt} = k_p \phi_m \bar{q} \left[\frac{N}{N_{Avo}}\right] \left[\frac{d_m}{d_p}\right] \tag{3.46}$$

Substitution of the value for total number of particles, N, from Equation 3.33 yields:

$$\frac{dP}{dt} = 0.208\ A^{0.6}\ k_p \left[\frac{d_m}{d_p}\right] \left[\frac{\phi_m}{N_{Avo}}\right] \left[\frac{R}{K}\right]^{0.4} \bar{q} \tag{3.47}$$

Finally, the value of the constant K can be substituted to give the polymerization rate:

$$\frac{dP}{dt} = 0.369 \left[\frac{k_p \cdot d_m \phi_m \cdot A}{N_{Avo}\ d_p}\right]^{0.6} (R(1 - \phi_m - \phi_a))^{0.4} \bar{q} \tag{3.48}$$

For the assumptions made above, the rate of polymerization is found to be proportional to the surfactant concentration to the power 0.6, and to the initiator concentration to the power 0.4.

It is hypothesized that both the average number of radicals per particle, $\bar{n}$, and also the total number of particles, N, are constant during interval II. If the volume fraction of monomer in the particles, ϕ_m, is assumed constant, the rate of polymerization would be constant because

all the other variables are constant, as described by Equation 3.46. However, as discussed earlier, the decrease of monomer concentration in the droplets results in the decrease of monomer concentration in the particles. Thus ϕ_m continues to decrease with increasing conversion. The rate of polymerization, therefore, is expected to fall continously and approach zero asymptotically as the monomer becomes depleted.

An equation for the average molecular weight for interval II may be determined assuming a constant volume fraction of monomer in the particles and for an average number of radicals per particle equal to 0.5. The volume rate of polymer production in a single growing particle is 2(dP/dt)/N. The factor 2 is required to take into account that only half of the particles are growing at any time. The average time interval between the entry of two radicals into a growing polymer particle is N/R and this is the time during which a single polymer chain grows. In this case the number average molecular weight will be:

$$\bar{M}_n = 2N_{Avo} \left[\frac{d_p}{R}\right]\left[\frac{dP}{dt}\right] \qquad (3.49)$$

If the value of dP/dt is substituted from Equation 3.46, the following equation results:

$$\bar{M}_n = K_p d_m \phi_m \left[\frac{N}{R}\right] \qquad (3.50)$$

Further substitution for the value of N from Equation 3.33 yields:

$$\bar{M}_n = 0.208\ k_p d_m \phi_m \left[\frac{A}{R}\right]^{0.6} \left[\frac{1}{K}\right]^{0.4} \qquad (3.51)$$

Finally, when the value of K is substituted Equation 3.51 becomes:

$$\bar{M}_n = 0.369\left[\frac{k_p d_m \phi_m A}{R}\right]^{0.6} \left[N_{Avo}\, d_p (1 - \phi_m - \phi_a)\right]^{0.4} \qquad (3.52)$$

This Equation indicates that for interval II, the number average molecular weight is proportional to the 0.6 power of the surfactant concentration and inversely proportional to the 0.6 power of the initiator concentration. Similar conclusions can also be drawn for interval I, where the number average molecular weight is obtained by substitution for K and N from Equations 3.32 and 3.33 respectively into Equation 3.43. Comparison of the number average molecular weights for intervals I and II, that is, Equations 3.43 and 3.50 shows that the average molecular weight value of interval I is 44% higher than that calculated for interval II. However, it is not likely that in reality the average molecular weight for interval I is higher than the interval II value. It is assumed for the calculation of $\bar{M}_n$ in interval I, that a particle grows from size zero. This assumption may

result in a serious error in the calculated value of $\bar{M}_n$. It can be said that according to the proposed model the $\bar{M}_n$ for interval II should not differ significantly from the interval I value.

The assumption taken for the above analysis includes the instantaneous termination of radicals inside the particles and the similar viscosities of the monomer and the additive. However, the addition of an additive may affect the viscosity of the reaction medium in the particles. The additive molecules surrounding a chain radical may affect the diffusion of a monomer molecule and another radical for the polymerization and the termination reactions, respectively. As discussed previously, at higher conversions and at high viscosities a particle may contain more than one free radical. The increase in the average number of radicals in the particles is expected to increase the rate of polymerization. The average molecular weight of polymer, which is indicated by Equation 3.48, is also expected to increase.

The proposed model will be employed to explain the effects of the addition of heptane and cyclohexane on the kinetics of emulsion polymerization of butadiene. The experimental results were obtained at constant temperature 10 °C. The analysis of the experimental results and the application of the proposed model are presented in Chapter 6.

Chapter IV

PROPERTIES OF MATERIALS

The useful properties of materials used in the present investigation are presented in various tables. The materials were obtained from different companies. The monomer, butadiene, of 99 mole% purity was purchased from Matheson of Canada, Limited. The cylinder pressure at 21 °C was 148 kPa. Butadiene was supplied containing an inhibitor (.01 to .02% tert-butycatechol) to prevent premature polymerization. The inhibitor was removed by scrubbing the gaseous butadiene with an aqueous sodium hydroxide solution. Subsequent drying with calcium carbonate removed vaporized water. The gaseous butadiene was condensed at -5 °C by means of a chilled solution of water and glycol circulating around the butadiene collection tube. The volume scale attached to the tube was used to measure the volume of liquified butadiene collected. Some of the physical properties of butadiene found useful in this work may be found in Table 2. Some of these properties were taken from the literature (68). The thermodynamic properties can be found in the Research Paper of National Bureau of Standard (69). The vapor-pressure-equation coefficients are presented in Table 3.

The surfactant, potassium laurate, having a specified purity of 95% was purchased from K and K Laboratories. Potassium laurate is highly soluble in water. Solubilities of potassium laurate are reported in the International Critical Tables by McBain (70). McBain reported that potassium laurate is so soluble that a solution having a concentration of less than 2 mol.kg^{-1} of water can not be salted out by potassium chloride at room temperature. At 50 °C the reported potassium laurate solubility is 8.5 mol.kg^{-1} of water. Bury and Parry (71) reported that dilute solutions of potassium laurate exhibit a tendency to deposit the acid soap. This tendency increases on standing and is favoured at low temperatures possibly because of carbon dioxide absorption. Therefore, fresh surfactant solutions were prepared when required for the experiments and were kept stoppered to limit carbon dioxide absorption.

Hydroperoxide-polyamine system was used as the initiator. Cumenehydroperoxide was purchased from K and K laboratories and tetraethylenepentamine was obtained from Eastman Organic Chemicals, Rochester. To prevent the coagulation of the emulsion latex, potassium hydroxide was added to keep the pH of the emulsion between 10 and 10.5. In a neutral or acid medium, the emulsion latex would coagulate. The heptane used was of 99+ mole% purity manufactured by Matheson Coleman and Bell. The physical properties of heptane used are presented in Table 4. The cyclohexane used had less than

0.005% nonvolatile matter and was from BDH Chemicals. Nitrogen was bubbled through each solvent for several hours. The solvents were then stored under nitrogen at room temperature until required for use. Nitrogen was also bubbled through the distilled water, used for the polymerization experiments. Polybutadiene samples were dissolved in tetrahydrofuran for measuring the molecular weight by Gel Permeation Chromatography.

Styrene of reagent grade was purchased from Eastman Kodak Company. It was further purified by vacuum distillation and was stored under nitrogen at -15°C until required for use. The physical properties of styrene are given in Table 5.

TABLE 2

Physical properties of butadiene (68)

Molar mass	54.09 $g.mol^{-1}$
Boiling point at 101.325 kPa	268.75 K
Freezing point at 101.325 kPa	164.24 K
Critical temperature	425.16 K
Critical pressure	4326.58 kPa
Enthalpy of vaporization	
at 298.16 K	384.36 $kJ.kg^{-1}$
at b.p. at 101.325 kPa	406.45 $kJ.kg^{-1}$
Solubility parameter at 298.16 K	14527.8 $J^{1/2}.m^{-3/2}$
Gaseous heat capacity, c_p	
at 273.16 K	1358.62 $J.kg^{-1}.K^{-1}$
at 298.16 K	1471.66 $J.kg^{-1}.K^{-1}$
at 373.16 K	1779.81 $J.kg^{-1}.K^{-1}$
Liquid density	
at 263.16 K	656.8 $kg.m^{-3}$
at 273.16 K	645.2 $kg.m^{-3}$
at 283.16 K	633.3 $kg.m^{-3}$
at 293.16 K	621.1 $kg.m^{-3}$
at 323.16 K	581.8 $kg.m^{-3}$
Gaseous molar volume	
at 277.16 K	21698.42 $cm^3.mol^{-1}$
at 298.16 K	23791.23 $cm^3.mol^{-1}$
at 323.16 K	25806.92 $cm^3.mol^{-1}$
Pitzer's acentric factor	0.195
Liquid viscosity	
at 277.16 K	0.50116 mPa.s
at 298.16 K	0.3967 mPa.s
at 323.16 K	0.3128 mPa.s

TABLE 3

Antoine vapor-pressure-equation coefficients (46)

$$\ln (p) = A - B/(T+C)$$

p in mm Hg and T in Kelvin

Component	A	B	C
Butadiene	15.7727	2142.66	-34.30
Styrene	16.0193	3328.57	-63.72
Heptane	15.8737	2911.32	-56.51
Water	18.3036	3816.44	-46.13
Cyclohexane	15.7527	2766.63	-50.50

TABLE 4

Physical properties of heptane (31,72)

Molar mass	100.20 $g.mol^{-1}$
Boiling point at 101.325 kPa	371.56 K
Freezing point at 101.325 kPa	182.56 K
Critical temperature	540.16 K
Critical pressure	2735.77 kPa
Enthalpy of vaporization	
at b.p. at 101.325 kPa	3165.22 $kJ.kg^{-1}$
Solubility parameter at 298 K	15243.94 $J^{1/2}.m^{-3/2}$
Molar volume	
277.16 K	143.35 $cm^3.mol^{-1}$
283.16 K	146.0 $cm^3.mol^{-1}$
298.16 K	147.0 $cm^3.mol^{-1}$
323.16 K	151.5 $cm^3.mol^{-1}$

* Molar Mass of Potassium Laurate ($C_{11}H_{23}COOK$)=238.272

TABLE 5

Physical properties of styrene (31,73).

Molar mass	104.14 $g.mol^{-1}$
Boiling point at 101.325 kPa	418.16 K
Freezing point at 101.325 kPa	242.56 K
Critical temperature	642.16 K
Critical pressure	3809.82 kPa
Solubility parameter at 298 K	19029.35 $J^{1/2}.m^{-3/2}$
Molar volume	
277.16 K	113.78 $cm^3.mol^{-1}$

Chapter V

EXPERIMENTAL EQUIPMENT AND PROCEDURE

Several sets of equipment were used in this research. A reactor was specifically designed to carry out emulsion polymerizations of butadiene. Auxiliary equipment for the reactor was designed to measure the heat evolved by the the reaction to determine the rate of polymerization. Polybutadiene samples were dissolved in tetrahydrofuran for analysis by means of gel permeation chromatography and infrared spectrophotometry for its molecular weight distribution and molecular structure respectively. Butadiene solubility and diffusivity in the liquid phase were measured in several solvents by means of the appropriate solubility and diffusivity apparatus. All of the equipment used and the experimental procedure followed are described in this chapter.

5.1 POLYMERIZATION REACTOR AND OPERATING PROCEDURE

Emulsion polymerization of butadiene was carried out in a batch reactor which was specifically designed to include the essential features of commercial reactors. The reactor was kept small, approximately 400 cm^3 in volume, for safety reasons. The main body of the reactor, as shown in Figure 5, was constructed of glass, stainless steel and teflon. The reactor was made of a three inch diameter QVF glass end

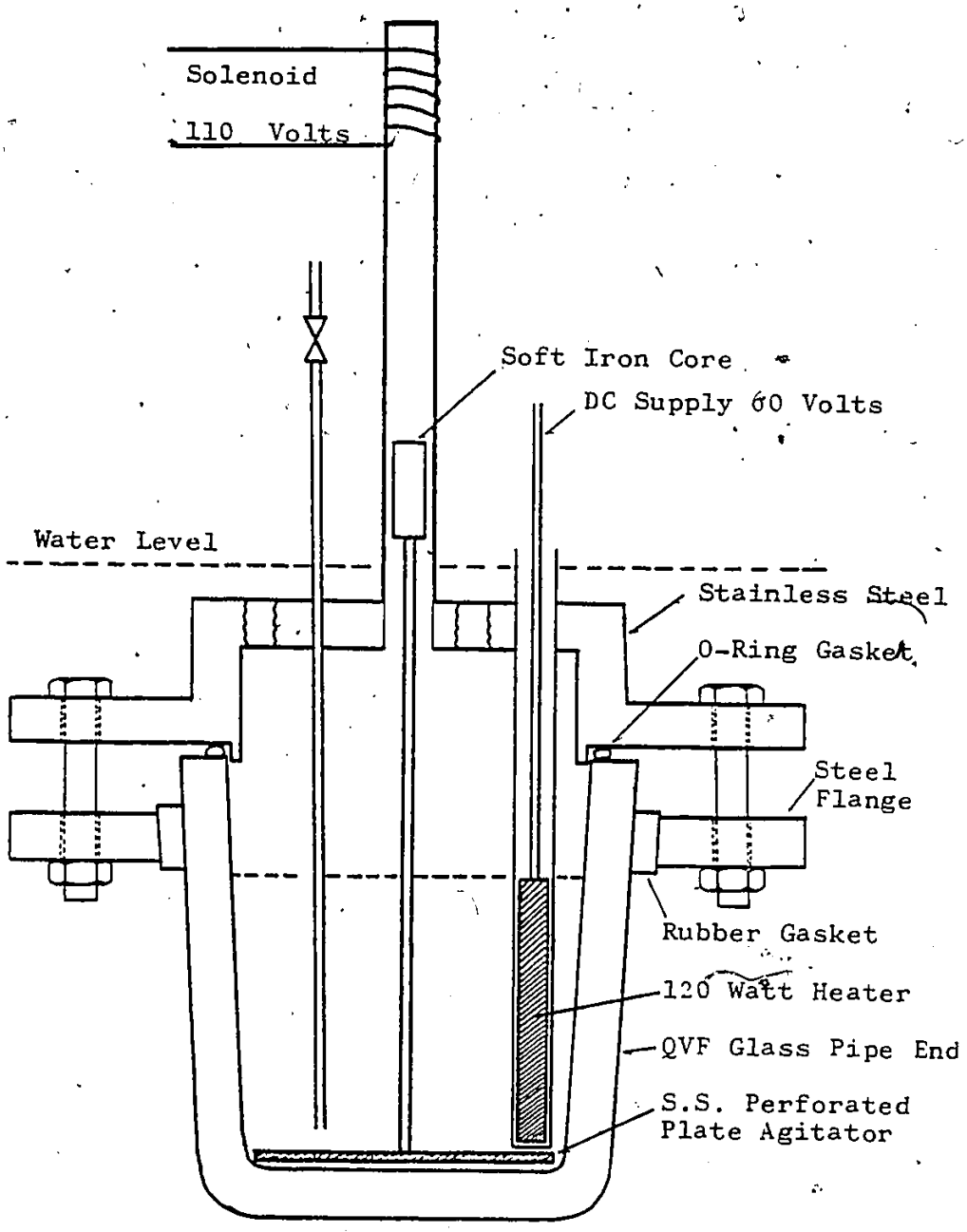

Figure 5 - Reactor details

buttress, topped by a machined stainless steel cover. The two pieces were bolted together using flanges with an O-ring forming the seal. The reactor was tested and found capable of withstanding pressure up to 690 kPa. There were two teflon valves from O.H. John's Scientific connected with the stainless steel top. These valves facilitated purging the reactor with nitrogen and for adding liquified butadiene.

The emulsion inside the reactor was agitated by means of a perforated plate agitator connected to a soft iron core with a stainless steel rod. The soft iron core housed in a 1/4-inch diameter stainless steel sheath was moved up and down by means of an external solenoid connected to a timer operating at one cycle per second. Thus, the agitator was especially a churn with the force for the downward stroke provided by the weight of the plunger. Initial trial runs determined that an agitation rate of one cycle per second was sufficient to form and maintain an emulsified mixture in the reactor.

A stainless steel thin walled tube of 3/8-inch diameter immersed in the emulsion, served as a heater sheath. A commercial heating element of 120 ohms resistance was inserted in the sheath, which was partially filled with oil to increase the rate of heat transfer from the heater to the sheath, and subsequently to the emulsion mixture. An additional stainless steel tube of 1/8-inch diameter was provided for injecting the initiator by means of a syringe. A rub-

ber septum was provided on the top of the tube for this purpose. Provisions were also made in the reactor cover for the insertion of a thermistor probe, and a pressure gauge for pressure measurement and a thermocouple for temperature measurement.

The auxiliary equipment was designed to use the reactor as a calorimetric reactor in that the rate of heat evolution during the polymerization could be measured. The principle involved in the design of the calorimetric reactor involved the use of a cooling device which was capable of removing all of the heat of polymerization. In conjunction with the cooling device was included a small auxiliary heater which could provide a quantity of heat comparable to that from the reaction and hence maintain a constant temperature in the reactor even when there was no reaction. Hence, when a reaction was in progress, the reduction in heat produced by the heater was equivalent to that produced by the reaction. This type of calorimetric reactor had been previously utilized by Laudie (74). Details of the equipment are now presented. During operation the reactor was immersed in a vessel with constant temperature water flowing around it, as shown in Figure 6. Water at 7 °C was pumped from a constant temperature bath into the bottom of the vessel through a rotameter. The rotameter was used to continuously check and maintain a constant flow rate. The water flowed up and around the reactor and overflowed back into the constant temperature bath.

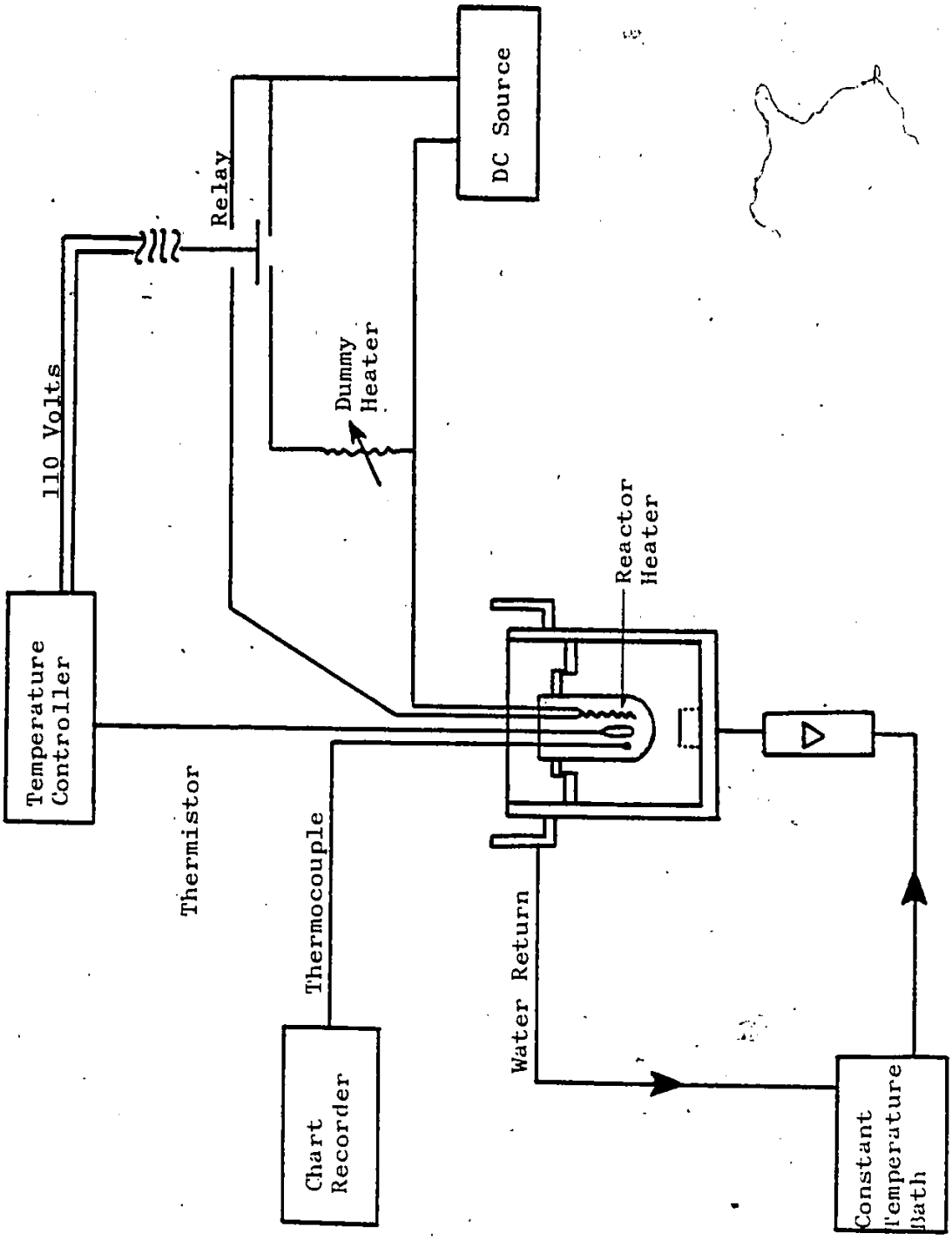

Figure 6 -- Reactor temperature control circuit

This arrangement assured a constant external heat transfer coefficient at the reactor wall. The thermistor probe installed within the reactor was connected to a thermotrol unit from the Precision-Scientific company which was operated as an on-off temperature controller, and which was set at the reaction temperature of 10 °C. The reaction temperature was controlled to ± 0.01 °C. The load output of the controller which normally is connected to a heating element was instead connected to a solenoid coil of a relay. When the solenoid coil was energized the relay connections were made between the internal heating element and a 60 volt DC source. The DC source was in fact a rectifier and voltage regulating device purchased from Trygon Electronics. The combination of heat produced by the heater and by the reactor was designed to keep the reaction mixture exactly at the reaction temperature. When the controller was off, the current was directed through a dummy heater which had the same resistance as the internal heater.

In addition, a system of timing clocks was arranged to measure the on and off time for the internal heating element and so to determine the heat generated by the reaction. A schematic diagram for the timing system is shown in Figure 7, and for the electronic circuit in Figure 8. The timers used were of the digital type from Automatic Timing and Controls, having an elasped time range of up to 9999.9 seconds and specified to have an accuracy of 0.011 seconds per oper-

ation. The time relays of 1 to 10 minutes and of 3 to 30 minutes were purchased from Agastat Company. The circuit was designed to measure electrically the heat evolved by the polymerization reaction over a short time interval (10 minutes) and to repeat this measurement every 20 minutes so that an almost continuous record of heat evolved could be obtained. When in operation, the total on-timer indicates the cumulative time the heater remains on, whereas, the on-timer and off-timer indicate the duration of time the heater remains on and off respectively in 10 minute interval.

The procedure for determining the heat evolved by the reaction involved initially charging all the components except the cumenehydroperoxide into the reactor and bringing the mixture to the reaction temperature. The monomer was liquified and mixed with an additive (heptane or cyclohexane) before charging into the reactor. The rate of heat supplied by the internal heater to maintain the reactor content at 10 °C, without reaction, was then determined by measuring the fraction of on-time of the internal heater for a ten minute interval (one beginning every 20 minutes). The rate of heat addition without reaction was used as a basis for the determination of the rate of heat generation by the polymerization reaction. When the initiator was added, the heat of reaction was estimated from the decrease in heating time required and the rate of electrical energy supplied to the heater. The heat requirement without reaction was expected

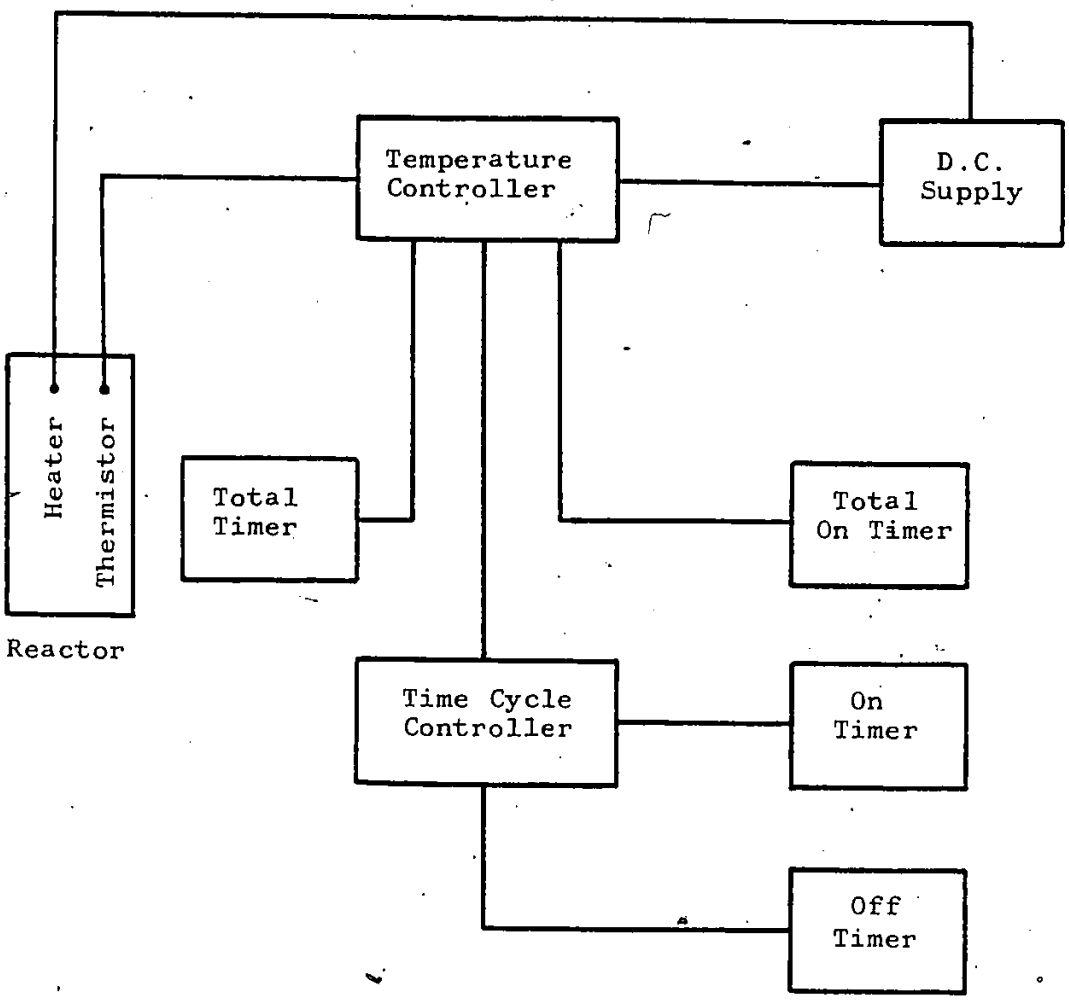

Figure 7 - Schematic diagram of isothermal kinetic calorimeter

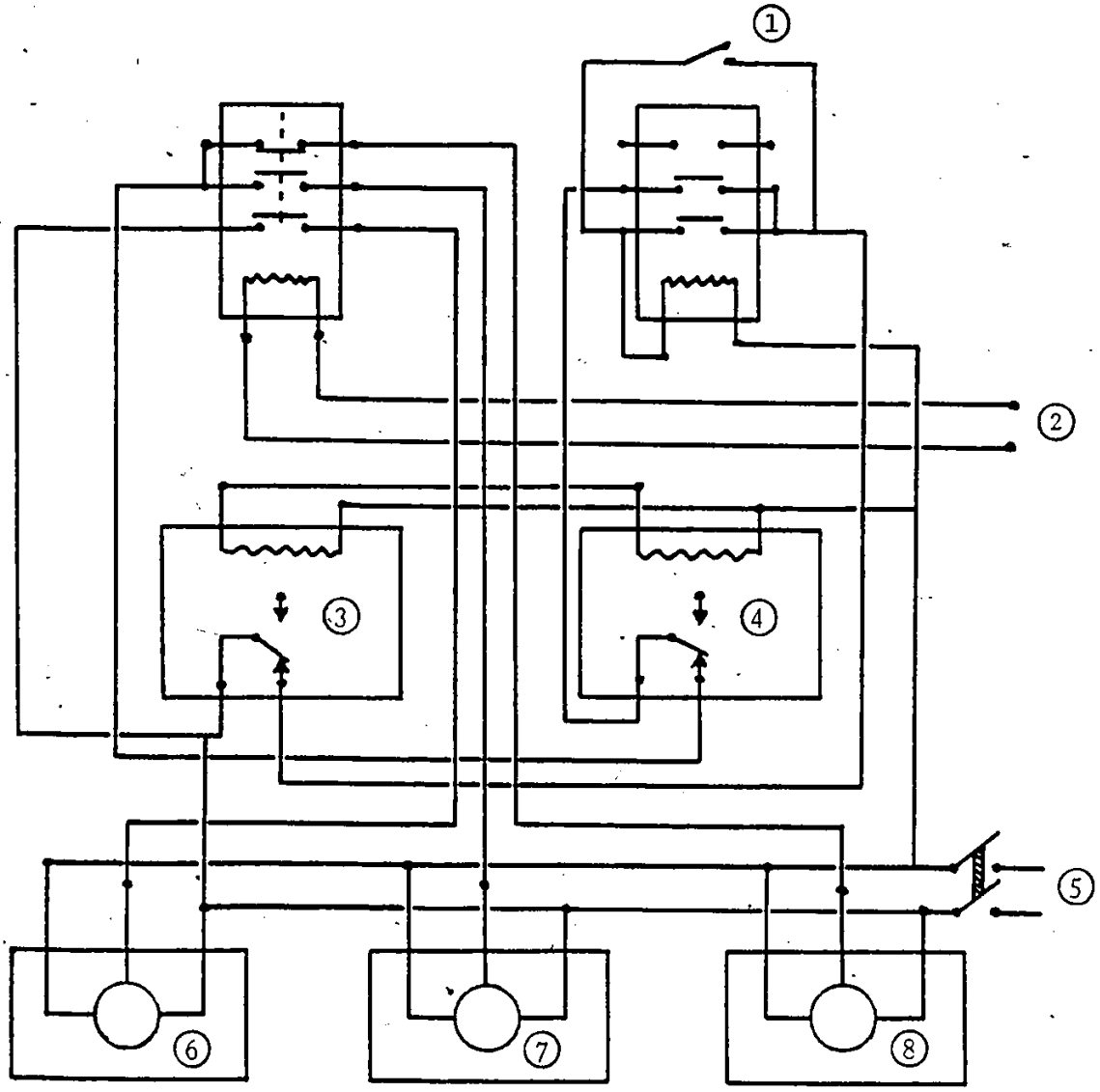

1) Push Button
2) To Temperature Controller
3) Time Relay, 3-30 min
4) Time,Relay, 1-10 min
5) 110 Volts Supply
6) Total On Timer
7) On Timer
8) Off Timer

Figure 8 - Electronic circuit

to change with conversion during polymerization as the specific heat of the latex was different from that of the original emulsion. Therefore, to determine the variation of required steady state rate of heat input with conversion, the reaction was stopped at different conversions by injecting shortstop and the steady state rate of heat input was measured. During polymerization heat was supplied by the internal heater as well as by the reaction. The sum of these two was considered to be equal to the steady state rate of heat input. The conversion during polymerization was estimated from a knowledge of the cumulative heat generated by the reaction and by using the heat of polymerization of butadiene of 75.36 $kJ.mol^{-1}$ (75). The method used for calculating the conversion was the same as that used by Anderson (76,77) and by Laudie (74). The rate of heat evolved from the reaction, in watts, is related to the polymer production rate by the following equation:

$$\bar{r}_p = (10^{-3})\ M_m\ [\frac{W_R}{\Delta W_p}] \qquad (5.1)$$

The basic recipes used in this research are reported in Table 6. The solvent quantity added was calculated on the basis of butadiene solubility in the solvent, so that the complete amount of butadiene could be dissolved in the solvent. Thus, the polymerization in the presence of the sol-

vent could be performed at atmospheric pressure. The butadiene was completely mixed with the solvent before charging into the reactor. The potassium laurate and initiator concentrations were varied by a factor of two about this standard recipe. The ratio of cumenehydroperoxide to tetraethylenepentamine was always kept constant during initiator concentration variations.

The experiments were started by putting all of the ingredients of the recipe into the reactor, except for the butadiene and associated solvent, if any, and the cumenehydroperoxide. The reactor was closed and submerged in the coolant recirculation vessel. Next, the reactor was tested for leaks by means of nitrogen pressure applied to the reactor. The nitrogen was first vented then evacuated before the butadiene and associated solvent were charged into the reactor. The agitator was then started and the temperature inside the reactor was recorded. When the reaction temperature was obtained, the timing system was started to measure the heat supplied by the internal heater. Finally cumenehydroperoxide was injected to start the polymerization, and the timing system was used to determine the heat evolved by polymerization as described before.

When the desired conversion was reached, shortstop (hydroquinone and hydrogenperoxide) was injected into the reactor to stop the reaction. The reactor was removed from the vessel and the excess butadiene was slowly vented. Finally,

nitrogen was bubbled in the reactor to remove any residual dissolved butadiene. The reactor was dismantled and, before coagulating the latex with sodium chloride solution and sulfuric acid, the antioxidant N-Phenyl-2-Naphthylamine was added. The antioxidant was found necessary to prevent any molecular weight change of the polymer during the drying and solution processes prior to analysis. The polybutadiene obtained was filtered and thoroughly washed with distilled water to remove soap, sodium chloride and other chemicals. The product was vacuum dried in a dessicator until constant weight was achieved before it was finally dissolved and analyzed.

TABLE 6

Recipe for emulsion polymerization of butadiene

Component	Recipe A, (g)	Recipe B, (g)
Butadiene	100.0	100.0
Water	180.0	180.0
Potassium laurate	5.0	5.0
Potassium hydroxide	0.112	0.112
Potassium chloride	0.8	0.8
Cumene hydroperoxide	0.21	0.21
Tetraethylenepentamine	0.40	0.40
Heptane/Cyclohexane	-	85.0 to 222.0

5.2 ANALYTICAL INSTRUMENTS AND OPERATING PROCEDURE

The polybutadiene samples prepared under different conditions were analysed by Gel Permeation Chromatography (GPC), and Infrared Spectrophotometry for the determination of their molecular weight, and molecular structure, respectively. The samples were dissolved in tetrahydrofuran for analysis. The instrument used for GPC was a high pressure liquid chromatograph supplied by Waters Associates. The Microstyragel columns were used as recommended by Waters Associates. The columns were 30 cm long and 0.8 cm in internal diameter. The packing material used was a fully porous and highly cross-linked styrene-divinylbenzene copolymer having a particle size of 10 microns. The column packing was specified to have a solid volume of 20%, a pore volume of 40% and an interstitial volume of 40%. A single column of 30 cm in length was specified to provide 3000 theoretical plates for the separation of polymer of different molecular weights.

The principle of operation of the GPC was discussed in Section 2.7. Polystyrene standards from Waters Associates were used for calibrating the GPC. The universal calibration curve of log ($[\eta]M$) versus retention volume was obtained. This calibration curve is shown in Figure 36 in Appendix E. The Mark-Houwink coefficients used for polystyrene (78), and for polybutadiene (79), are given in Equations 5.2, and 5.3, respectively:

$$[\eta] = 1.25(10^{-4})M^{0.713} \qquad (5.2)$$

$$[\eta] = 2.27(10^{-4})M^{0.75} \qquad (5.3)$$

An Infrared Spectrophotometer used for the determination of polybutadiene structures was originally purchased from Perkin Elmer (model 267) . Sodium chloride cells were used for analysis. The wave lengths assigned to trans-1,4 and vinyl structures were 10.3 and 11.0 μm. These values were taken from the literature (32). A wave length of 13.8 μm was found to be characteristic of the cis-1,4 structure by analysing the cis-1,4 polybutadiene sample obtained from Polysar Limited. The operating procedure and the calculation for the analysis has been discussed by Godon (80).

5.3 SOLUBILITY APPARATUS AND OPERATING PROCEDURE

The apparatus used to measure the butadiene solubility in heptane, in styrene-heptane mixtures, in water and in aqueous surfactant solutions at atmospheric pressure was essentially of the same design as that described by Hayduk and Chang (81). The apparatus used is shown in Figure 9. It consisted mainly of a gas burette, a contacting chamber in the form of a glass tube spiral, a small manometer and a solvent burette all enclosed in a glass jacket through which water at constant temperature was circulated. The gas burette at its lower end was connected with tygon tubing to a bottle

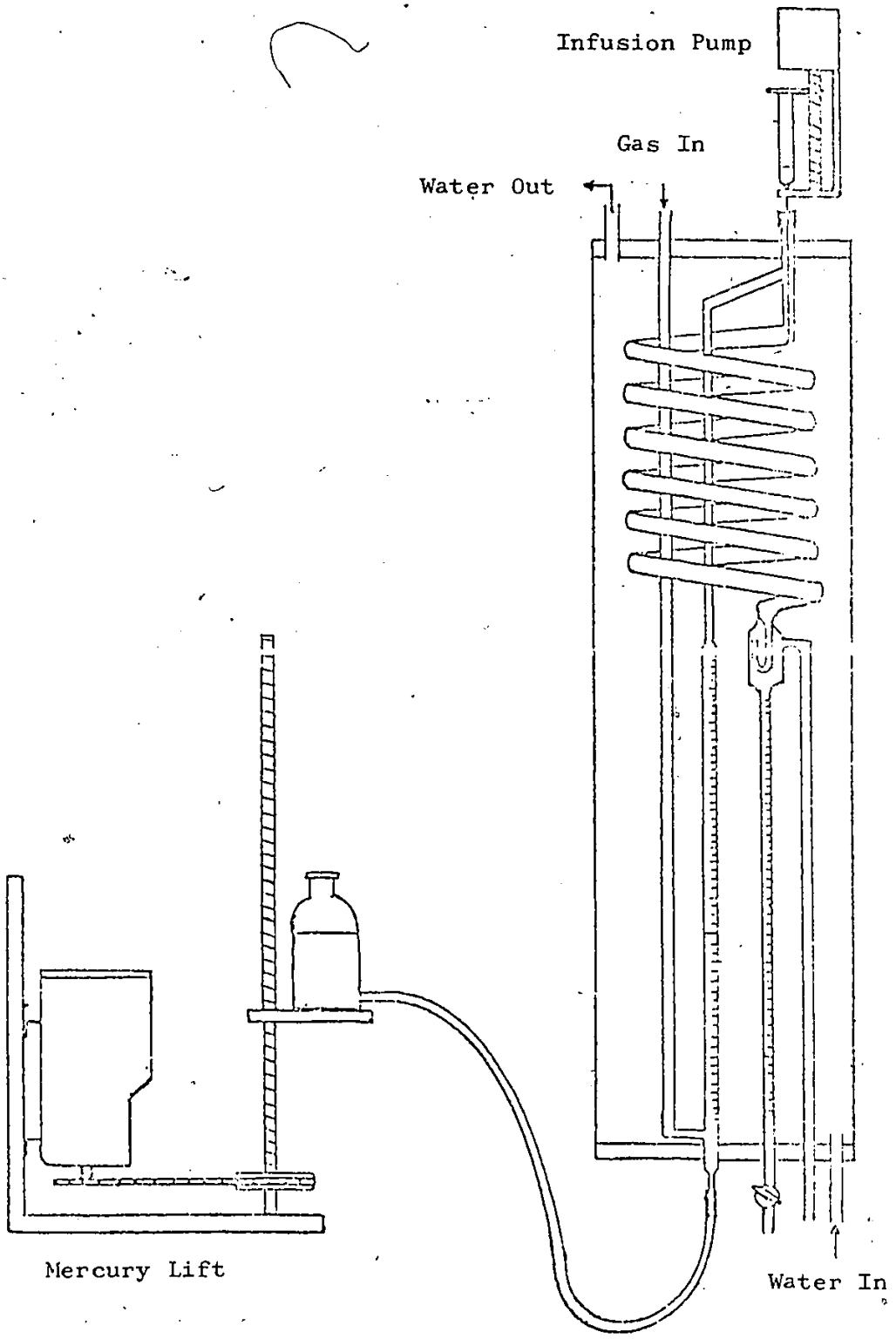

Figure 9 - Solubility apparatus

filled with mercury. The mercury filled bottle could be raised by means of a rotating threaded shaft, chain-driven by a variable-speed motor. The top end of the glass spiral was closed with a rubber septum. The solvent was brought into the contacting chamber through the rubber septum by the use of a syringe attached to a syringe pump.

The solubility apparatus used for measuring the butadiene solubility in heptane at 25 and 50°C, contained a gas burette of 100 cm^3 in capacity with graduations of 0.1 cm^3 and a solution burette of 5 cm^3 in capacity with graduations of 0.01 cm^3. Deaerated solvent was supplied by means of a Harvard Apparatus syringe pump equipped with a 20 cm^3 gas tight Hamilton syringe. The solvent flow rate was kept constant with a motor of 1/10 rpm and 1/20 rpm for the syringe pump for solubility measurements at 50°C , and for 25°C , respectively.

Preliminary measurements for the solubility, at 4°C and atmospheric pressure, of butadiene in heptane and styrene-heptane solutions indicated that the solubilities were very high. In this case, another solubility apparatus was constructed with a gas burette of 250 cm^3 capacity graduated in 0.5 cm^3 divisions and with a solution burette of 5 cm^3 capacity graduated in 0.01 cm^3 divisions. The solvent was injected with a 10 cm^3 gas-tight Hamilton syringe using a motor speed of 2 rph.

On the other hand, the solubility of butadiene in water and surfactant solutions at 4 °C and atmospheric pressure was low. The solubility apparatus used in this case had a gas burette of 5 cm^3 capacity graduated in 0.01 cm^3 divisions and a solution burette of 10 cm^3 capacity graduated in 0.02 cm^3 divisions. The syringe used was 20 cm^3 in volume while the motor speeds used were 1/2, 1/4 and 1/5 rpm. The volumetric infusion rates for the different motor speeds were accurately determined by weighing the quantities of distilled water discharged in a certain time interval.

Constant temperature water at 25 and 50 °C was circulated through the jacket of the solubility apparatus by a bath circulator. The bath was controlled to within ± 0.05 °C of the set temperature. The water was replaced by water-glycol solution for the experiments at 4 °C. A Neslab refrigeration unit was used for cooling the antifreeze solution in the circulating bath when required.

The procedure for measuring gas solubility has been described in detail by Hayduk and Chang (81). The degassing apparatus used for deaerating the solvent, is shown in Figure 10. Calibration plots were prepared to determine the composition of degassed solvent for styrene-heptane mixtures. Calibration plots were obtained by measuring the density and refractive index of solutions of known composition and are shown in Figures 34 and 35 in Appendix C. The calibration data, tabulated in Table 14 in Appendix C, were obtained by weighing different proportions of heptane and

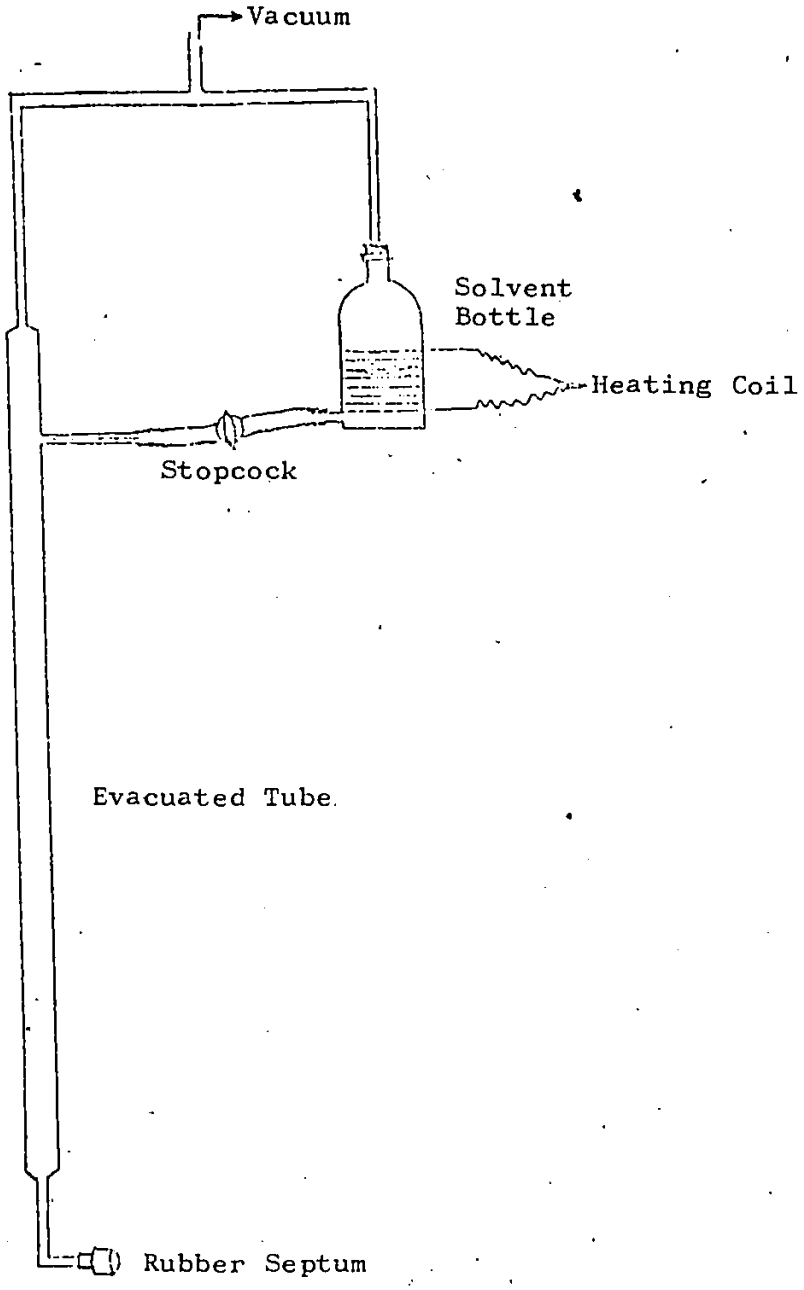

Figure 10 - Degassing apparatus

styrene, mixing them and measuring their refractive indices and densities at 25 °C.

5.4 DIFFUSIVITY APPARATUS AND OPERATING PROCEDURE

Diffusivities of dissolved butadiene were measured at various temperatures using the steady state capillary cell method originally described by Malik and Hayduk (82). A diffusion cell, consisting of a capillary sealed in a closed reservoir which could be filled with degassed solvent by means of two valves located on either side of the reservoir is shown in Figure 11. The end of the capillary in the reservoir was conically ground to facilitate the dissipation of solute. The capillary used was of 1 mm diameter for the measurement of the butadiene diffusivities. Whereas diffusivities in heptane at 25 and 50 °C were measured without difficulty, the measurement of butadiene diffusivity at 4 °C, caused a great deal of experimental difficulty. The liquid level in the capillary continued to increase, due to high solubility of butadiene in heptane at 4 °C and made it impossible to take reliable volume readings. On the other hand the bead movement in case of water as solvent was extremely slow for a 1 mm diameter capillary. Another cell was made having two capillaries, one attached to the other. The top capillary was of 0.6 mm in diameter and lower capillary was of 1.5 mm in diameter. Again the movement of bead in the capillary remained extremely slow and no reliable diffusivity for butadiene in water was obtained.

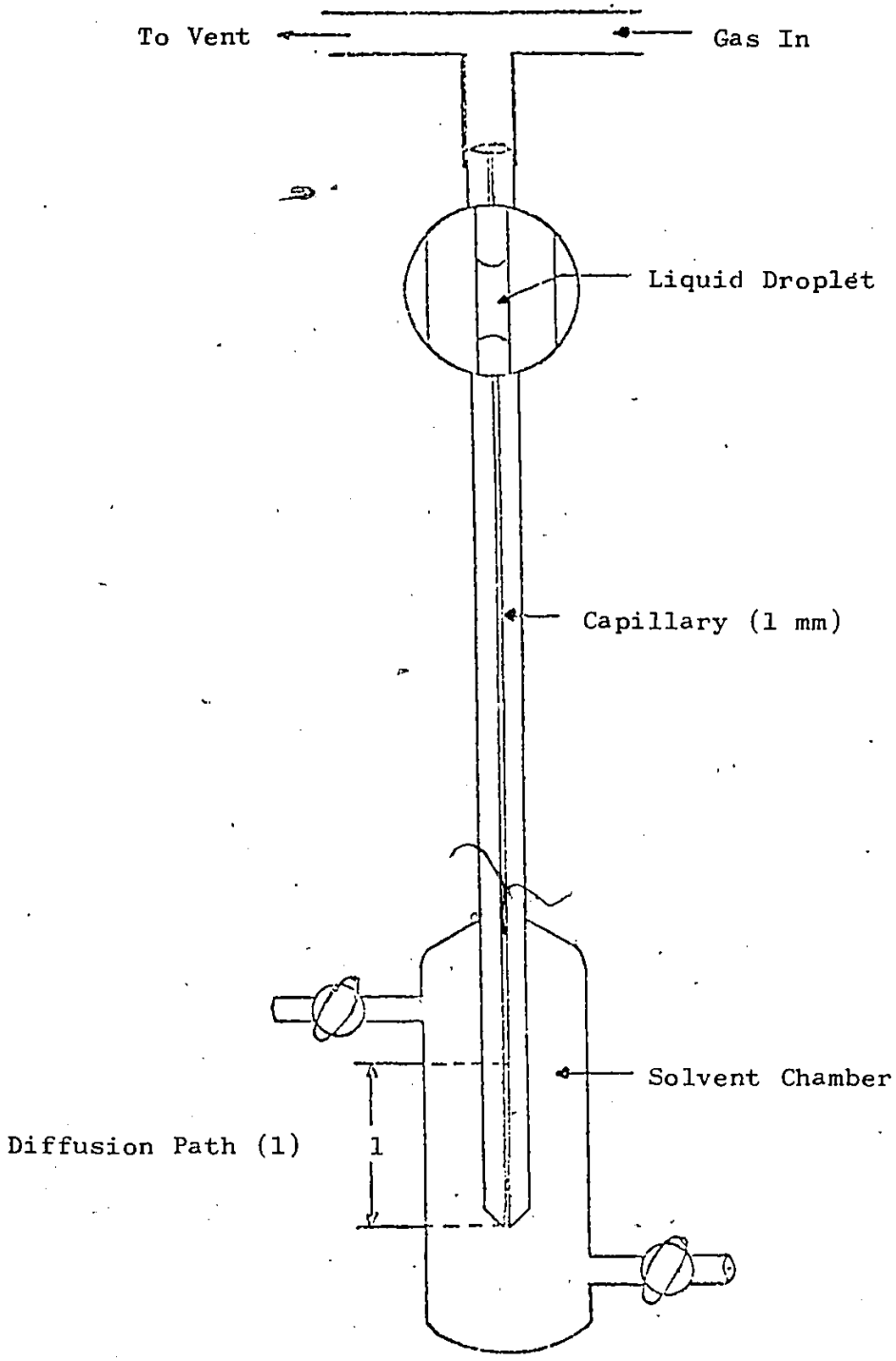

Figure 11 - Diffusivity cell

5.5 EQUIPMENT FOR MEASURING LIQUID VISCOSITIES AND DENSITIES

Two additional laboratory devices were used for measuring the physical properties of soap solutions at various concentrations. Solution viscosities were measured with calibrated Cannon-Fenske viscometry tubes immersed in a constant temperature bath. An Anton Paar Model DMA 02C digital precision densitometer was used to measure the solution densities. This instrument utilized a vibrating reed, the frequency of which was related to the density of the fluid in which the reed was immersed. The instrument required calibration with two fluids of accurately known density, usually dried air and distilled water. The calibration constant, B, was obtained from the fluid densities and corresponding vibration frequencies:

$$d_A - d_B = \frac{1}{B}\left(T_A^2 - T_B^2\right) \qquad (5.4)$$

The instrument was capable of providing densities to at least four-figures accuracy if the cell temperature is controlled to ± 0.001 °C. For calibration purposes densities of dried air and deaerated water were obtained from Weast (83) and Perry et al. (84) respectively.

Chapter VI

RESULTS AND DISCUSSIONS

The presentation and discussion of the experimental results has been separated into various sections. Section one deals with the determination of the properties of aqueous surfactant solutions and latices. The solution and transport properties of dissolved butadiene, its solubility and diffusivity in certain solvents are discussed in section two. In the third section, the results are presented for the effects of nonreactive liquid additives on the kinetics of emulsion polymerization of butadiene. In this section a discussion is also included for the effects of the variation in surfactant and initiator concentrations on the kinetics of the emulsion polymerization of butadiene in the presence of nonreactive solvents. These results are discussed on the basis of the theoretical model developed earlier. Limitations in utilization of the model developed, as well as its possible uses are discussed in the third section. Finally, in the last section the results of the development of several diffusivity correlations are discussed.

6.1 CRITICAL MICELLE CONCENTRATION OF POTASSIUM LAURATE

It was useful to determine the cmc of potassium laurate while studying the kinetics of emulsion polymerization of butadiene. The surfactant concentration was always kept above cmc to ensure micelle formation. Three types of cmc values have been reported by Sata and Tyuzyo (85) and by Hess et al. (86). The first corresponds to a change from dilute homogeneous molecular solution to one containing surfactant clusters or dispersed micelles. The second corresponds to the change to an ordered micelle structure, and the third corresponds to the start of micelle crowding. In this work, only the first cmc was considered to be of importance because of the solubilizing effect of the micelles for butadiene even at relatively low surfactant concentrations.

Two properties of potassium laurate solutions were measured at 4 °C in order to determine the cmc. The viscosities and densities of potassium laurate solutions may be observed to have a measurable change in behaviour at the cmc. When the experimental results are inspected, it is apparant that the value of the cmc, that is the most reliable, is that obtained from a reduced viscosity versus concentration plot as shown in Figure 12. The value of the cmc for potassium laurate at 4 °C was determined as 2.5 $g.dm^{-3}$. The viscosity data are given in Table 9 of Appendix A. The variation of density of potassium laurate solutions with concentration is also shown in Figure 12. The density-concentration relation

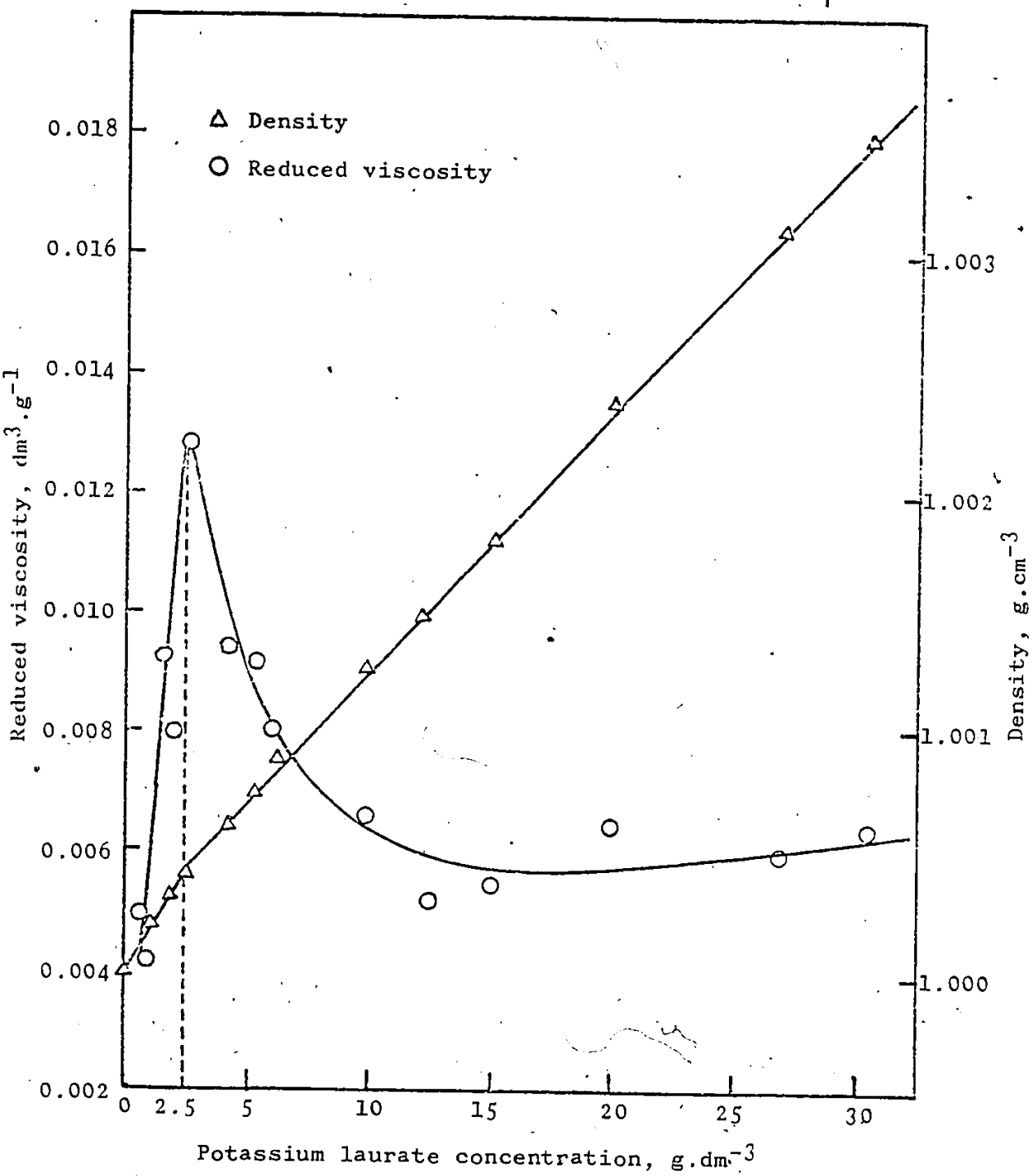

Figure 12 - Density and reduced viscosity of potassium laurate solutions at 4 °C

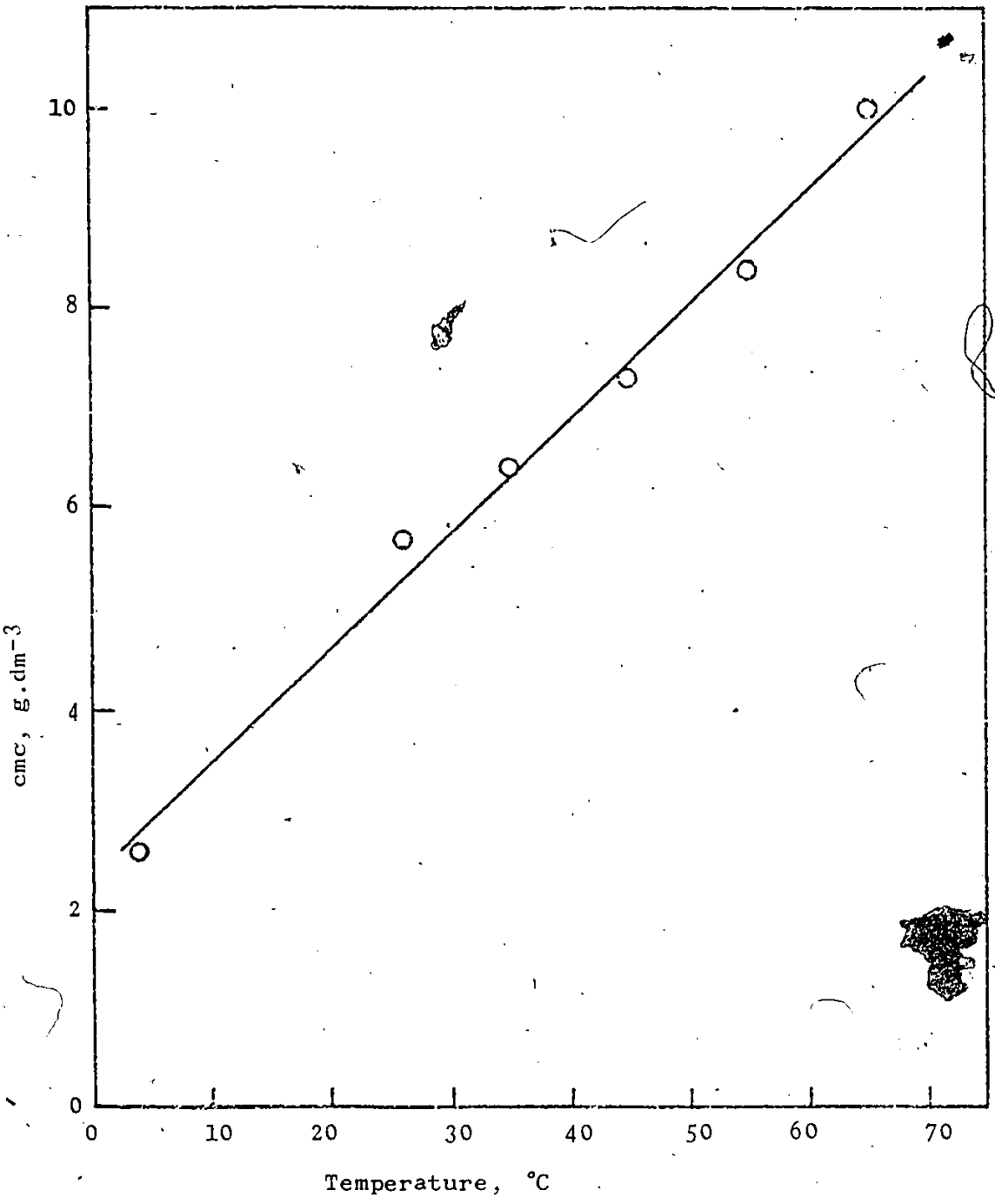

Figure 13 - Temperature versus critical micelle concentration

is observed to have an inflection at the cmc of 2.5 $g.dm^{-3}$. The density data are also given in Table 9 of Appendix A.

No published data for the cmc of potassium laurate at low temperatures was found in the literature. Harkins (87) reported the cmc for potassium laurate at 26°C. At higher temperatures, the cmc for potassium laurate was reported by Klevens (88). Both the experimental and the literature values of the cmc versus temperature is shown in Figure 13. It may be noted that the cmc increases with increasing temperature. The values of the cmc at various temperatures are given in Table 10 of Appendix A.

6.2 SOLUBILITY AND DIFFUSIVITY OF BUTADIENE

It is useful to know the solubility and diffusivity of butadiene in water, in aqueous surfactant solutions and non-reactive solvents. The solubility of butadiene in heptane at various temperatures and at atmospheric pressure expressed as the mole fraction and Ostwald coefficient is presented in Table 11 of Appendix B. Butadiene is highly soluble in heptane even at atmospheric pressure. The logarithm of solubility in mole fraction versus the inverse of the absolute temperature is shown in Figure 14. Butadiene solubility calculated from Raoult's law and the regular solution theory is also shown in Figure 14. It may be noted that butadiene solubility in heptane at low temperatures is close to the predicted value based on Raoult's law and the regular

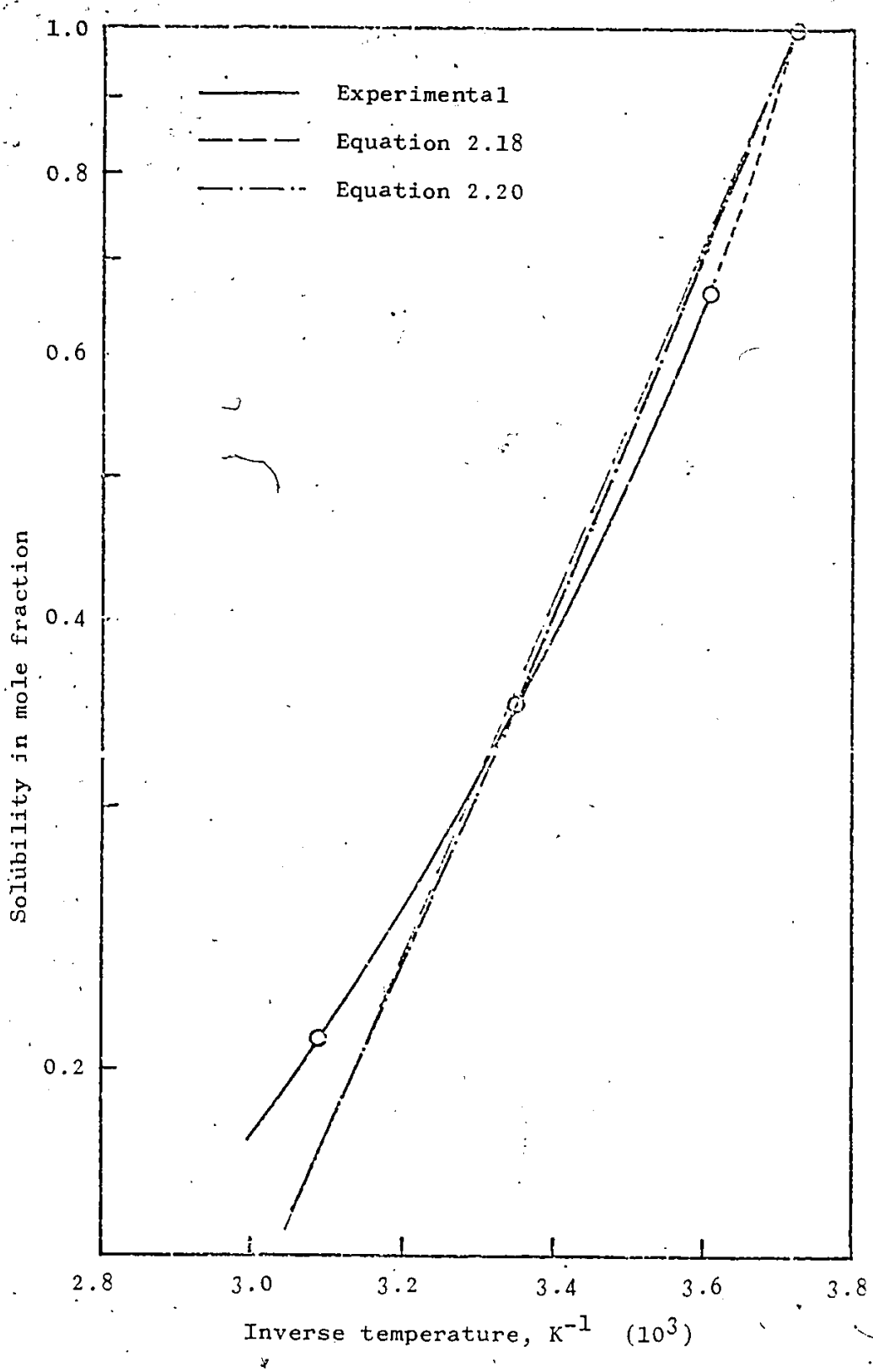

Figure 14 - Solubility of butadiene in heptane at various temperatures

solution theory. Deviation between predicted and experimental values increases with increase in temperature. Hayduk and Castaneda (89) obtained similar results while studying butane solubility in paraffin solvents particularly in hexane and in heptane. Thus, Raoult's law and the regular solution theory are occasionally useful in predicting solubilities but even then probably only for very high solubilities in nonpolar solvents. Predicted and experimental values of butadiene solubility in heptane is given in Table 12 of Appendix B.

The solubility of butadiene in water and in aqueous potassium laurate solutions, at 4 °C and atmospheric pressure, is shown in Figure 15. It may be noticed that the solubility of butadiene in water is extremely small. As discussed in Section 2.3, the function of surfactant is to increase the amount of butadiene dissolved in the liquid phase. The quantity of butadiene above its solubility in water is held in the micelles, which are formed when potassium laurate concentration exceeds the cmc. It is noted from the experimental results that the solubility is increased considerably with an increase in potassium laurate concentration. Klevens (42) also observed that the solubilizing power of a soap increases quite sharply as its concentration is increased. He studied the solubilization of ethylbenzene in aqueous solutions of various n-alkanoates. Stearns et al. (45) provided evidence that the increase in solubility in the surfactant solutions is associated with the presence of an

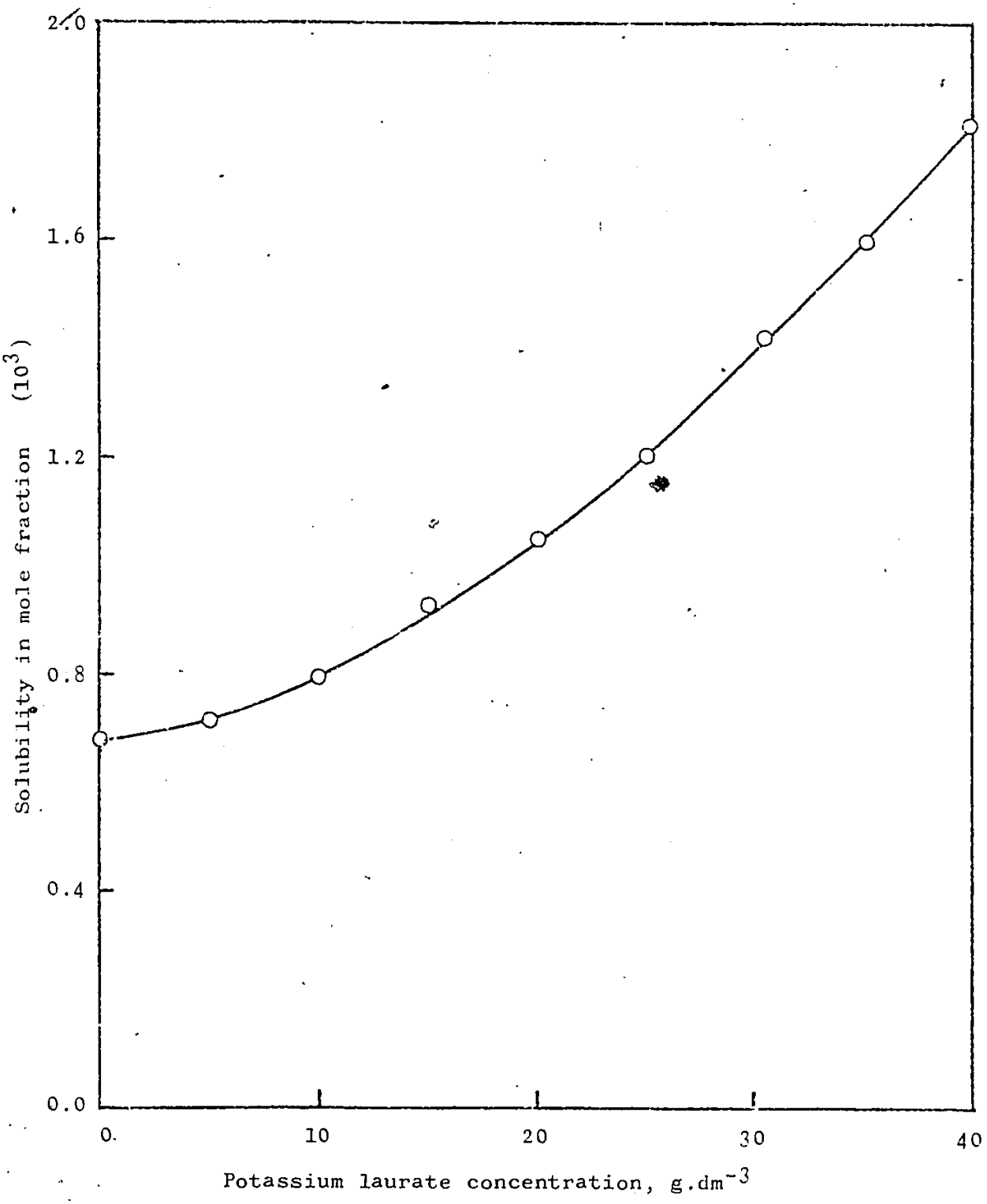

Figure 15 - Solubility of butadiene in potassium laurate solutions at 4 °C

increasing number of micelles, and so is interpreted as being the result of imbibition within the micelles. The ratio of solubility of butadiene in surfactant solutions, x_s , to that in water, x_w , versus surfactant concentration is shown in Figure 16. The solubility increases almost three fold at a potassium laurate concentration of 40 $g.dm^{-3}$. Hall and Pethica (90) suggested that, at saturation concentration of the monomer, the amount of monomer solubilized increases linearly with the total concentration of the surfactant. However, the experimental results show that the amount of butadiene solubilized does not increase linearly with the amount of potassium laurate in solution. Stearns et al. (45) reported a similar observation while reporting the solubilization of other hydrocarbons in potassium laurate solutions. Tabulated values for butadiene solubilities in surfactant solutions are listed in Table 13 of Appendix B.

The solubility of butadiene in styrene-heptane mixtures at 4 °C and atmospheric pressure was also measured. These measurements were not of direct relevance to the present investigation, but would be useful while studying the effect of heptane on emulsion copolymerization of styrene-butadiene. The solubilities of butadiene in the mixed solvents are shown in Figure 17 expressed as Ostwald coefficient. It may be seen from Figure 17 that butadiene is highly soluble in styrene-heptane mixtures and the solubility reaches a maximum at a mole fraction of 0.8 for styrene . The

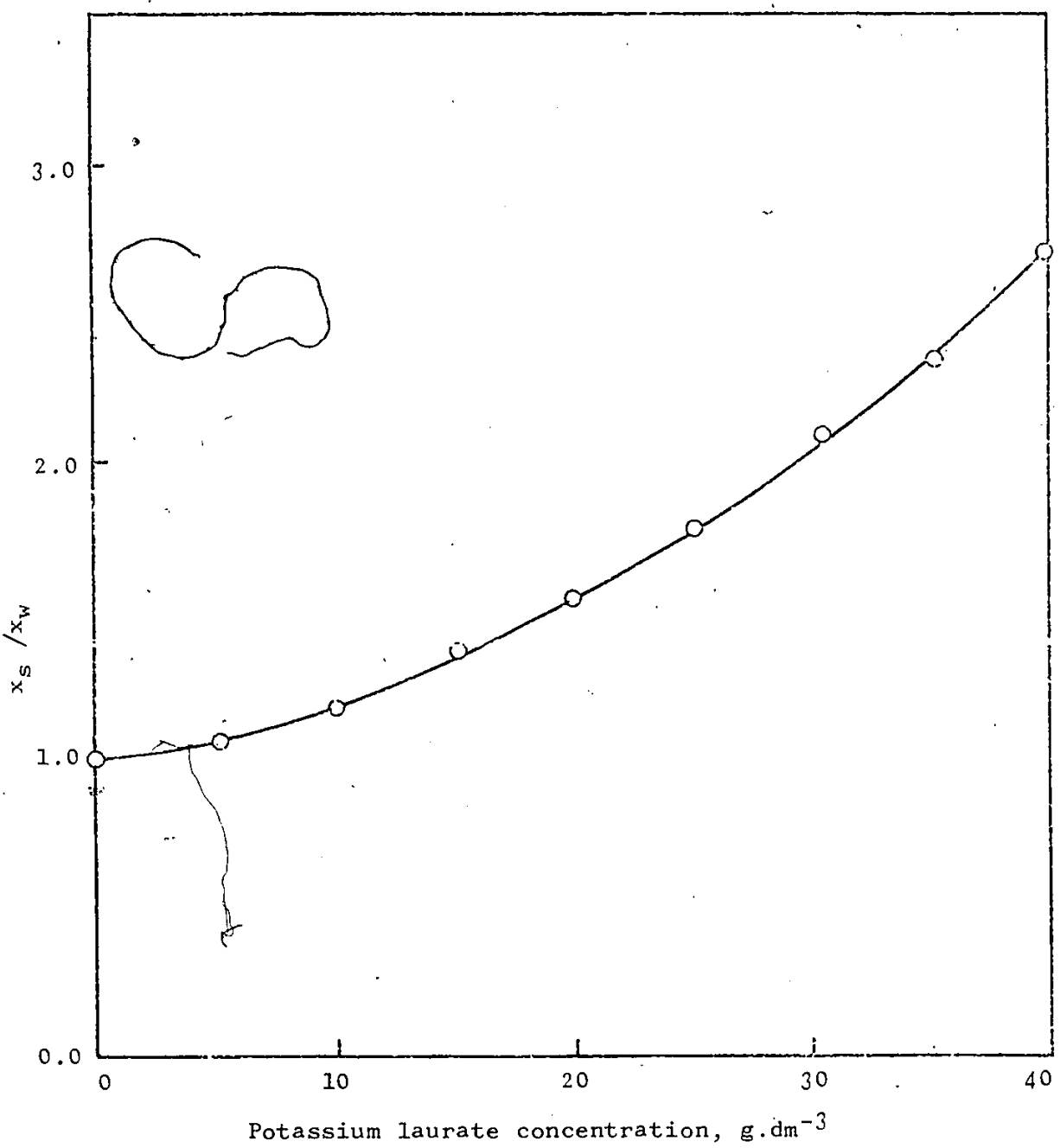

Figure 16 - Solubilization of butadiene in potassium laurate solutions at 4 °C

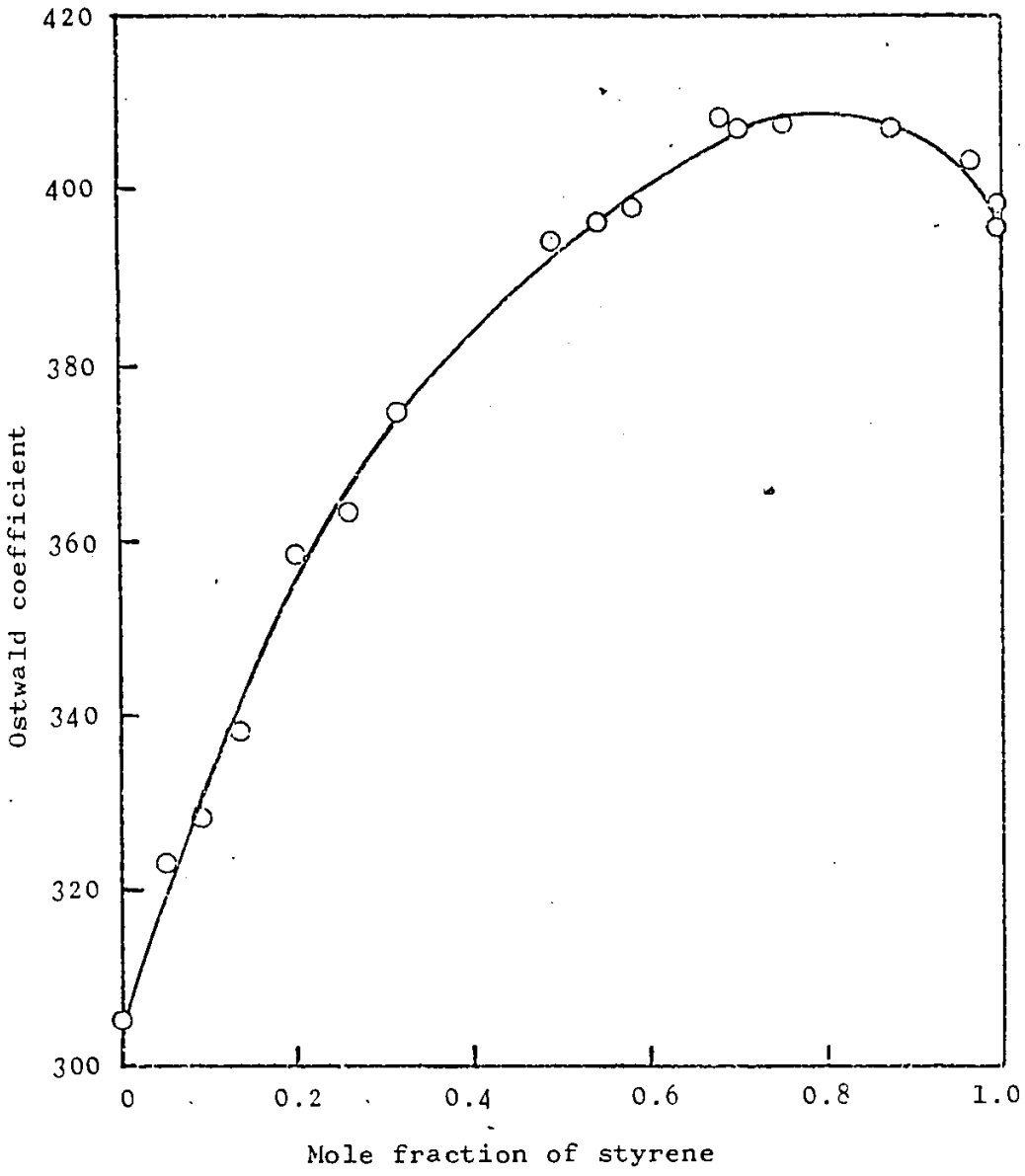

Figure 17 - Butadiene solubility in styrene-heptane mixtures at 4 ℃

numerical data of butadiene solubility in styrene-heptane mixtures is reported in Table 15 of Appendix C. The experimental values of solubilities were compared with the values predicted by means of Raoult's law, the regular solution theory and other equations discussed in Section 2.8.1. The comparison data is presented in Tables 16 and 17 of Appendix C and graphically shown in Figure 18. It may be observed that Equation 2.20 of the regular solution theory is a better approximation of the experimental values as compared to Raoult's law and Equation 2.21. However, large error may be noticed when predicting butadiene solubility in styrene by means of the regular solution theory. Equation 2.24 which is for ideal solvent mixtures, gives a good approximation of the actual butadiene solubility for styrene-heptane mixtures. However, when the binary interaction constant is added to take into account the nonideality of the mixture, that is when Equation 2.25 is used, the deviation of predicted values from the experimental values increases. The binary interaction constant was calculated from Equation 2.26 assuming styrene and heptane as nonpolar solvents. This assumption might have resulted in a larger deviation. The binary interaction constant was estimated empirically to represent the solubility data with minimum error. The estimated value of the constant is 0.17 as compared to 0.8 estimated by assuming styrene and heptane as nonpolar solvents. The predicted values by using the value of binary constant

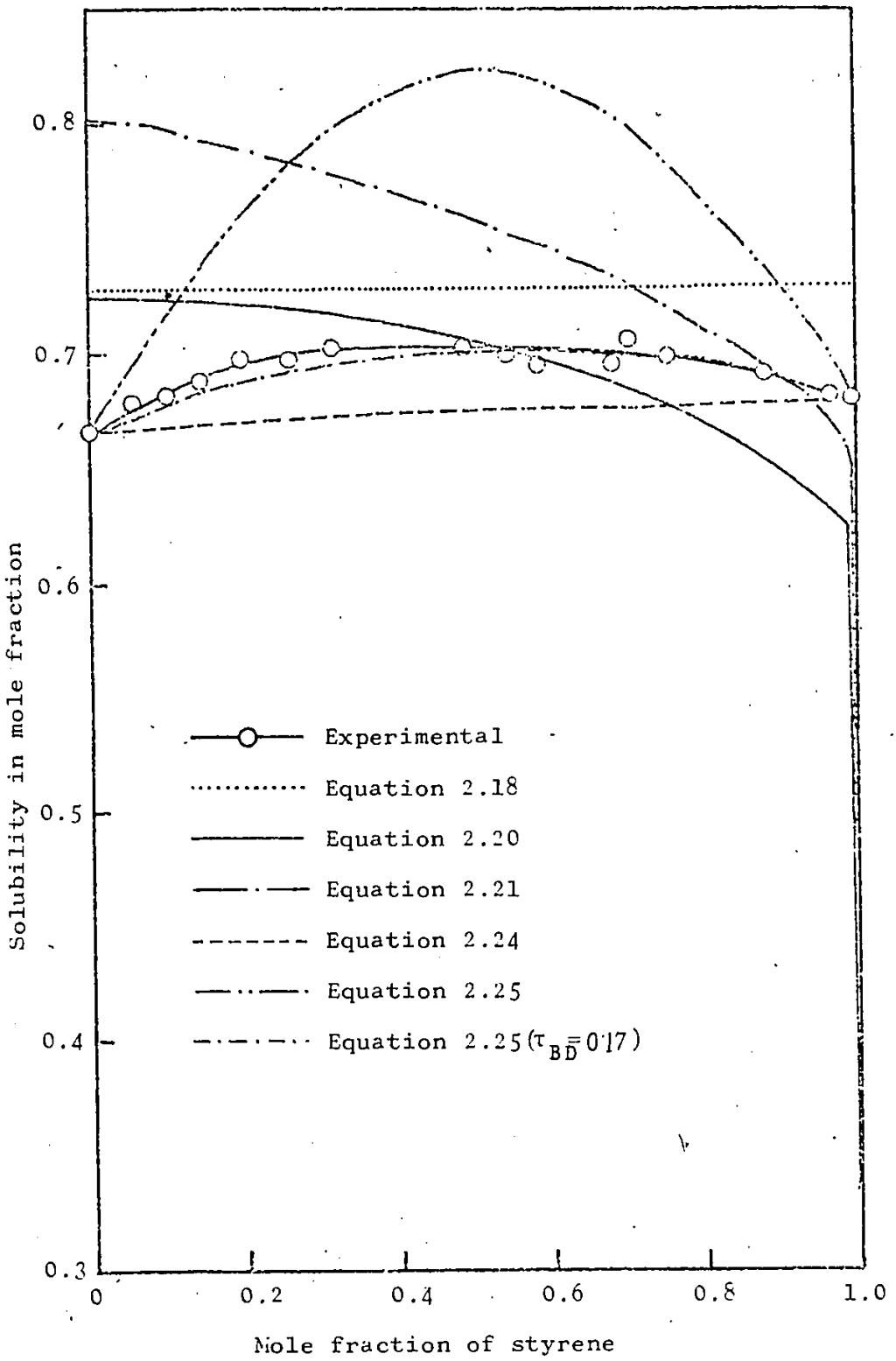

Figure 18 - Comparison of experimental solubility of butadiene in styrene-heptane mixtures at 4 °C with those predicted from theoretical correlations

as 0.17 is also shown in Figure 18, which is in good agreement with the experimental values.

The diffusion coefficient for dissolved butadiene in heptane at 25 and 50°C are listed in Table 18 of Appendix D. The accurate measurement of diffusivity at lower temperatures by the steady state capillary cell method was not successful as a result of the extremely high solubility of the butadiene. The liquid level in the capillary kept on increasing (because of the volume occupied by the dissolved butadiene) at such a rate that even a pseudo steady-state could not be reached. On the other hand, diffusivity measurements in water and surfactant solutions were unsuccessful because of the extremely low solubility of butadiene in those solvents. In this case, the liquid bead moved so slowly in the capillary that accurate readings of the volume change within the capillary were impossible. Hence, further measurements of diffusivity for these complex systems were abandoned.

6.3 EMULSION POLYMERIZATION OF BUTADIENE IN THE PRESENCE OF NONREACTIVE DILUENTS

Having obtained some useful information about potassium laurate solutions and of the solubility of butadiene as discussed in the above two sections, it was then possible to attempt to analyse the experimental results for the emulsion polymerization of butadiene in the presence of nonreactive liquid additives. The values for butadiene solubility in

heptane were used for determining the quantity of heptane to be added to perform the emulsion polymerization at atmospheric pressure. The knowledge of the cmc was used to ensure that, for all of the experiments, the surfactant concentration exceeded the cmc. The other data obtained, such as the solubility of butadiene in water and surfactant solutions and the butadiene diffusivity, were useful for interpreting the experimental data.

The experimental results of emulsion polymerization of butadiene in the presence of the nonreactive liquid additives , heptane and cyclohexane, are presented in this section. The process variables studied include reaction time, reaction temperature, additive concentration, surfactant concentration and initiator concentration. The effects of the additives on the rate of polymerization and the molecular weight are also compared.

To obtain a meaningful interpretation of the experimental results, the conversion during the emulsion polymerization was kept low, to about 40%. The molecular weight also remained approximately constant at the low conversions. It was expected that at higher conversions the latex would thicken and the molecular weight would continue to increase (74). This was considered to be caused by the formation of branches and cross links on the polymer molecules previously formed. For this reason, the conversion was kept low for the polymerization experiments.

Butadiene was polymerized at 4 °C using the recipe shown in Table 6 in Section 5.1. Except for the quantity of solvent that was systematically added the same recipe was used for all of the experiments. A typical conversion-time relationship for polymerization with (or without) the added solvent is shown in Figure 19. The polymerization in the presence of heptane was performed at atmospheric pressure. The heptane was charged at a weight ratio of heptane to butadiene of 0.85. It may be seen from Figure 19 that the addition of heptane causes a reduction in the rate of polymerization. The conversion-time data are reported in Table 20 of Appendix F. The lower conversion rate resulted in a correspondingly lower heat evolution due to polymerization. Further experiments were performed at 10 °C in order to obtain a higher rate of polymerization and higher rate of heat evolution to measure it more accurately with the designed apparatus.

The data for the effect of an increase in polymerization temperature on the conversion-time relationship are given in Table 21 of Appendix F and graphically represented in Figure 20. As expected the conversion obtained at 10 °C was always higher than that obtained at 4 °C for the same reaction time. Almost 50% conversion was achieved at 10 °C as compared with 35% conversion achieved at 4 °C in a period of 4.5 hours.

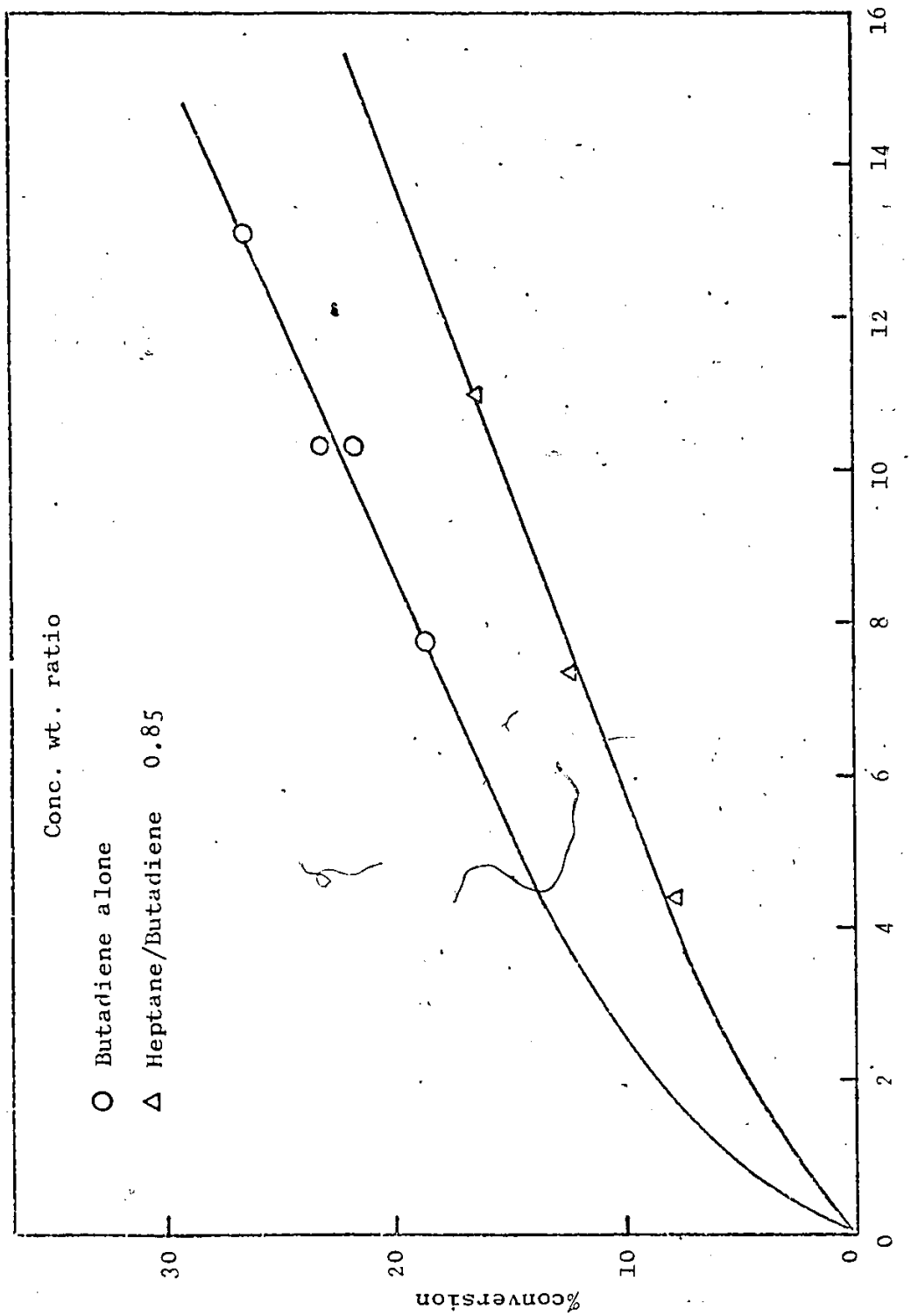

Figure 19 - Effect of concentration of heptane on conversion-time relationship for polymerization of butadiene at 4°C

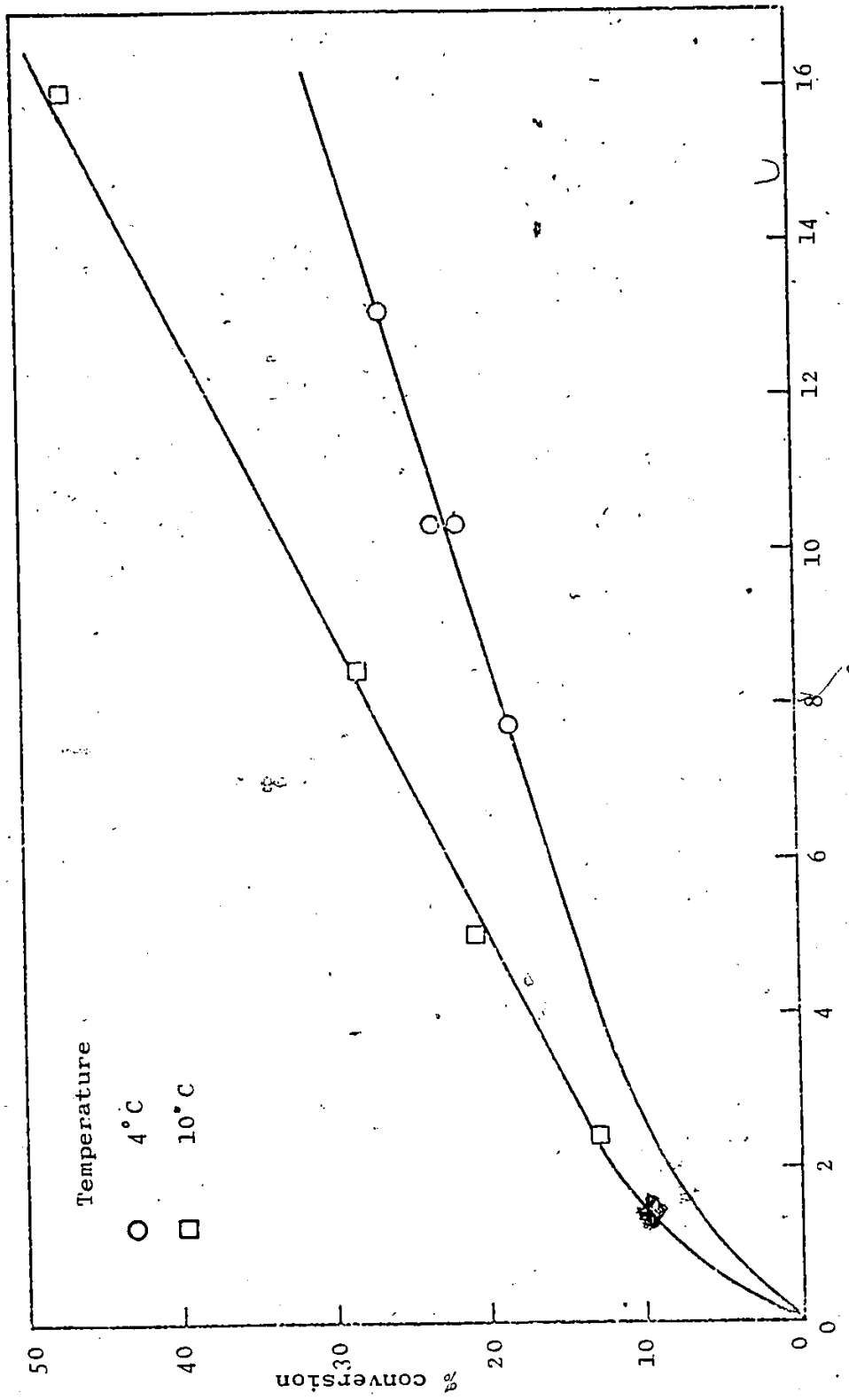

Figure 20 - Effect of temperature on conversion-time relationship for polymerization of butadiene

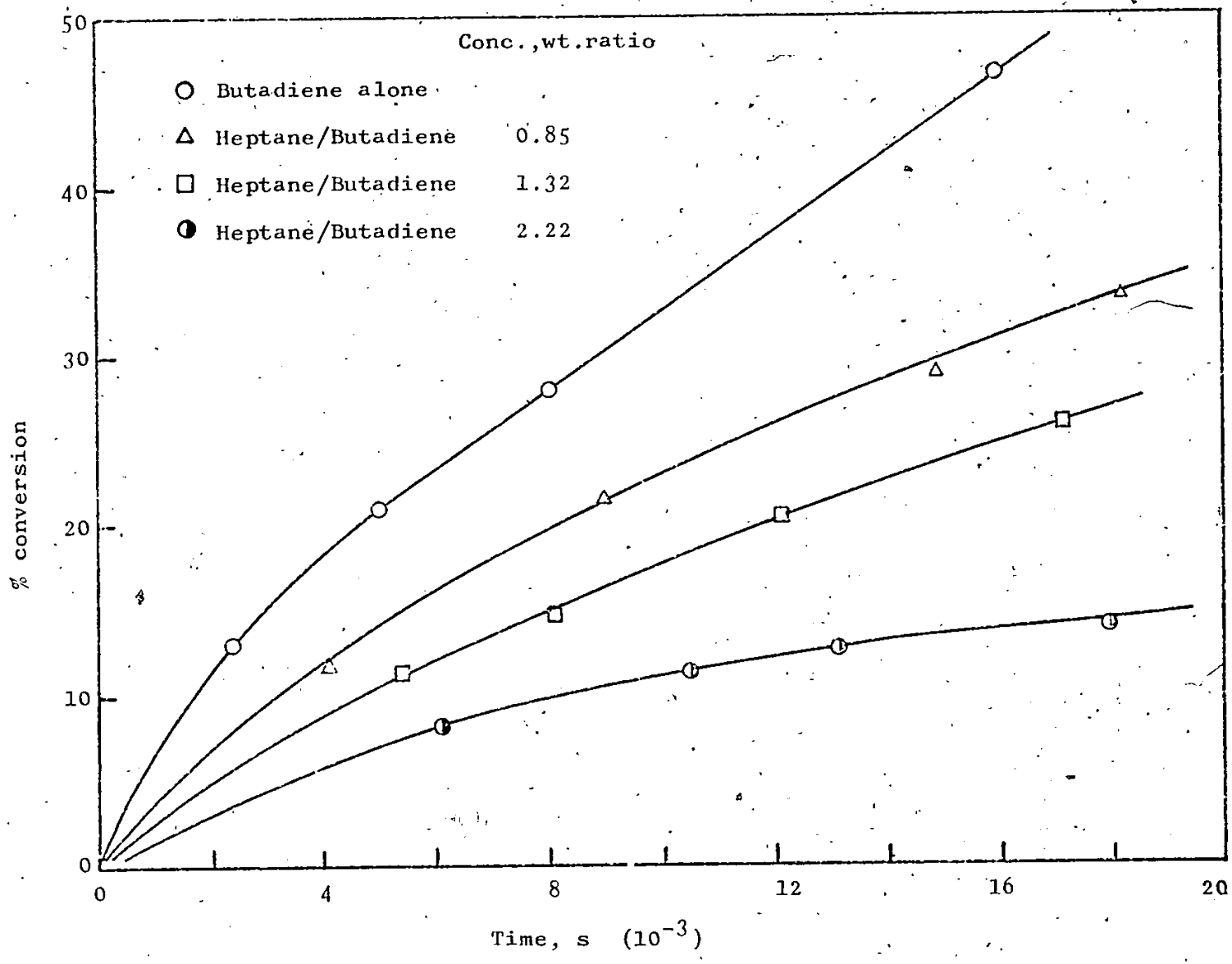

Figure 21 - Effect of concentration of heptane on conversion-time relationship for polymerization of butadiene at 10°C

The effect of the addition of heptane on the conversion-time relationship is shown in Figure 21. The different concentrations of heptane were obtained by varying the amount of heptane while the butadiene quantity was always kept constant. It may be observed that the presence of heptane retards the rate of polymerization and that as the quantity of heptane is increased further retardation results. This type of retardation in the rate of polymerization was also observed by other investigators (1,3,4) while polymerizing styrene in the presence of various nonreactive additives including heptane. The effect of viscosity on the emulsion polymerization of butadiene was observed by replacing heptane (0.457 mPa.s at 10 °C) (72) with the more viscous cyclohexane (1.21 mPa.s at 10 °C) (73). The effect of the addition of cyclohexane on the conversion-time relationship is shown in Figure 22. It may be seen from Figure 22 that the presence of cyclohexane also retards the rate of polymerization and that as the concentration of cyclohexane is increased further retardation results. The data for the effect of the addition of heptane and cyclohexane on the conversion-time relationship are given in Tables 22 and 23 of Appendix G.

The addition of an additive is expected to reduce the rate of polymerization because it reduces the butadiene concentration in the monomer phase as well as in the micelle phase. The rate of polymerization is considered to be directly proportional to the monomer concentration as

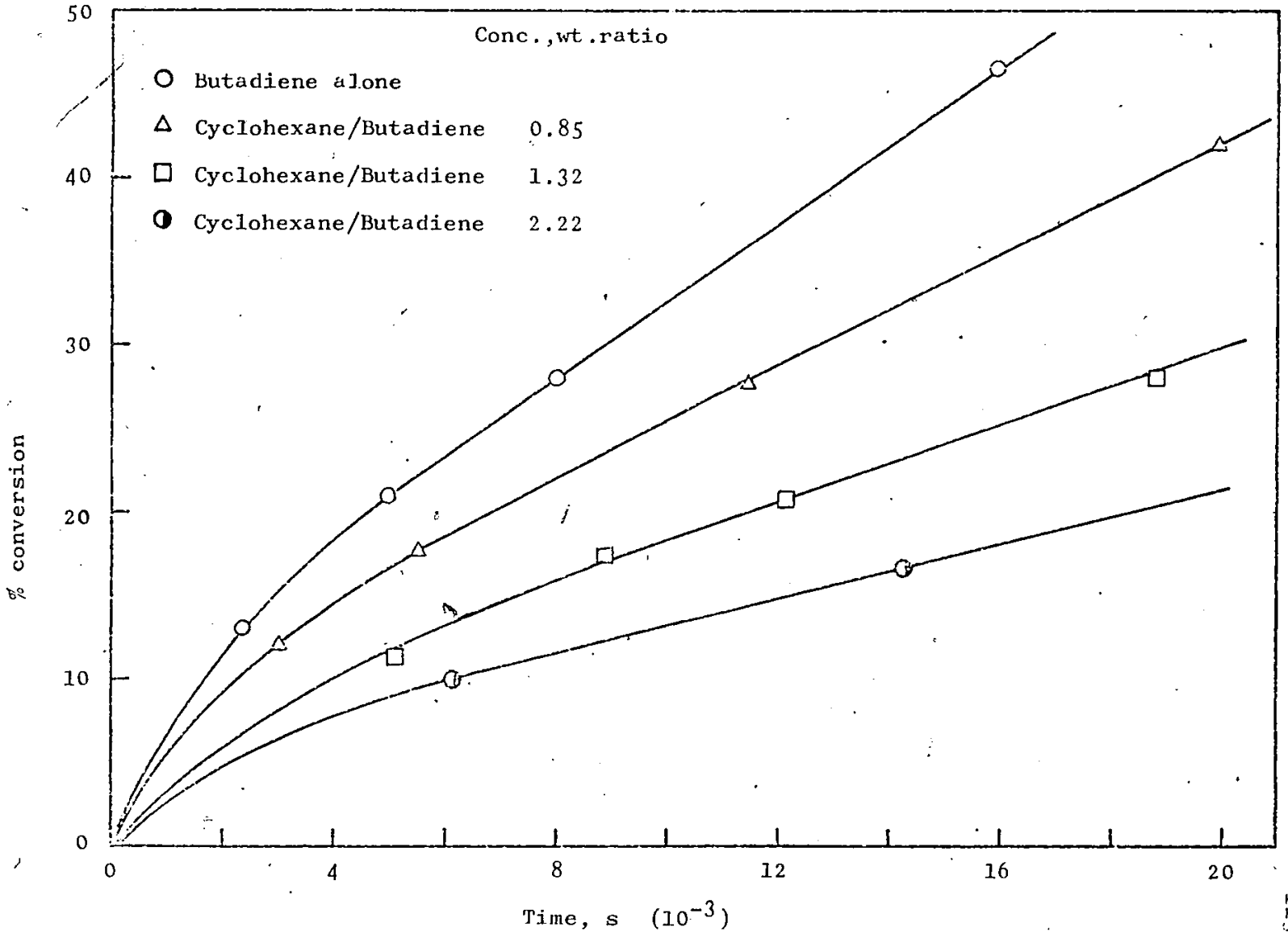

Figure 22 - Effect of concentration of cyclohexane on conversion-time relationship for polymerization of butadiene at 10°C

expressed by emulsion polymerization theories (16,17). However, the retardation in the presence of heptane and cyclohexane appears to be more than that expected on the basis of mere monomer dilution by the additives. The experimental values for the polymerization rates are compared with predicted values calculated on a basis of a reduced monomer concentration resulting from a dilution with solvent, as shown in Figure 23. The experimental values for the rate of polymerization were determined for the straight line portion of the conversion-time curves. These values are listed in Table 24 of Appendix G. The predicted values for the rates were calculated by considering the initial concentration of butadiene in the monomer phase. The percent deviation of the predicted values with the experimental values of the polymerization rates is given in Table 25 of Appendix G. Figure 23, shows that the experimental values were less than the calculated ones. It also shows that the rates of polymerization obtained in the presence of the more viscous cyclohexane were always higher than those obtained in the presence of heptane. Seymour et al. (1) also observed that viscous nonreactive additives were less effective in reducing the rate of polymerization. They studied the emulsion polymerization of styrene in the presence of various nonreactive additives. The observation is made therefore, that the viscosity of an additive is most likely an important property which may significantly affect the kinetics of

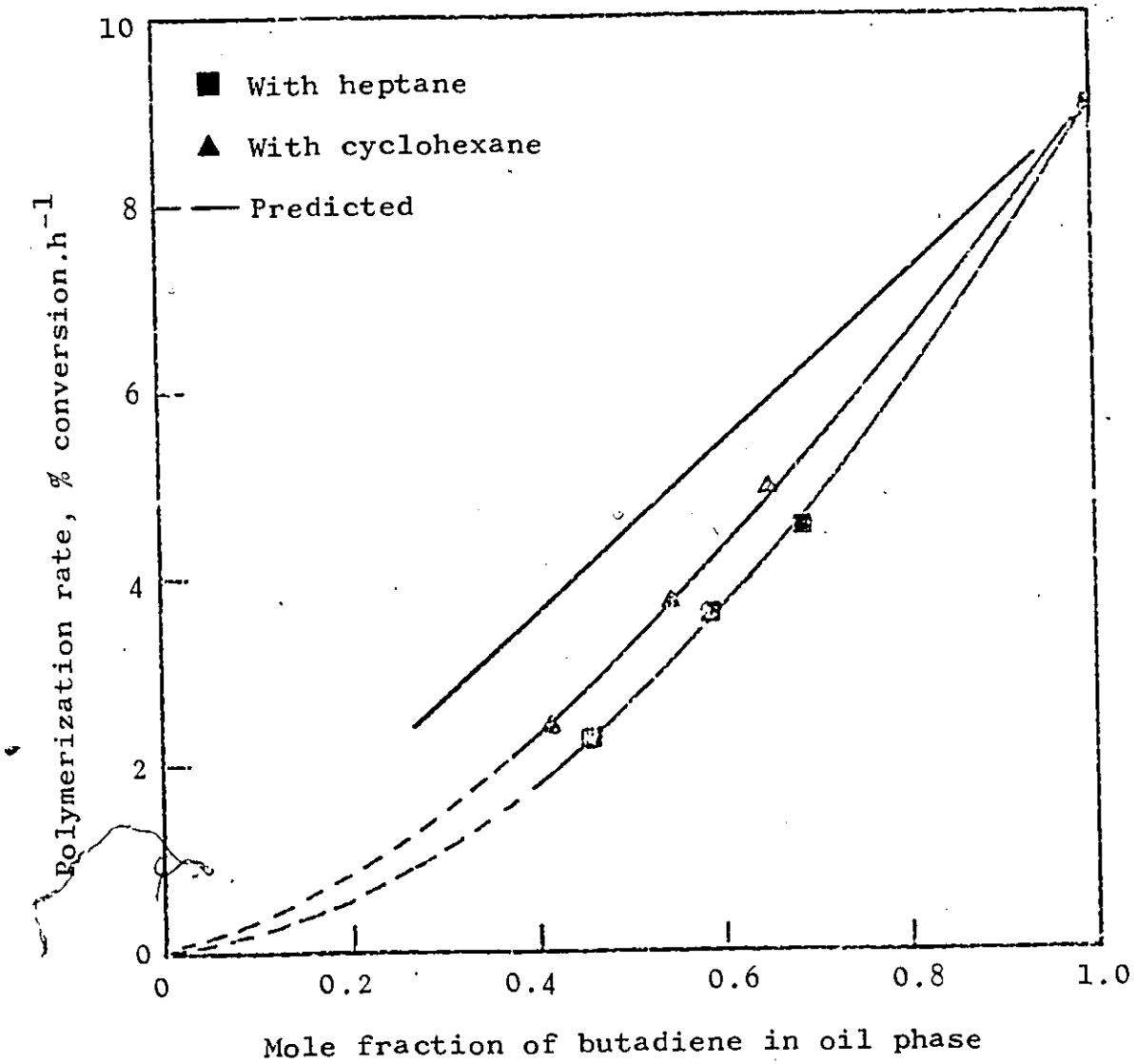

Figure 23 - Comparison of experimental rate of polymerization in the presence of heptane and cyclohexane at 10°C with the predicted rate of polymerization

emulsion polymerization. The retardation in the rate of polymerization in the presence of a solvent suggests that the rate of polymerization is dependent on monomer concentration to an order higher than first order. It appears that the rate of polymerization can be expressed in terms of the monomer concentration by the following equation:

$$R_p = C_3[M]^{\theta_3} \qquad (6.1)$$

The index θ_3 was determined by measuring the slope of the double logarithmic plot of the rates of polymerization versus initial monomer concentration in the hydrocarbon phase as shown in Figure 24. It is equal to 1.70 in the presence of heptane and 1.48 in the presence of cyclohexane. Thus, the rate of polymerization is dependent on monomer concentration to a greater extent in the presence of heptane. These data were correlated with a computer program to get the best fit and the value of the index θ_3. Blackley (3) found that the equivalent index θ_3 for the emulsion polymerization of styrene in the presence of aromatic diluents was 2.75, whereas in the presence of cyclohexane it was of the order of 1.

The molecular weights of polybutadiene samples were determined by Gel Permeation Chromatography by following the procedure previously discussed in Section 5.2. A typical chromatographic molecular weight distribution is shown in Figure 37 of Appendix E. The sample calculation for the

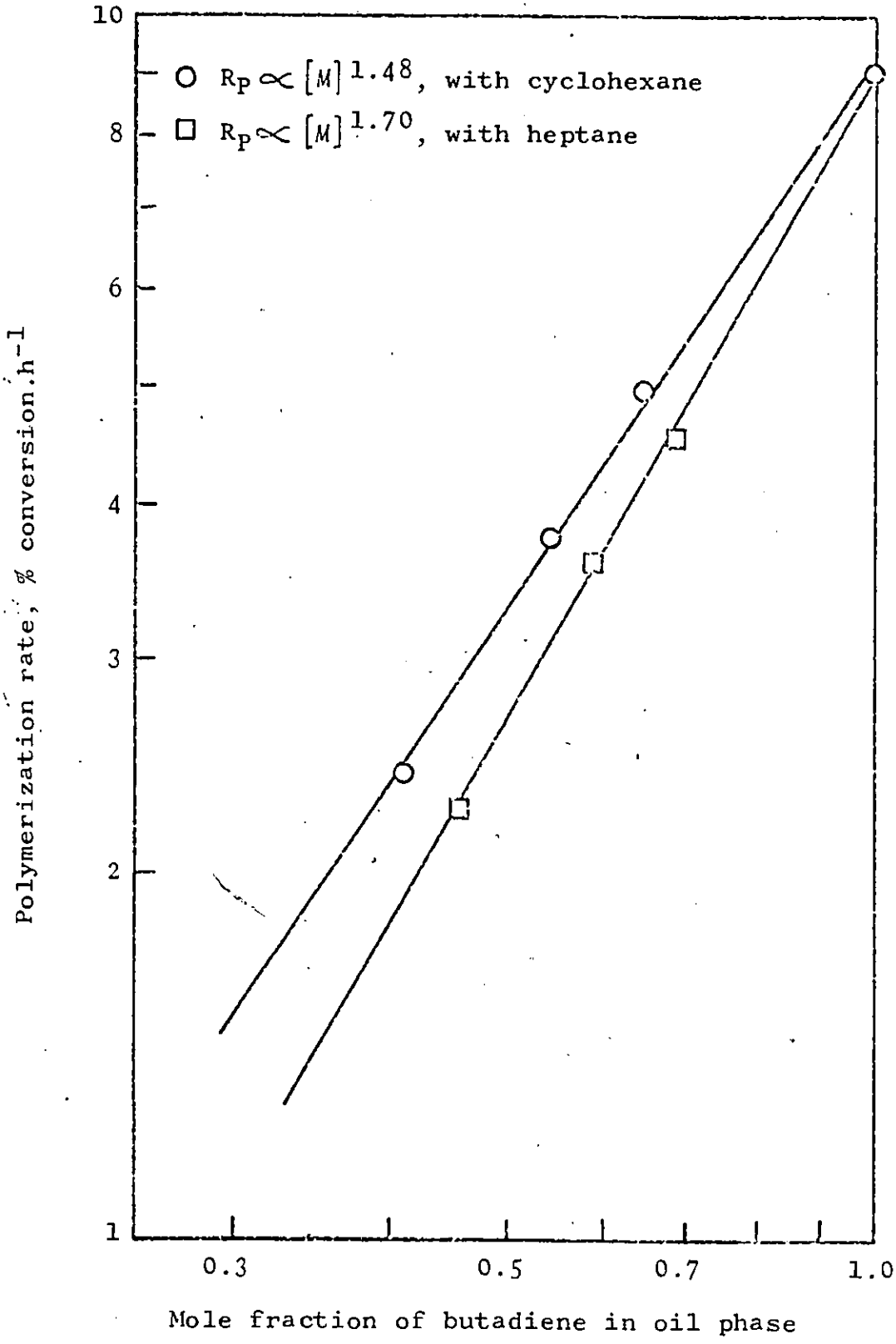

Figure 24 - Effect of concentration of cyclohexane and heptane on rate of polymerization of butadiene at 10°C

determination of the number average and the weight average molecular weights is also presented in Appendix E.

The molecular weights of polybutadiene samples obtained at different concentrations of heptane and cyclohexane are reported in Table 26 of Appendix G. The molecular weights of polybutadiene samples obtained at different reaction times were also determined. It was found that the molecular weights were independent of reaction time. A similar observation was also noted by other investigators including the molecular weight of polyvinylchloride as obtained by Laudie (74). Emulsion polymerization theories are often based on the assumption that a constant molecular weight of polymer is obtained for increasing reaction times at low conversions (17). It is observed that the addition of either heptane or cyclohexane reduces the polymer molecular weight. Molecular weights further reduce as the quantity of additive is increased. Heptane was found to reduce the molecular weight more than cyclohexane. The reduction in molecular weight in the presence of a solvent was also observed by other investigators (1), while studying the emulsion polymerization of styrene.

Molecular structure of polybutadiene samples were determined by Infrared Spectrophotometry as previously discussed in Section 5.2. A typical spectrum of a polybutadiene sample is shown in Figure 38 of Appendix G. The relative proportions of cis-1,4, vinyl and trans-1,4 structures of poly-

butadiene samples obtained at different concentrations of heptane and cyclohexane are presented in Table 27 of Appendix G. The results indicate that the presence of heptane or cyclohexane has no effect on polybutadiene structure.

The data for the effect of changes in surfactant concentration upon butadiene conversion while the other variables were all kept constant are given in Table 28 of Appendix H and graphically represented in Figure 25. As expected it may be observed that for a particular reaction time the conversion increases with an increase of surfactant concentration. Although the number of particles in the latex was not measured, it is well known that the number of particles increases with the surfactant concentration, as described by various investigators including Ugelstad et al. (91). The increase in surfactant concentration was expected to cause an increase in the number of particles which in turn increased the reaction rate and butadiene conversion for the same reaction time. The effect of changes in surfactant concentration on the butadiene conversion in the presence of heptane is shown in Figure 26. The heptane concentration was kept constant at heptane to butadiene weight ratio of 1.32 in all the experiments. All of the other variables were held constant to obtain this conversion-time relationship. Figure 26 depicts the increase of conversion with the increase of surfactant concentration for any particular reaction time. The data for the effect of variation in surfactant

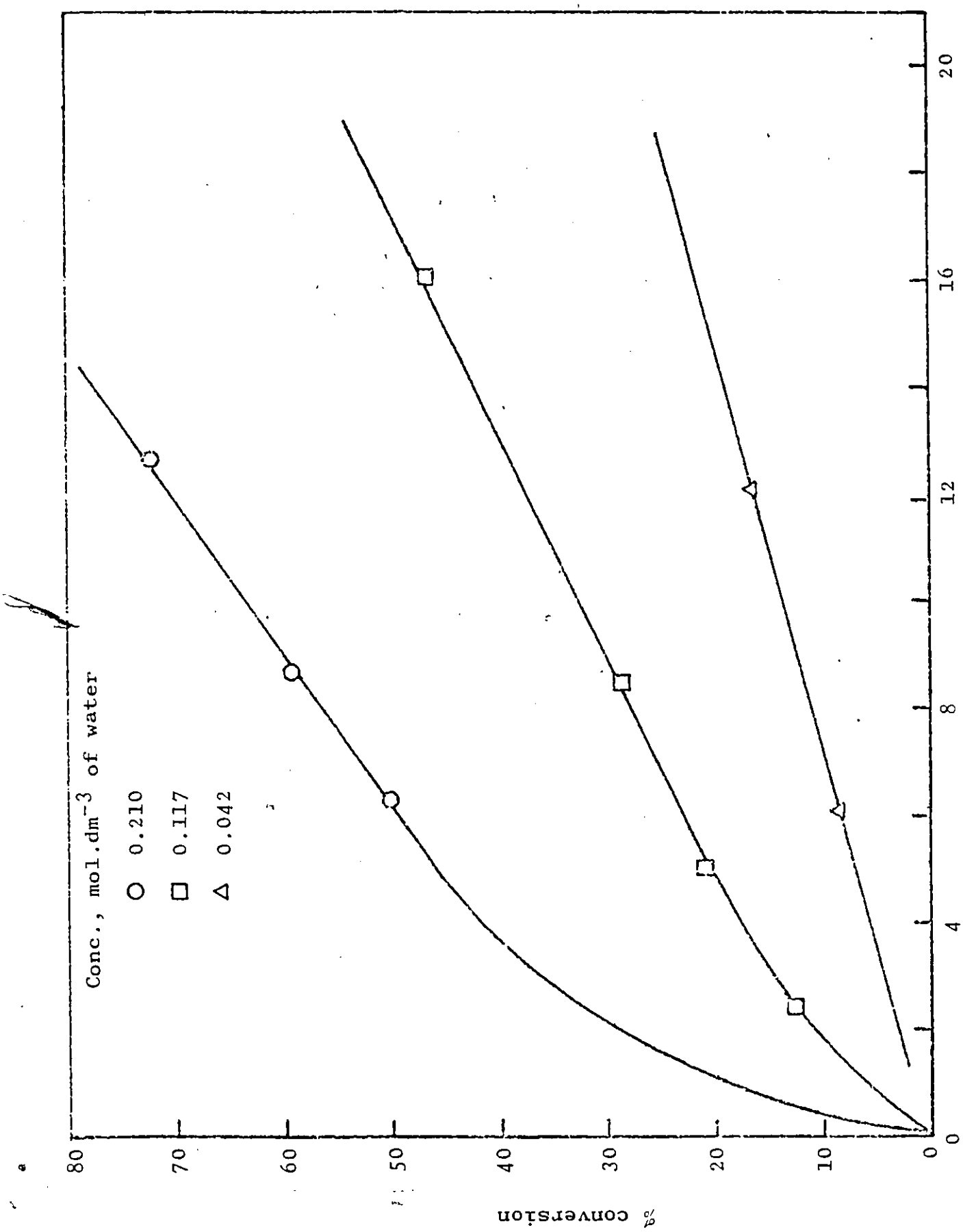

Figure 25 - Effect of concentration of potassium laurate on conversion-time relationship of butadiene at 10°C

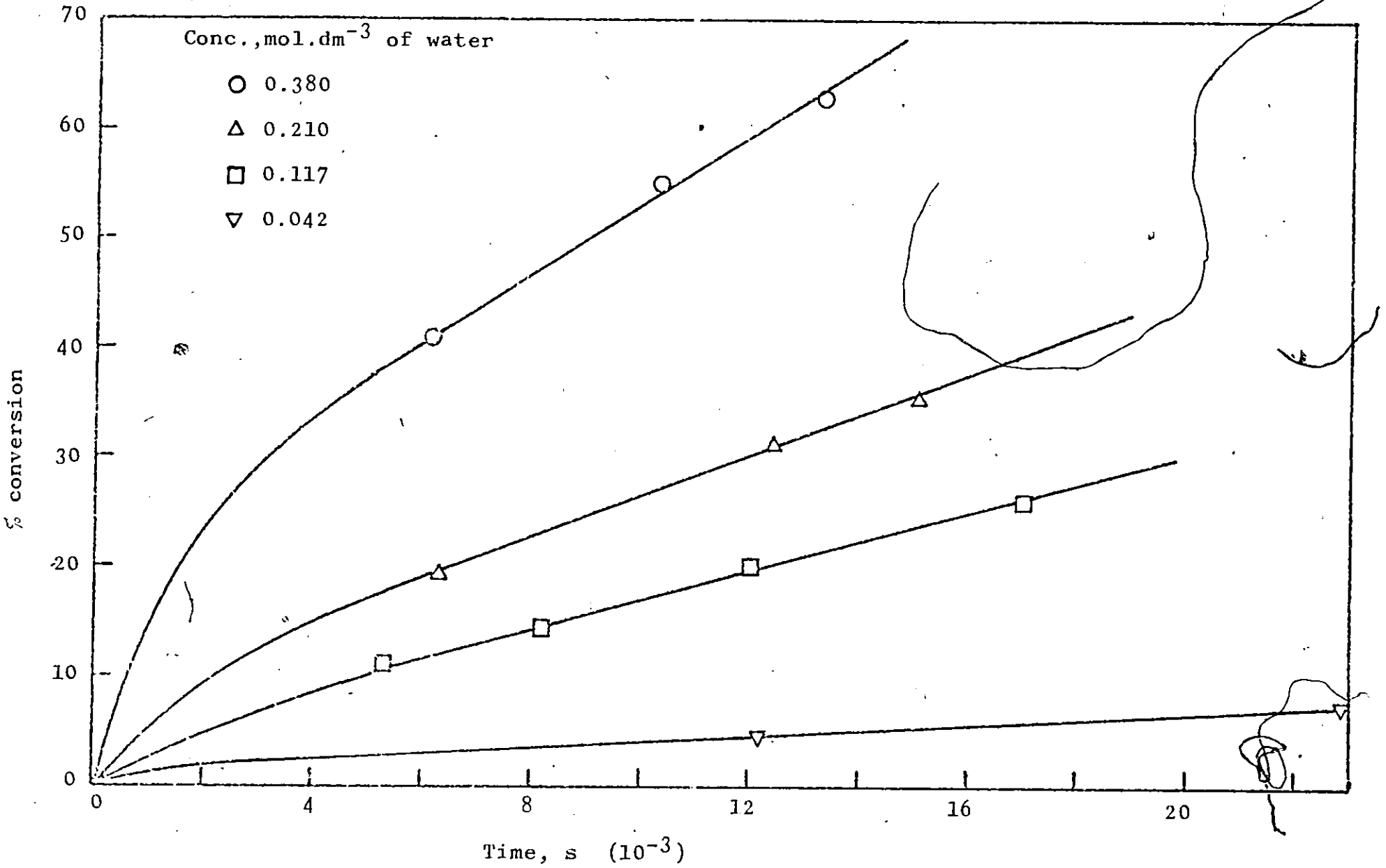

Figure 26 - Effect of concentration of potassium laurate on conversion-time relationship for polymerization of butadiene at 10°C in the presence of heptane at heptane to butadiene weight ratio of 1.32

concentration upon butadiene conversion in the presence of heptane are presented in Table 29 of Appendix H.

When the results corresponding to Figures 25 and 26 are compared, it may be seen that the conversion rate dependency on the surfactant concentration is greater in the presence of heptane. To analyse these observations, the rates of polymerization at various surfactant concentrations were compared for the constant rate portions of the conversion-time relationship. These constant rates of polymerization were plotted against surfactant concentration as shown in Figure 27. The rates of polymerization may be observed to increase with an increase in surfactant concentration and this dependence can be represented by:

$$R_p \propto [A]^{\theta_4} \qquad (6.2)$$

The exponent θ_4 for the butadiene polymerization in the absence of solvent was found to be 0.59. This is comparable with an exponent of 0.6 predicted from the Gardon theory of emulsion polymerization (17). An exponent of the order of 0.6 was also observed by Morton and Salatiello (92) for the emulsion polymerization of butadiene. In the presence of heptane solvent, however, the value of the index θ_4 increased to 1.12. This may be compared with the exponent of 1.8 which was obtained by Seymour et al. (2) for the emulsion polymerization of styrene in the presence of Nujol at styrene to Nujol ratio of 1 to 0.025. Therefore, it may be concluded

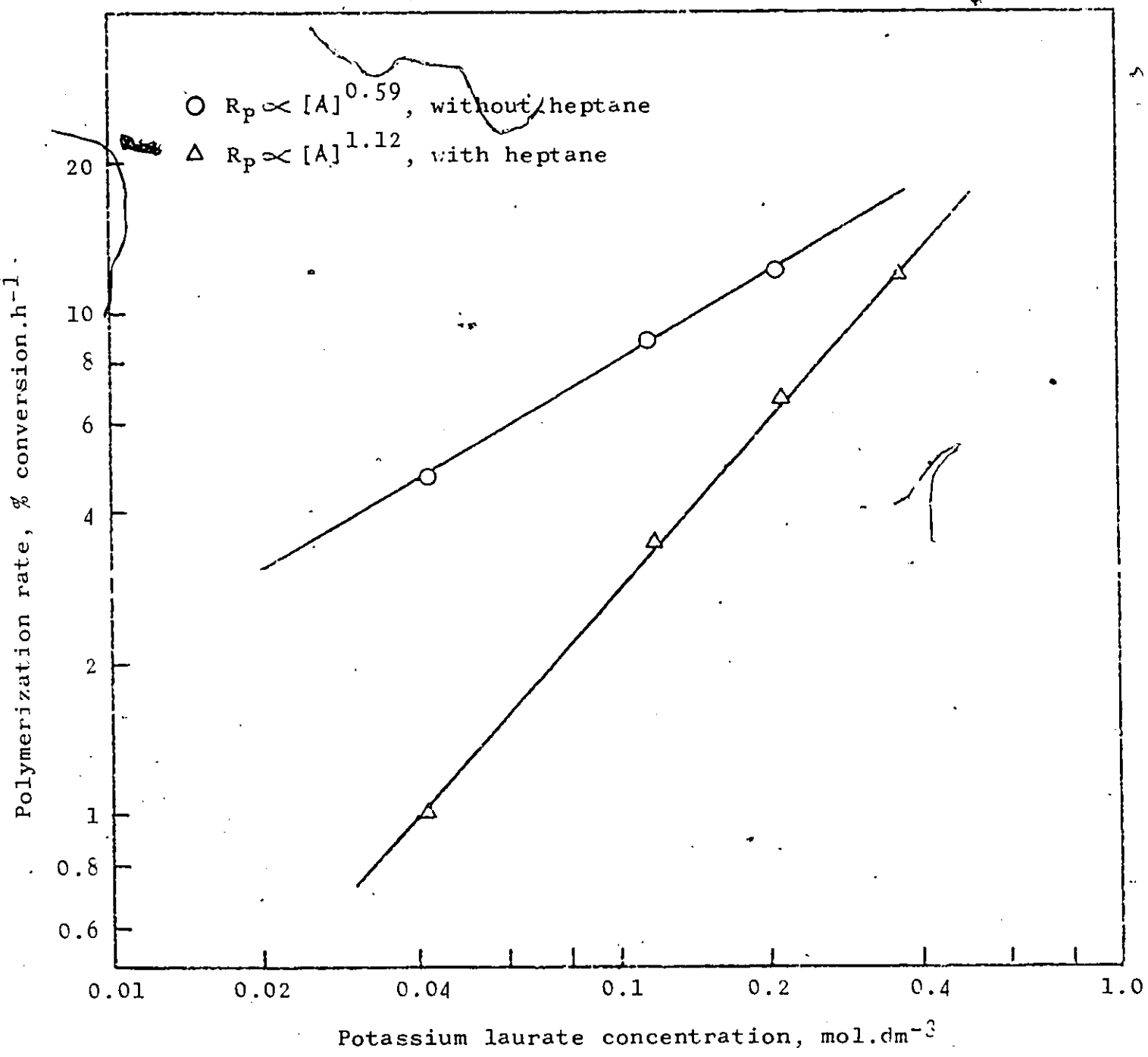

Figure 27 - Effect of concentration of potassium laurate on polymerization rate of butadiene with and without heptane at 10°C

that the rate of polymerization is influenced by the surfactant concentration to a greater extent in the presence of a nonreactive liquid additive than without it. The data for the rate of polymerization versus potassium laurate concentration are given in Table 30 of Appendix H.

Figure 28 demonstrates the effect of a variation in surfactant concentration upon the average molecular weight of polybutadiene produced while the other variables are held constant. The molecular weight may be observed to increase with increasing surfactant concentration in the absence as well as presence of heptane. This observation is in agreement with the prediction based on the Gardon theory for this situation. It is also clear from Figure 28 that the polydispersity of the polymer produced also increases with an increasing surfactant concentration. In the absence of a solvent the polydispersity at the surfactant concentration of 0.04 $mol.dm^{-3}$ is 4.14, while at a surfactant concentration of 0.4 $mol.dm^{-3}$ the polydispersity is observed to increase to 5.7. It may be seen from Figure 28 that the addition of heptane caused a reduction in the polydispersity of polybutadiene formed at all surfactant concentrations. The polydispersity increased from 2.62 to 4.85 when the surfactant concentration was varied from 0.04 to 0.4 $mol.dm^{-3}$. The dependence of $\bar{M}_n$ and $\bar{M}_w$ on surfactant concentration can be represented by:

$$\bar{M}_n \propto [A]^{\theta_5} \qquad (6.3)$$

$$\bar{M}_w \propto [A]^{\theta_6} \qquad (6.4)$$

The values of the indices θ_5 and θ_6 have been determined from the slope of the plots in Figure 28 and are presented in Table 7 (page 135). The complete numerical data for the variation of molecular weight with surfactant concentration are presented in Table 31 of Appendix H.

Infrared spectra of polybutadiene samples were obtained to analyse the effect of a variation in surfactant concentration on the molecular structure. The relative proportions of cis-1,4, vinyl and trans-1,4 structures of the polybutadiene samples are presented in Table 32 of Appendix H. From the results obtained it may be noted that the polybutadiene structure is essentially independent of the concentration of surfactant used.

A number of experiments were conducted to study the effect of a variation in initiator concentration for otherwise constant polymerization conditions. Based on recent emulsion polymerization theories (16,17), it may be expected that the polymerization rate will be constant for a variation in initiator concentration provided that the number of particles is also constant. Gardon (17) while developing the emulsion polymerization theory used potassium persulfate as the initiator. According to his theory, the steady-state rate of polymerization is affected by the initial initiator

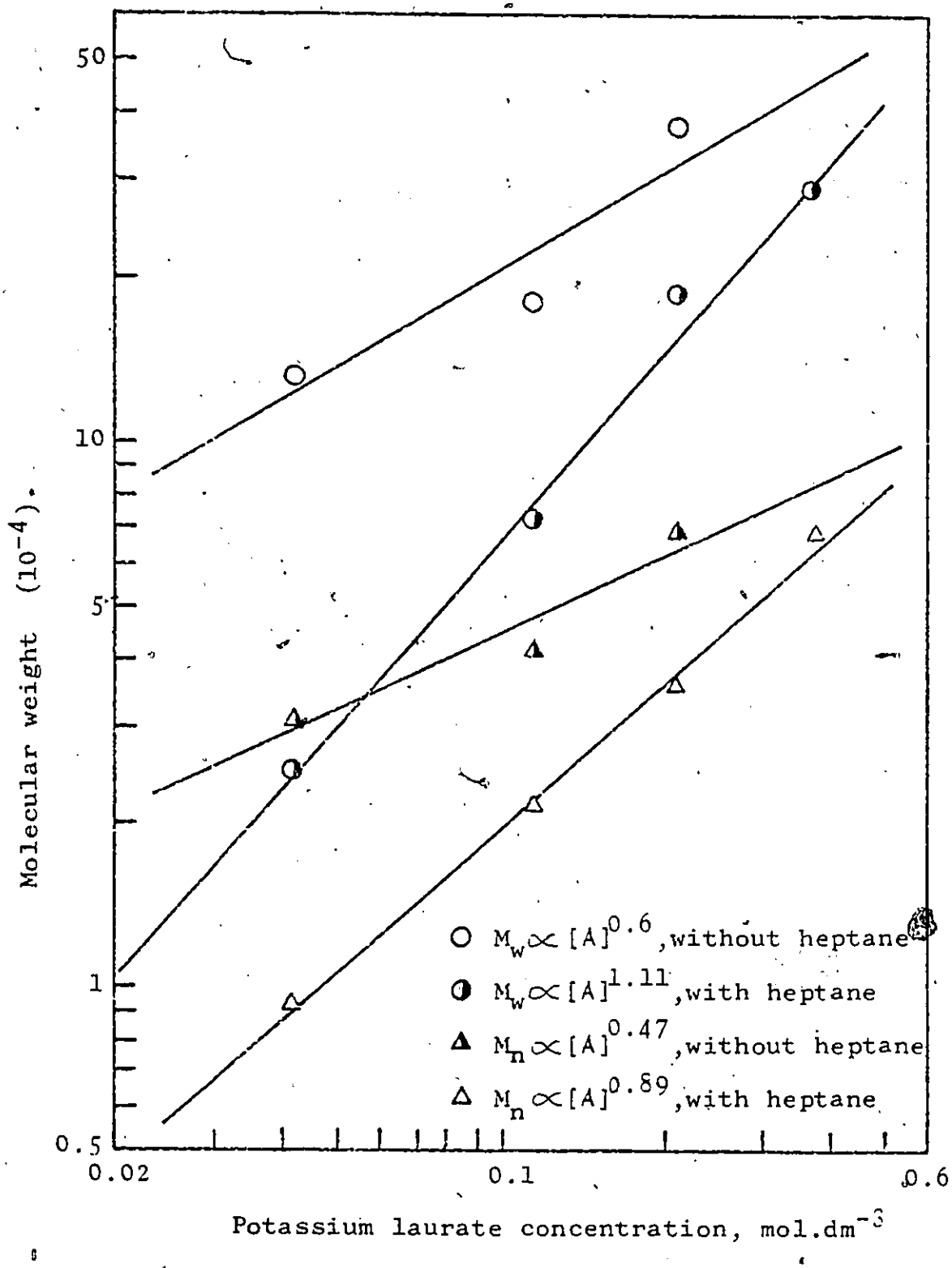

Figure 28 - Effect of concentration of potassium laurate on molecular weight of polybutadiene formed with and without heptane

concentration because of its effect upon the formation of the number of latex particles during the initiation stage. In this case the rate of polymerization is expected to be proportional to the 0.4 power of the initiator concentration. However, in this investigation a redox initiation system consisting of cumenehydroperoxide-tetraethylenepentamine was used. Therefore, it was assumed that the effect of changes in initiator concentration in the present results might not be the same as predicted by the emulsion polymerization theories. In this work, the cumenehydroperoxide to tetraethylenepentamine ratio was kept constant so that it was expected that the number of free radicals generated was proportional to the concentration of either ingredient.

The effect of varying the initiator concentration on butadiene conversion is shown in Figure 29. For otherwise similar conditions, the quantity of polybutadiene produced or the butadiene conversion essentially remained constant with a variation in initiator concentration. The effect of varying the initiator concentration on the butadiene conversion in the presence of heptane is also shown in Figure 29. The heptane concentration in all of the experiments was held constant at an heptane to butadiene weight ratio of 1.32. It may be seen that the conversion in the presence of heptane also remained constant with a variation in the initiator concentration. The conversion obtained in the presence of heptane was lower than that obtained with butadiene

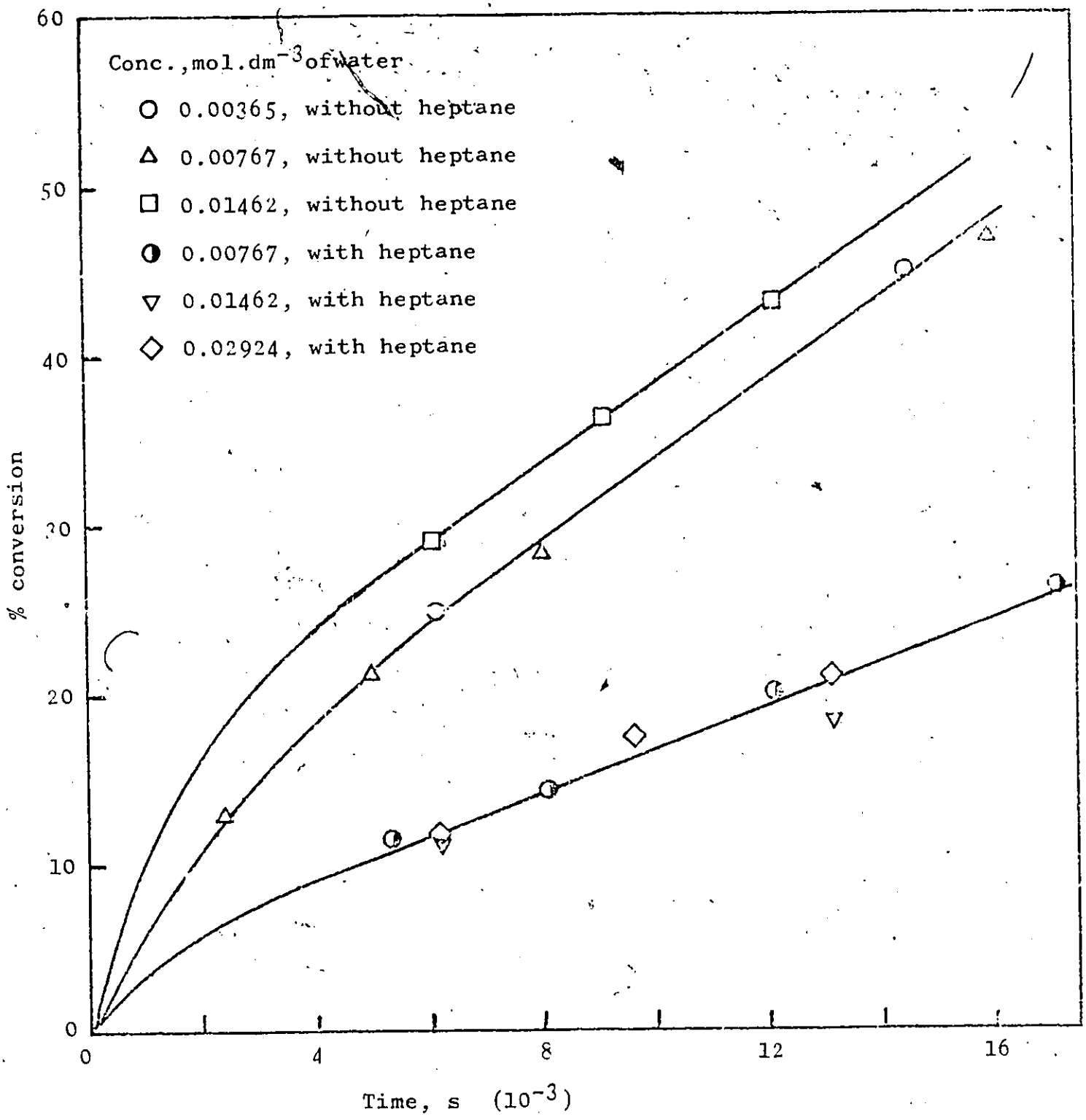

Figure 29 - Effect of concentration of cumenehydroperoxide on conversion-time relationship for polymerization of butadiene with and without heptane at 10°C

alone for the same initiator concentration. The data for the effect of changes in initiator concentration on butadiene conversion are given in Tables 33 and 34 of Appendix I. The effect of the addition of heptane was determined by comparing the rate of polymerization for every initiator concentration as determined from the slopes of conversion-time curves in Figure 29. The logarithm of the rates of polymerization and the initiator (cumenehydroperoxide) concentration are shown in Figure 30. The results indicate that the rate of polymerization remains at least approximately constant with a variation in initial concentration of the initiator and can be represented by:

$$R_p \propto [I]^{\theta_7} \qquad (6.5)$$

When the data were correlated the value of the index θ_7 was found to be 0.08 for polymerization of butadiene alone and 0.06 for polymerization of butadiene in the presence of heptane. The results obtained indicate that the rate of polymerization of butadiene, with or without heptane, essentially remains independent of the redox initiator concentration. The polymerization rate data for the various initiator concentrations are presented in Table 35 of Appendix I.

The effect of a change in initiator concentration on polybutadiene molecular weight is shown in Figure 31. It may be observed that an increase in initiator concentration

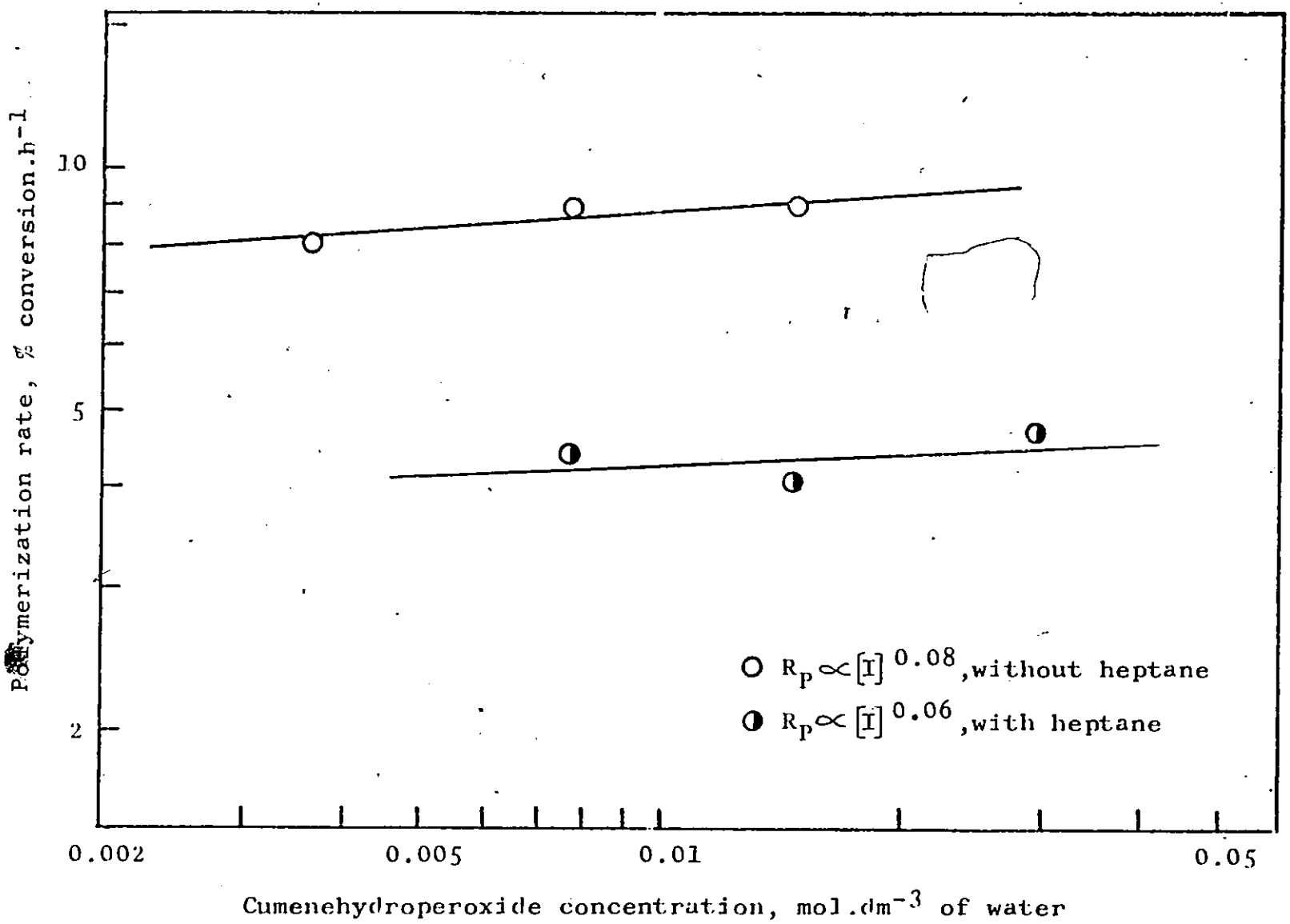

Figure 30 - Effect of concentration of cumenehydroperoxide on polymerization rate of butadiene with and without heptane at 10°C

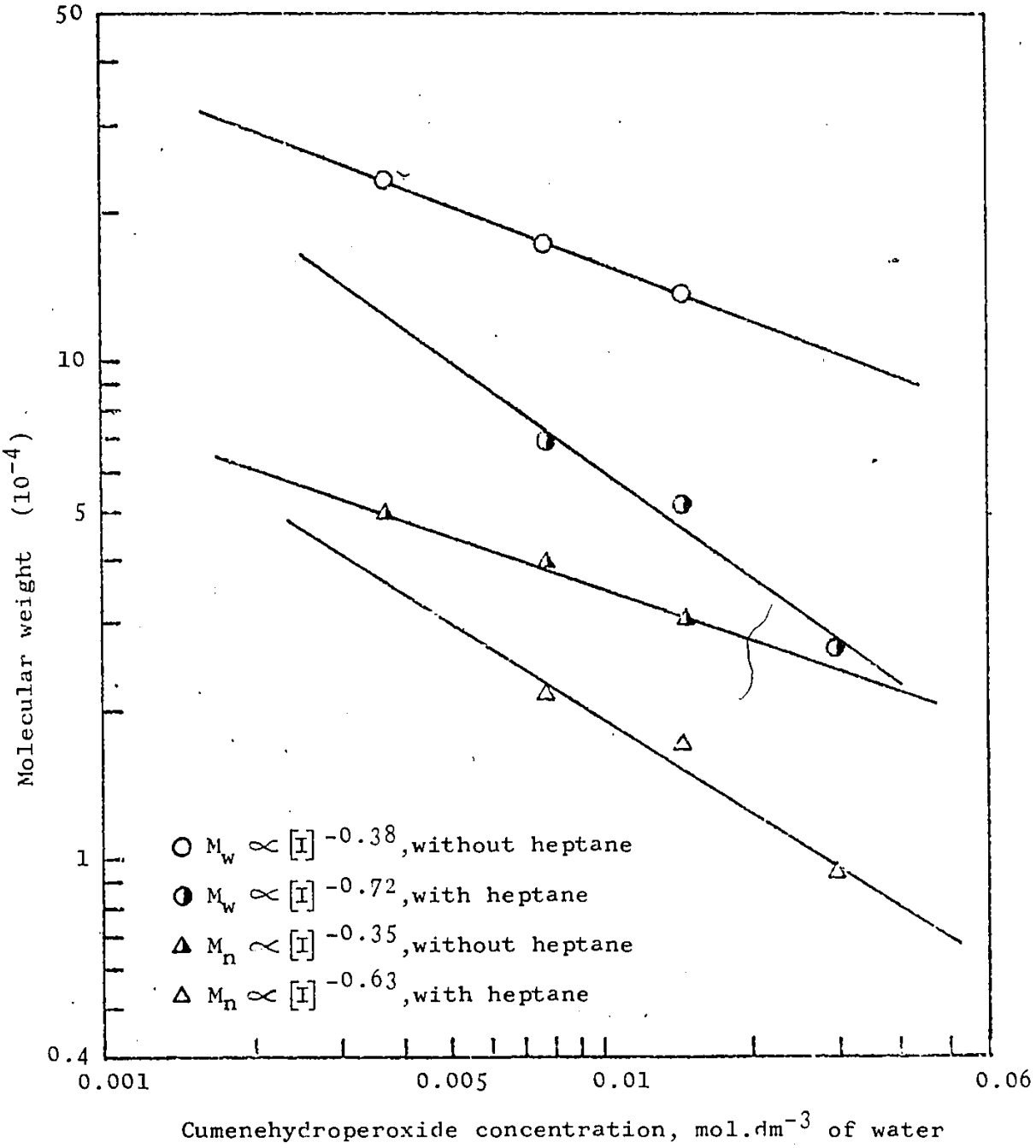

Figure 31 - Effect of concentration of cumenehydroperoxide on molecular weight of polybutadiene formed with and without heptane at 10°C

resulted in a reduction in both $\bar{M}_n$ and $\bar{M}_w$ for butadiene polymerized alone as well as in the presence of heptane. The molecular weights were reduced to a greater extent by an increase in the initiator concentration in the presence of heptane solvent. The molecular weight was correlated as a function of the initiator concentration as follows:

$$\bar{M}_n \propto \frac{1}{[I]^{\theta_8}} \tag{6.6}$$

$$\bar{M}_w \propto \frac{1}{[I]^{\theta_9}} \tag{6.7}$$

The best values of indices θ_θ and ϵ_9 obtained for the effect of initiator concentration on $\bar{M}_n$ and $\bar{M}_w$ are given in Table 8. The value of the indices indicates that the reduction in $\bar{M}_n$ and $\bar{M}_w$ caused by the increase of initiator concentration is greater in the presence of heptane.

Infrared spectra of polybutadiene samples were obtained to analyse the effect of a variation in initiator concentration on the molecular structure. The relative proportions of cis-1,4, vinyl and trans-1,4 structures for the polybutadiene samples are presented in Table 37 of Appendix I. It is apparent from this table that the relative proportion of polybutadiene isomers are essentially independent of the initiator concentration used for polymerization.

TABLE 7

The effect of surfactant concentration on $\bar{M}_n$ and $\bar{M}_w$

θ_5/θ_6	Index	Remarks
θ_5	0.47	Without heptane
θ_5	0.89	With heptane
θ_6	0.60	Without heptane
θ_6	1.11	With heptane

TABLE 8

The effect of initiator concentration on $\bar{M}_n$ and $\bar{M}_w$

θ_8/θ_9	Index	Remarks
θ_8	0.35	Without heptane
θ_8	0.63	With heptane
θ_9	0.38	Without heptane
θ_9	0.72	With heptane

The experimental results were used to modify the model for emulsion polymerization as originally developed by Gardon (17) for the situation in which a solvent was present. The model, as presented in Chapter 3, will now be examined to see whether it actually describes the results obtained. If the monomer volume fraction in a particle, ϕ_m, is assumed to be constant up to a certain conversion, then the rate of polymerization would be expected to be constant as expressed by Equation 3.46:

$$\frac{dP}{dt} = k_p \phi_m \bar{q} \left[\frac{N}{N_{Avo}}\right] \left[\frac{d_m}{d_p}\right] \qquad (3.46)$$

In the above expression, all of the other variables including number of particles, N, are constant. Constant rates of polymerization were obtained in the presence of heptane and cyclohexane after certain conversions as shown in Figures 21 and 22. Constant rates of polymerization were also observed by Blackley and Haynes (3), for the emulsion polymerization of styrene in the presence of ethylbenzene solvent. Seymour et al. (1,2) also observed constant rates of polymerization of styrene in the presence of a number of different solvents including hexane, heptane, octane, dibutylphthalate and diisoctylphthalate. Therefore, the polymerization rate in interval II can be assumed constant up to a certain conversion. Above this conversion, the decrease in monomer concentration in the latex particles, as

discussed in Chapter 3, is expected to reduce the rate of polymerization.

The retardation in the rates of polymerization caused by the addition of nonreactive liquid additives is more than that calculated on the basis of a reduced monomer concentration resulting from a dilution with solvent. This phenomenon may be explained by the model described earlier. As mentioned in Chapter 3, the presence of a relatively water insoluble additive depresses the activity of the monomer, and thus concentrates the monomer in the droplets. Therefore, at equilibrium the concentration of monomer in the latex particles is less than that calculated from simple dilution. Thus, the rate of polymerization obtained in the presence of heptane and cyclohexane was lower than that calculated on the basis of monomer dilution as shown in Figure 23. However, heptane was found to cause a greater degree of retardation (than cyclohexane) of the rate of polymerization as indicated in Figure 23. This reduction in the polymerization rate may be explained by diffusivity considerations within the polymer particles. As mentioned in Chapter 3, viscosity effects are quite prevalent in emulsion polymerization. Within the polymer particles, an increase in viscosity restricts the diffusion of all components including the macroradicals, the new radicals as well as the monomer itself. The monomer and a chain radical must diffuse through a region of solvent surrounding the active chain radical for

polymerization and termination reactions, respectively, to take place. This diffusive resistance through the solvent is an additional rate controlling resistance. As discussed in Chapter 3, it has been observed that a change in the viscosity of the reaction medium mainly affects the termination process and the influence on the propagation process is significantly less (27,28,66). Termination rate constants have been related to the viscosity of the medium by Equation 3.18:

$$\frac{k_t}{k_{t_0}} = \left[\frac{\eta_{p_0}}{\eta_p}\right] \qquad (3.18)$$

In the above equation, the rate of termination is inversely proportional to the viscosity. Hence, the addition of cyclohexane, which is more viscous than heptane retards the termination rate more than does heptane. This is expected to result in the existence of a number of chain radicals in a single particle, which in turn increases the molecular weight of the polybutadiene as well as the polymerization rate.

It has been ascertained by Ugelstad (93,94) and Blackley (3) that the addition of nonreactive solvents to the emulsion mixture increases the number of particles in the emulsion system. The emulsion polymerization theories (16,17) predict that the increase in surfactant concentration increases the number of particles in the emulsion. An attempt

will be made to explain the experimental results for various surfactant concentrations in the presence of heptane by postulating that the increase in the number of particles in the emulsion, when the surfactant concentration is increased, is greater in the presence of heptane. It is essential to test the validity of this postulate before using it to explain the experimental results. The experimental data for the rate of polymerization and the molecular weight were analysed to test the validity of the assumption. Utilizing Equation 3.46, it may be seen that a variation in surfactant concentration affects only the number of particles, N, all other parameters remaining constant.

$$\frac{dP}{dt} = k_p \phi_m \bar{q} \left[\frac{N}{N_{Avo}}\right] \left[\frac{d_m}{d_p}\right] \qquad (3.46)$$

Therefore, the equation for the rate of polymerization can be written as:

$$R_p = C_4 \cdot N \qquad (6.8)$$

At two levels of surfactant concentration, 1 and 2, the above equation can be written as:

$$\frac{R_{P_1}}{R_{P_2}} = \frac{N_1}{N_2} \qquad (6.9)$$

The rates of polymerization for surfactant concentrations of 0.3 and 0.03 mol.dm^{-3} as obtained from the Figure 27, are respectively, 15.3 and 4% conversion h^{-1}. The ratio of these rates are:

$$\frac{N_1}{N_2} = 3.82 \qquad (6.10)$$

If the increase in rate is attributed solely to an increase in number of particles, the number of particles were increased approximately four fold. If the concentration had been increased to 1 mol.dm^{-3}, the increase in the number of particles would have been 14.1 times as great:

$$N_1 = 14.1\ N_2 \qquad (6.11)$$

When the data for the rate of polymerization in the presence of heptane were inspected, the number of particles appeared to increase by a factor of 36.6 for an increase of surfactant concentration to 1 mol.dm^{-3}:

$$N_1 = 36.6\ N_2 \qquad (6.12)$$

Thus, it appears possible that the increase in the number of particles on increasing the surfactant concentration is enhanced by the presence of heptane.

Another test of the postulate concerning the effect of solvent on the number of particles will be attempted by com-

paring the resulting polymer molecular weights. It may be observed that in Equation 3.50 if all of the variables remain constant with an increase of surfactant concentration except the number of particles, the equation can be written as:

$$\bar{M}_n = C_5 \cdot N \qquad (6.13)$$

Comparing the molecular weights at two different level of surfactant concentrations the above equation can be written as:

$$\frac{\bar{M}_{n1}}{\bar{M}_{n2}} = \frac{N_1}{N_2} \qquad (6.14)$$

A comparison of the corresponding molecular weights showed an increase in the number of particles by a factor of 11 on increasing the surfactant concentration by 1 $mol.dm^{-3}$:

$$N_1 = 11\ N_2 \qquad (6.15)$$

The comparable ratio of number of particles obtained in the presence of heptane was

$$N_1 = 28.2\ N_2 \qquad (6.16)$$

These results also clearly support the assumption.

A comparison of Equations 6.11 and 6.12 with Equations 6.15 and 6.16 indicates little differences in the numerical values. The analysis of Equations 6.11 and 6.12 shows that the increase in the number of particles, when the surfactant concentration is increased by 1 $mol.dm^{-3}$, is enhanced by a factor of 2.59 by the presence of heptane. A similar analysis of Equations 6.15 and 6.16 indicates that this enhancement is by a factor of 2.56. However, the difference in the increase of number of particles from the rate of polymerization and molecular weight data analysis does not affect the postulate that there is an increase in the number of particles resulting from the presence of solvent. The difference in the numerical values is attributed to the fact that little is known regarding the precise chemistry of the hydroperoxide-polyamine initiation system as discussed in Section 2.1. In the development of theoretical model, the assumptions taken involve the production of identical free radicals, which may not be true for the redox initiation system used in the present investigation.

The experimental results for various surfactant concentrations in the presence of heptane may be explained by the postulate. As discussed in Chapter 3, the polymerization rate and the molecular weight of the polymer formed are directly proportional to the number of particles, and the number of particles increases with the increase in surfactant concentration. Therefore, the increase in surfactant concen-

tration results in an increase of the polymerization rate as well as the molecular weight of the polymer formed. However, the increase in the number of particles, when the surfactant concentration is increased, is greater in the presence of a solvent. Therefore, the increase in the rate of polymerization and in the molecular weight with an increase of surfactant concentration, is greater in the presence of heptane.

It may be seen from the theoretical model presented in Chapter 3 that the rate of polymerization is independent of the initiator concentration provided the number of particles remains constant. The experimental rate of polymerization of butadiene, with and without heptane, remained essentially independent of the redox initiator concentration. It may be considered from this observation that the number of particles are independent of the redox initiator concentration.

As is shown in Figure 31, the molecular weight reduces with the increase of initiator concentration. It is consistent with the prediction from the theoretical model that the increase in the initiator concentration causes a reduction in the molecular weight. However, the reduction observed in the presence of heptane was greater. As discussed above, the presence of heptane increases the viscosity of the reaction medium which may result in the presence of more than one free radical in the particle. The number of free radicals present in the particles is expected to increase with the increase of initiator concentration. As discussed in Sec-

tion 2.1 , the free radicals, generated by the hydroperoxide-amine initiation system, are not identical. Thus, the increase in number of free radicals might increase the rate of termination of the radicals which are more active. This would result in a greater reduction in the molecular weight.

The experimental results indicate that the addition of heptane and cyclohexane caused a reduction in the rate of polymerization as well as in the molecular weight of the polybutadiene obtained. Heptane was found to cause a greater degree of reduction (than cyclohexane) of the rate of polymerization and of the molecular weight. The addition of the additives have very little, if any, effect on the molecular structure of polybutadiene. The effect of the variation of surfactant concentration on the rate of polymerization and on the molecular weight was more dominant in the presence of an additive.

6.4 DEVELOPMENT OF DIFFUSIVITY CORRELATIONS FOR DILUTE LIQUID SOLUTIONS

Diffusivity data available in the literature were used for the development of a number of new correlations for the prediction of diffusion coefficients in liquid solutions. Different correlations were developed for different types of solutions including normal paraffin solutions, nonpolar solvents, and for aqueous solutions. A general correlation for all solvents and solutes was also developed. The correlating parameters used for the development of correlations included the molar volume, the parachor and the radius of gyration for both solutes and solvents.

A nonlinear optimization technique was used for developing the correlations. This technique is based on Box-modified Gauss method. The computer program for this technique is available at the University of Ottawa Computer Centre and is stored under the subroutine name NONLIN. The NONLIN program was modified to accomodate 800 data points whereas, the original version was programmed for only 100 data points. To use this program the form of the relationship and the choice of parameters needed to be specified, while the parameters best representing the data were calculated. Various forms of correlating equations of increasing complexity were utilized in each case and the resulting deviation between predicted values and experimental values were expressed as the sum of squares.

A viscosity-diffusivity map (95) for normal paraffin solutes dissolved in normal paraffin solvents at 25°C is shown in Figure 32. It was used as a basis for correlating diffusivities in normal paraffin solutions. It was found that diffusivities at one solvent viscosity could be correlated as a function of solute molar volume. The slopes of the lines were determined and related again to the solute molar volume. Thus a basic form of the correlation was obtained. The temperature was taken into account by considering the temperature index to be variable. The equation developed was:

$$D^{\circ}_{AB} = 13.3(10^{-8}) \frac{T^{1.47}}{V_A^{0.71}} \eta_B^{[\frac{10.2}{V_A} - 0.791]} \qquad (6.17)$$

This correlation was developed utilizing 58 data points for normal paraffin solutes containing 5 to 32 carbons and for normal paraffin solvents containing 5 to 16 carbons. These data were taken from sources listed in references (53) and (95). After a number of trials using equations of different form, Equation 6.17 yielded the lowest average deviation of 3.4% from the experimental results. Such a good correlation suggests that the mechanism for diffusion of all long-chained paraffin solutes in paraffin solvents is similar. In addition, an inspection of the complex index of the viscosity term in Equation 6.17 indicates the existance of an

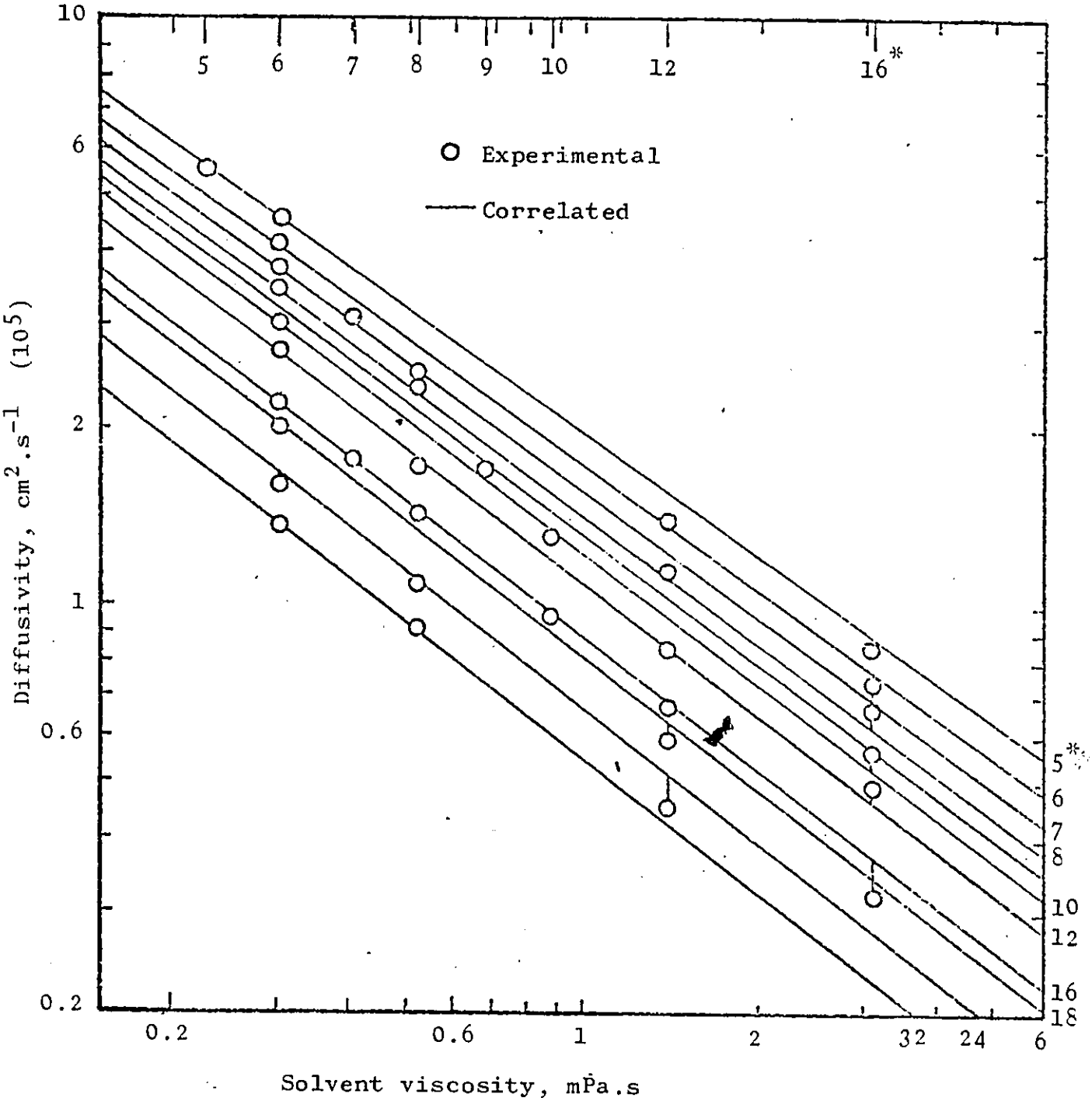

Figure 32 - Diffusivities at infinite dilution and at 25°C of normal paraffins in normal paraffin solvents

*number of carbons in normal paraffins

interaction between the solute molar volume and solvent viscosity.

A comparison of experimental data with the predicted values for solutions of paraffins is shown in Figure 33. The predicted values are generally in very good agreement with the experimental ones. Minor deviations are observed with the low diffisivities in the high molecular weight solvents, dodecane and hexadecane. Statistical tests were performed to ensure that the equation adequately represented the data. These are outlined in Appendix J.

It was next determined whether further improvements to the predictive equations for diffusivity at infinite dilution in water were possible utilizing the nonlinear regression technique. Seven different nonlinear models were developed and compared utilizing some 237 data points referred to by Tyn and Calus (53) and Hayduk and Laudie (55). All of the correlations developed are compared in Table 38 of Appendix J. The average percent absolute error may be seen to decrease with an increase in complexity of the form of equation. The slightly complex form of the equation giving the lowest average deviation from the experimental data is as follows:

$$D^{\circ}_{AB} = \left[\frac{1.25}{V_A^{0.19}} - 0.365\right](10^{-8})\, \eta_B^{\left[\frac{9.58}{V_A} - 1.12\right]}\, T^{1.52} \qquad (6.18)$$

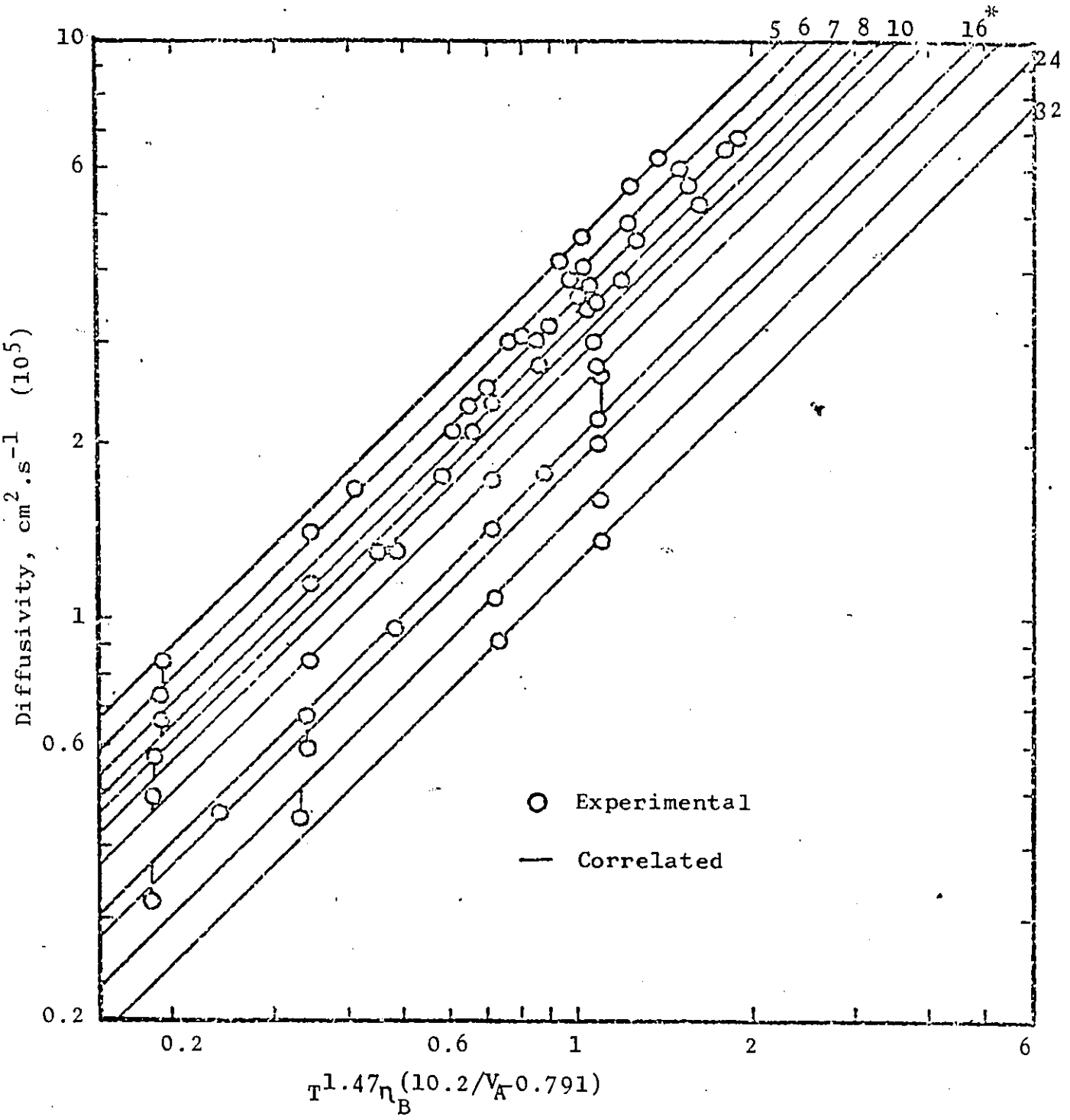

Figure 33 - Diffusivities at infinite dilution in normal paraffin solutions versus the factor $T^{1.47}\eta_B(10.2/V_A-0.791)$ at various temperatures

*number of carbons in normal paraffins

Equation 6.18 yielded an average deviation of 9:4% as compared with a comparable deviation of 10.3% from the Hayduk and Laudie correlation and was considered a significant improvement for predicting diffusivities in water. A residual plot indicated that the form of the equation was adequate.

Yet another general correlation was developed for the prediction of diffusion coefficients based on all of the data points available including those for paraffin solutions and aqueous solutions. The data sources may be found in several compilations (47,53,55,95). The new general correlation, based on parachor values for both solute and solvent and yielding the lowest average error for prediction purposes is as follows:

$$D^{\circ}_{AB} = 1.55(10^{-8}) \frac{T^{1.29}}{\eta_B^{0.92}} \frac{1}{V_B^{0.23}} \frac{\mathbb{P}_B^{0.5}}{\mathbb{P}_A^{0.42}} \qquad (6.19)$$

Equation 6.19 was compared with the Tyn and Calus and with Wilke-Chang correlations in Table 39 of Appendix J. Equation 6.19 yielded an average error for prediction of 13.9%, as compared with 14.2%, and 16.1% for the Tyn and Calus, and the Wilke-Chang correlations, respectively. It was further observed that the equations based on the parachor values had significantly lower average errors than those simply based on molar volumes. It was possible to exclude the molar volume of the solute entirely from the correlations and to obtain good correlations as long as the corresponding parachor values were utilized. The rules applied for the polar or

associating substances were the same as those specified by Tyn and Calus in their correlation. The adequacy of the general correlation was tested by plotting the residuals versus the predicted values; a random distribution was observed. Statistical tests were also performed for the adequacy of the correlation as discussed in Appendix J.

A general correlation was also developed using the radius of gyration as a parameter for both solutes and solvents. Only available radius of gyration values for most common substances were utilized; hence, not all of the diffusivity data available could be utilized in the development of correlations. Based on 436 data points for which radii of gyration were available, the following correlation was obtained:

$$D^{\circ}_{AB} = 6.916(10^{-10}) \frac{T^{1.7}}{\eta_B^{0.8}} \frac{R_B^{0.2}}{R_A^{0.4}} \qquad (6.20)$$

Equation 6.20 was effective in correlating the data with an average error of 14.3% which can be compared with the average error of 14.2% for the Tyn and Calus correlation as shown in Table 39 of Appendix J. In this case, although the form of the equation is somewhat simpler than that of Tyn and Calus, no improvement in accuracy was obtained. A correlation was also developed for nonpolar solvents only. Based on 254 diffusivity data for which radii of gyration were easily available, the following correlation was developed:

$$D^{\circ}_{AB} = 13.82(10^{-10}) \frac{T^{1.6}}{\eta_B^{0.78}} R_B^{0.31} R_A^{-0.4} \qquad (6.21)$$

Equation 6.21 correlated the data with an average error of 13.4% which is identical to the average error obtained from Equation 6.20 when used only 254 data for nonpolar solvents. Therefore, it is considered that Equation 6.20 can be used as effectively as Equation 6.21 for predicting diffusivities in nonpolar solvents.

A comparison of the various equations on the basis of percent average error are summarized in Table 40 of Appendix J. Several of the newly developed correlations yield significantly lower probable errors when compared with those for other available correlations. These correlations have been reported in the literature (67).

Chapter VII

CONCLUSIONS

Although it has been shown that emulsion polymerization of butadiene can be performed at atmospheric pressure by dissolving it in heptane or cyclohexane, the addition of these additives caused a significant reduction in the rate of polymerization and the molecular weight of the polymer formed. This was considered to indicate that the presence of water insoluble additive depresses the monomer activity in the polymerizing particles resulting in the reduction of polymerization rate and the molecular weight. It was found that, in the presence of an additive, though the rate of polymerization was always lower, its dependence on the surfactant concentration was greater than for comparable conditions without an additive. Thus, it was concluded that in the presence of an additive there is a greater fractional increase in number of particles in the emulsion when the surfactant concentration is increased than without an additive.

As in the emulsion polymerization of butadiene without any solvent, a variation of initiator concentration was found to have very little effect on the rate of polymerization. Hence, it was concluded that the number of latex particles was independent of the initiator concentration as for

conventional emulsion polymerization. It was also concluded that an increase in initiator concentration reduced the molecular weight of the polymer to a greater extent in the presence of a solvent than without it. Finally, it is concluded that the relative proportions of cis-1,4, vinyl and trans-1,4 structures remain essentially constant upon the addition of heptane or cyclohexane solvents to the butadiene emulsion mixture.

A theoretical model may be used to explain the experimental results by taking into account the viscosity of the additive and its effect on the activity of the monomer. The mathematical equation developed for the monomer concentration in the micelle in the presence of an additive is given below:

$$F_{m_2} = \frac{S_m x_m}{S_m x_m + S_a(1-x_m)} \qquad (3.3)$$

The resulting rate of polymerization and the molecular weight of the polymer are represented by the following equations:

$$\frac{dP}{dt} = 0.369 \left[\frac{k_p \cdot d_m \phi_m \cdot A}{N_{Avo}\, d_p}\right]^{0.6} (R(1 - \phi_m - \phi_a))^{0.4}\, \bar{q} \qquad (3.48)$$

$$\bar{M}_n = 0.369 \left[\frac{k_p d_m \phi_m A}{R}\right]^{0.6} [N_{Avo}\, d_p (1 - \phi_m - \phi_a)]^{0.4} \qquad (3.52)$$

Based on the solubility experiments it may be concluded that butadiene is only slightly soluble in water, but is solubilized in aqueous potassium laurate surfactant solutions. For a surfactant concentration of 40 $g.dm^{-3}$, the butadiene solubility increased by 300% at otherwise comparable conditions. Butadiene was also found to be highly soluble in heptane.

Based on the supplementary portion of this investigation involving the correlation of diffusivities, it is concluded that the two new correlations developed for estimating diffusivities in dilute aqueous and dilute paraffin solutions are significantly more accurate than those currently available in the literature. These correlations are for dilute aqueous solutions, and for dilute paraffin solutions, respectively:

$$D^{\circ}_{AB} = 13.3(10^{-8})\ \frac{T^{1.47}}{V_A^{0.71}}\ \eta_B^{\left[\frac{10.2}{V_A} - 0.791\right]} \qquad (6.17)$$

$$D^{\circ}_{AB} = \left[\frac{1.25}{V_A^{0.19}} - 0.365\right](10^{-8})\ \eta_B^{\left[\frac{9.58}{V_A} - 1.12\right]}\ T^{1.52} \qquad (6.18)$$

REFERENCES

1. Seymour, R.B., Owen, D.R., Tinnerman, W.N., Lasada, C.J., Polymer Preprints, 16, 1, 261-6 (1975)

2. Owen, D.R., McLemore, D., Liu, Wan-Li, Seymour, R.B., Tinnerman, W.N., ACS Symposium Series, No.24, 299 (1976)

3. Blackley, D.C., Haynes, A.C., British Polymer J., 9, 312 (1977)

4. Azad, A.R.M., Fitch, R.M., Namura, M., ACS Symposium Series, No.165, 357 (1981)

5. Bowden, M.J., in Macromolecules, An Introduction to Polymer Science, Ed. by Bovey, F.A., Winslow, F.H., Academic Press, N.Y. (1979)

6. Hakoila, E., Annals Universitatis Turkuensis, Ser. A, 66, 7 (1963)

7. Bacon, R.G.R., Q. Rev. Chem. Soc., 9, 287 (1955)

8. Whitby, G.S., Wellman, N., Floutz, V.W., Stephens, H.L., Ind. Eng. Chem., 42, 445 (1950)

9. Blackley, D.C., Emulsion Polymerization, Applied Science Publishers Ltd., London, P. 244 (1975)

10. Rodriguez, F., Principles of polymer Systems, Hemisphere Pub. Corp. N.Y., P. 116 (1982)

11. Blackley, D.C., Emulsion Polymerization. Applied Science Publishers Ltd., London, P. 260 (1975)

12. Shinoda, K., 'Solvent properties of nonionic surfactant in aqueous solutions' in 'Solvent Properties of Surfactant Solutions' (ed. K. Shinoda), Marcel Dekker, N.Y., PP. 27-63 (1967).

13. Bovey, F.A., Kolthoff, I.M., Medalia, A.I., Meehan, E.J., Emulsion Polymerization, Interscience Publishers Inc., N.Y., p 15, (1955)

14. Harkins, W.D., J. Chem. Phys., 13, 381 (1945)

15. Harkins, W.D., J. Chem. Phys., 14, 47 (1946)

16. Smith, W.V., Ewart, R.H., J. Chem. Phys., 16, 592 (1948)

17. Gardon, J.L., J. Polym. Sci., Pt. A-1, 6, 623 (1968)

18. Gardon, J.L., J. Polym. Sci., Pt. A-1, 6, 643 (1968)

19. Gardon, J.L., J. Polym. Sci., Pt. A-1, 6, 665 (1968)

20. Gardon, J.L., J. Polym. Sci., Pt. A-1, 6, 687 (1968)

21. Gardon, J.L., J. Polym. Sci., Pt. A-1, 6, 2853 (1968)

22. Gardon, J.L., J. Polym. Sci., Pt. A-1, 6, 2859 (1968)

23. Flory, P.J., Principles of Polymer chemistry, PP. 106-177, Ithaca, N.Y. Cornell Univ. Press (1953)

24. Norrish, G.W., Brookman, E.F., Proc. Royal Soc., London (A) 171, 147 (1939)

25. Trommsdorff, E., Kohle, H., Lagally, P., Makromol. Chem., 1, 106 (1947)

26. Bengough, W.I., Melville, H.W., Proc. Royal Soc., London (A) 230, 429 (1955)

27. Hayden, P., Melville, H.W., J. Polym. Sci., 43, 201 (1960)

28. Fischer, J.P., Mucke, G., Schulz, G.V., Ber. Bunsenges. Phys. Chem., 73, 154 (1969)

29. Fischer, J.P., Mucke, G., Schulz, G.V., Ber. Bunsenges. Phys. Chem., 74, 1077 (1970)

30. Bovey, F.A., Kolthoff, I.M., Medalia, A.I., Mechan, E.J., Emulsion Polymerization, Interscience Publishers, N.Y., P. 101 (1955)

31. Hildebrand, J.H., Scott, R.L., The Solubility of Non electrolytes, Reinhold Publishing Corp., N.Y., 3rd ed. (1950)

32. Hampton, R.R., Anal. Chem., 21, 923 (1949)

33. Benoit, M., Grubisic, Z., Rempp, R., J. Polym. Sci., 5, 753 (1967)

34. Binder, J.L., Analyt. Chem., 26, 1877 (1954)

35. Richardson, W.S., J. Polym. Sci., 13, 229 (1954)

36. Prausnitz, J.M., 'Molecular Thermodynamics of Fluid Phase Equilibria', Prentice-Hall Inc., Englewood Cliffs, N.J., PP. 351-384 (1969)

37. Hildebrand, J.H., Prausnitz, J.M., Scott, R.L., 'Regular and Related Solutions', Van Nostrand Reinhold Co., N.Y. (1970)

38. Hayduk, W., Laudie, H., AIChE J, 19, 1233 (1973)

39. Miyano, Y., Hayduk, W., Can. J. Chem. Eng., 59, 746 (1981)

40. Krischevsky, I.R., Zh. Fiz. Khim., 9, 41 (1937)

41. O'Connell, J.P., Prausnitz, J.M., Ind. Eng. Chem. Fundamentals, 3, 347 (1965)

42. Klevens, H.B., Chem. Rev., 47, 1 (1950)

43. McBain, M.E.L., Hutchinson, E., 'Solubilization and Related Phenomena', Acad. Press, N.Y. (1955)

44. McBain, J.W., Richards, P.H., Ind. Eng. Chem., 38, 642 (1946)

45. Stearns, R.S., Oppenheimer, H., Simon, E., Harkins, W.D., J. Chem. Phys., 15, 496 (1947)

46. Reid, R.C., Prausnitz, J.M., Sherwood, T.K., 'The Properties of Gases in Liquids', 3rd ed. McGraw Hill Book Co., N.Y., P. 567 (1977)

47. Ghai, R.K., Ertl, H., Dullien, F.A.L., AIChE J, 19,881 (1973)

48. Ghai, R.K., Ertl, H., Dullien, F.A.L., AIChE J, 20, 1 (1974))

49. Wilke, C.R., Chang, R., AIChE J, 1, 262 (1955)

50. Scheibel, E.G., Ind. Eng. Chem., 46, 2006 (1954)

51. Reddy, K.A., Doraiswamy, L.K., Ind. Eng. Chem. Fundamentals, 6, 77 (1967)

52. King, C.J., Hsueh, L., Mao, K-W, J. Chem. Eng. Data, 10, 348 (1965)

53. Tyn, M.T., Calus, W.F., J. Chem. Eng. Data, 20, 106 (1975)

54. Othmer, D.F., Thākar, M.S., Ind. Eng. Chem., 45, 589 (1953)

55. Hayduk, W., Laudie, H., AIChE J, 20, 611 (1974)

56. Himmelblau, D.M., Chem. Rev., 64, 527 (1964)

57. Lewis, G.N., Randall, M., 'Thermodynamics', Revised by Pitzer, K.S., Brewer, L., McGraw Hill Book Co., N.Y., PP. 243, 483 (1961)

58. Ugelstad, J., Makromol. Chem., 179, 815 (1978)

59. Ugelstad, J., Ellingsen, T., Kaggerud, K.H., 'Adv. in Organic Coating Sci., P. Techn. Athens 17-21 July (1978) Preprints.

60. Ugelstad, J., Polymer Colloid Group Newsletter, 9, 1, May (1980)

61. Ugelstad, J., Polymer Colloid Group Newsletter, 9, 1, June (1980)

62. Ugelstad, J., Mork, P.C., Paper presented at Third International Conference on Surface and Colloid Science, Stockholm, 20-25 August (1979) Preprints.

63. Ugelstad, J., Mork, P.C., Kaggerud, K.H., Ellingsen, T., Berge, A., Adv. in Coll. and Interface sci., 13, 101-140 (1980)

64. Ugelstad, J., Mork, P.C., Kahn, A.A., ACS Org. Coat. and plast. Chem., Preprints, 43, 514 (1980)

65. Mayer,G., Schulz, G.V., Makromol. Chem., 173, 101 (1973)

66. Allen, P.E.M., Patrick, C.R., 'Kinetics and Mechanics of Polymerization Reactions', P. 94, Halsted Press, N.Y. (1974)

67. Hayduk, W., Minhas, B.S., Can. J. Chem. Eng., 60, 299, (1982)

68. Saltman, W.M. in 'Encyclopedia of Polymer Science and Technology', Edited by Herman Mark, Bikales, N., Interscience Publishers, Inc., N.Y. Vol.2, PP. 680-683 (1965)

69. Mayers, C.H., Cragoe, C.S., Mueller, E.F., J. Res. Natl. Bur. Stds., 39, 507 (1947)

70. McBain, J.W., Int. Crit. Tables, 5 (1926)

71. Bury, C.R., Parry, G.A., J. Chem. Soc. (London) 626 (1935)

72. Gallant, R.W., 'Physical Properties of Hydrocarbons', Vol.2, Gulf Publishing Co., Houston, Texas (1970)

73. Gallant, R.W., 'Physical Properties of Hydrocarbons', Vol.1, Gulf Publishing Co., Houston, Texas (1970)

74. Laudie, H., 'Emulsion Polymerization of Vinyl Chloride', Ph.D. Thesis, University of Ottawa (1977)

75. Saltman, W.N., in 'Encyclopedia of Polymer Science and Technology', Edited by Herman Mark, Bikales, N., Interscience Publishers, Inc., N.Y. Vol.2, 69 6 (1965)

76. Anderson, H.M., J. Polym. Sci., A-1, 4, 783 (1966)

77. Anderson, H.M., J. Polym. Sci., A-1, 7, 2889 (1969)

78. Park, W.S., Graessley, W.W., J. Polm. Sci., Polymer Physics Ed., 15, 71-83 (1977)

79. Rochefort, W.E., Smith, G.G., Rachapudy, H., Raju, V.R., Graessley, W.W., J. Polym. Sci., Polymer Physics Ed., 17, 1197-1210 (1979)

80. Godon, S., 'Infrared Studies of Polymers for Classification Purposes', B.A.Sc. Thesis, University of Ottawa (1976)

81. Hayduk, W., Cheng, S.C., Can. J. Chem. Eng., 48, 93 (1970)

82. Malik, V.K., Hayduk, W., Can. J. Chem. Eng., 46, 462 (1968)

83. Weast, R.C., Ed., 'Handbook of Chemistry and Physics', 48th Edition, P. F-10, Chemical Rubber Publ., Cleveland, Ohio, 1967-68

84. Perry, R.H., Chilton, C.H., Eds., 'Chemical Engineers' Handbook', 5th Ed., P. 3-71, McGraw Hill, N.Y.

85. Sata, N., Tyuzyo, K., Bull. Chem. Soc., Japan, 26, 177 (1953)

86. Hess, V.K., Philippoff, W., Kiessig, H., Kolloid Z., 88, 40 (1939)

87. Harkins, W.D., J. Am. Chem. Soc., 69, 1428 (1947)

88. Klevens, H.B., J. Colloid Sci., 2, 301, (1947)

89. Hayduk, W., Castaneda, R., Can. J. Chem. Eng., 51, June (1973)

90. Hall, D.G., Pethica, B.A. in 'Nonionic Surfactants', Shick, M.J., Ed., Marcel Dekker, N.Y. (1967)

91. Ugelstad, J., Mork, P.C., Dahl, P., Rangres, P., J. Poly. Sci., 27, 49 (1969)

92. Morton, M., Salatiello, P.P., J. Polym. Sci., 8, 215 (1952)

93. Azad, A.R.M., Ugelstad, J., Fitch, R.M., Hensen, F.K., ACS Symposium Series, 24, (1976)

94. Azad, A.R.M., Fitch, R.M., Ugelstad, J., Polymer Reprints, 16, 1, 131-142 (1975)

95. Hayduk, W., Ioakimidis, S., J. Chem. Eng. Data, 21, 255 (1976)

Appendix A

Physical properties of aqueous potassium laurate solutions

A.1 TREATMENT OF DATA FOR DENSITY OF POTASSIUM LAURATE SOLUTIONS

Potassium laurate solutions densities were measured by Anton Model DMA02C digital precision densitometer. It was calibrated by two fluids, dried air and distilled water. The density for dried air at 4°C, 0.0012743 $g.cm^{-3}$, was obtained from Weast (83) and for distilled water at 4°C, 1.0 $g.cm^{-3}$, was obtained from Perry et al. (84). The measured vibration frequencies for dried air and distilled water were 176933 and 239554, respectively. The calibration constant, B, was calculated from the following equation:

$$d_A - d_B = 1/B(T_A^2 - T_B^2)$$

$$1 - 0.0012743 = 1/B((239554)^2 - (176933)^2)$$

$$B = 2.61141(10^{10})$$

Sample calculation:

For a 30.49 $g.dm^{-3}$ concentration of potassium laurate solution the vibration frequency obtained was 239742. Thus the density of this solution will be

$$d_A - 1 = 1/2.61141*10^{10}\ [(239742)^2 - (239554)^2]$$

$$d_A = 1.00345\ g.cm^{-3}$$

TABLE 9

Density and viscosity of aqueous potassium laurate solutions at 4°C

Concentration ($g.dm^{-3}$)	Density ($g.cm^{3}$)	Viscosity (mPa.s)	Reduced Viscosity ($dm^{3}.g^{-1}$)
0.000	1.0000	0.01547	
0.528	1.0001	0.01551	0.00496
0.970	1.0002	0.01553	0.00411
1.511	1.0003	0.01569	0.00922
1.997	1.0003	0.01572	0.00799
2.547	1.0004	0.01598	0.01285
3.964	1.0006	0.01605	0.00937
5.172	1.0007	0.01620	0.00917
5.958	1.0009	0.01621	0.00804
9.919	1.0013	0.01649	0.00663
12.052	1.0015	0.01641	0.00501
15.063	1.0018	0.01672	0.00536
19.946	1.0024	0.01737	0.00615
26.836	1.0031	0.01792	0.00589
30.490	1.0035	0.01855	0.00653

TABLE 10

Effect of temperature on critical micelle concentration for potassium laurate

Temperature (°C)	cmc ($g.dm^{-3}$)	Reference
4	2.5	Present work
26	5.72	84
35	6.43	85
45	7.27	85
55	8.34	85
65	10.0	85

Appendix B

Solubility of butadiene in heptane, water and aqueous potassium laurate solutions

B.1 TREATMENT OF DATA FOR SOLUBILITY OF BUTADIENE

Solubilities of butadiene, expressed as Ostwald coefficients, were calculated from the measured volume of vapor-free gas required to saturate the corresponding solvent volume by means of the following equation:

$$L = \frac{V_G P_t}{V_L [P_t - P_A^\circ (1-x_A)} \qquad (B.1)$$

The mole fraction solubility was determined by:

$$x_A = \frac{L/V_G}{L/V_G - 1/V_L} \qquad (B.2)$$

An iterative calculation process was used for calculating L and x. An initial value of x was chosen; L and x were then calculated. The calculation was repeated with the new value of x until the difference in successive calculated values of x was negligible. Gas molar volumes were obtained from literature sources (62,63).

TABLE 11

Solubility of butadiene in heptane at various temperatures

Temperature (°C)	x	x(average)	L	L(average)
4	0.6671	0.6680	304.1	305.4
	0.6689		306.6	
25	0.3590	0.3537	84.88	83.06
	0.3643		87.33	
	0.3578		84.29	
	0.3338		75.73	
50	0.2092	0.2104	36.43	36.67
	0.2117		36.92	

TABLE 12

Comparison of experimental solubility of butadiene in heptane with those predicted from theoretical correlations

Temperature (°C)	x_1	x_2	Equation 2.20	Equation 2.21
4	0.6880	0.7285(5.8)	0.7144(3.8)	0.8038(16.8)
25	0.3537	0.3610(2.1)	0.3545(0.2)	0.3964(12.1)
50	0.2104	0.1787(-15.0)	0.1758(-16.4)	0.1951(-7.3)

*value in brackets indicates percentage deviation

%Deviation = (Predicted - Expt'l)100/Expt'l

TABLE 13

Solubility of butadiene in water and aqueous potassium laurate solutions at 4°C

Potassium laurate ($g.dm^{-3}$)	Mol.fr.of butadine	Ostwald coeff.
0.0	0.00068	0.806
5.16	0.00072	0.852
10.05	0.00080	0.949
15.10	0.00093	1.112
20.07	0.00105	1.252
25.18	0.00120	1.434
30.47	0.00143	1.672
35.31	0.00160	1.897
40.11	0.00185	2.220

Appendix C

Solubility of butadiene in styrene-heptane mixtures

TABLE 14

Density and refractive index at 25°C for styrene-heptane mixtures

Styrene composition (% volume)	Density ($g.cm^{-3}$)	Refractive index
100	0.9012	1.544
90	0.8794	1.529
80	0.8575	1.514
70	0.8351	1.488
60	0.8132	1.483
50	0.7906	1.465
40	0.7684	1.450
30	0.7458	1.434
20	0.7234	1.421
10	0.7011	1.402
0	0.6789	1.386

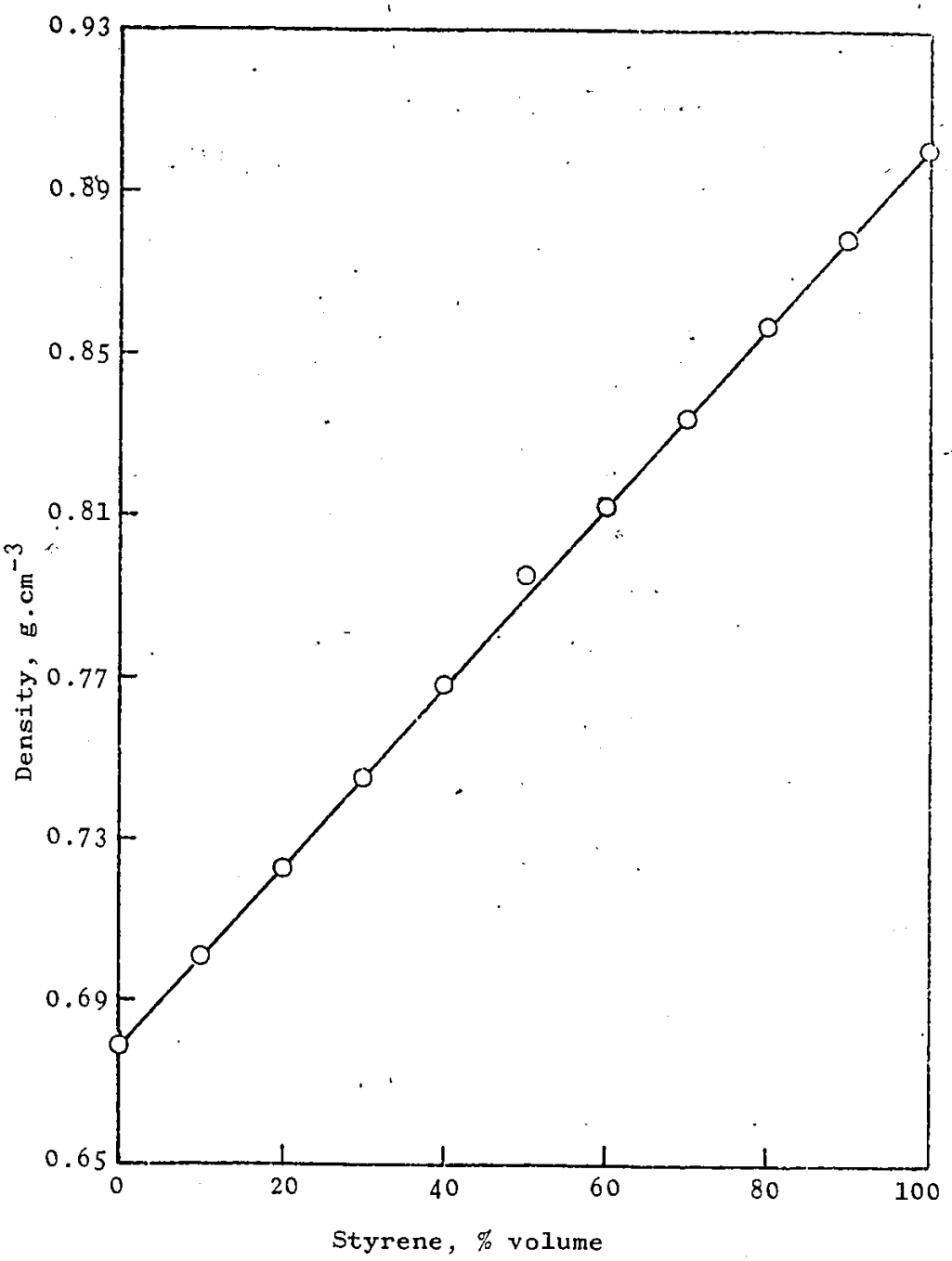

Figure 34 - Density of styrene-heptane mixtures versus mixture composition at 25°C

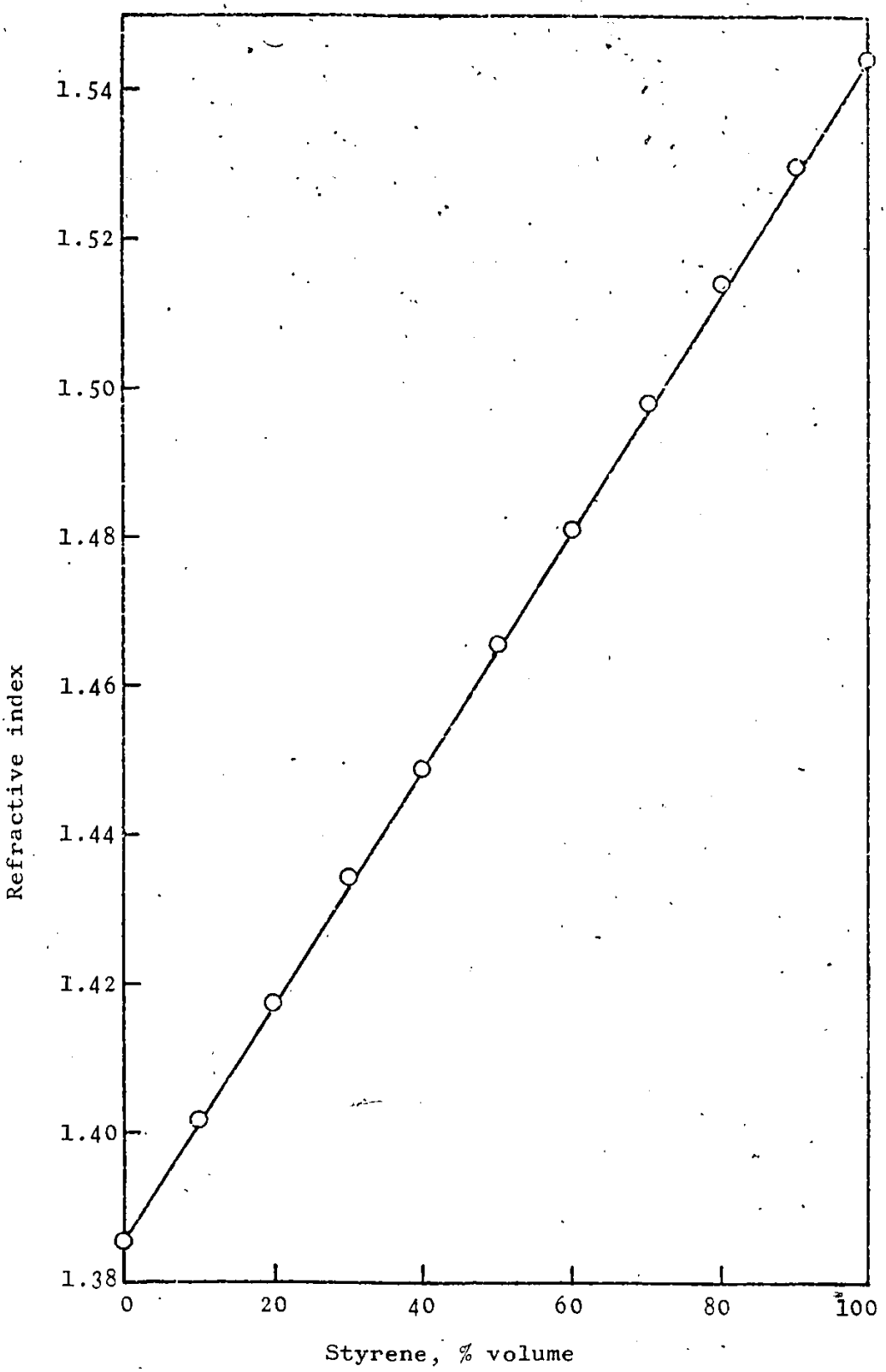

Figure 35 - Refractive index of styrene-heptane mixtures versus mixture composition at 25°C

TABLE 15

Solubility of butadiene in styrene-heptane mixtures at 4°C

Mol.fr. of styrene	Mol.fr. of butadiene	Ostwald coeff.
0.000	0.668	305.4
0.054	0.679	323.0
0.100	0.682	328.0
0.144	0.688	338.2
0.196	0.700	358.9
0.259	0.698	363.2
0.315	0.703	374.8
0.486	0.704	395.1
0.541	0.700	396.7
0.585	0.694	397.7
0.680	0.695	409.8
0.703	0.707	407.1
0.751	0.698	407.8
0.879	0.692	406.8
0.968	0.683	403.4
1.000	0.680	398.9
1.000	0.683	395.6

TABLE 16

Comaprison of experimentally determined solubility of butadiene in styrene-heptane mixtures at 4°C with those predicted from theoretical correlations

Mol.fr. of styrene	x	Equation2.20	Equation2.21
0.000	0.728(9.0)*	0.714(6.9)	0.804(20.3)
0.054	0.728(7.2)	0.725(6.8)	0.801(17.9)
0.100	0.728(6.7)	0.724(6.1)	0.797(16.8)
0.144	0.728(5.8)	0.723(5.0)	0.794(15.3)
0.196	0.728(4.1)	0.721(3.1)	0.789(12.8)
0.259	0.728(4.4)	0.719(3.0)	0.784(12.3)
0.315	0.728(3.5)	0.716(1.9)	0.778(10.7)
0.486	0.728(3.4)	0.706(0.3)	0.760(7.9)
0.541	0.728(4.1)	0.702(0.2)	0.754(7.6)
0.585	0.728(4.9)	0.698(0.5)	0.748(7.7)
0.680	0.728(4.7)	0.688(-1.1)	0.734(5.5)
0.703	0.728(3.1)	0.685(-3.1)	0.730(3.3)
0.751	0.728(4.4)	0.678(-2.8)	0.722(3.4)
0.879	0.728(5.3)	0.656(-5.1)	0.695(0.5)
0.968	0.728(6.6)	0.633(-7.3)	0.670(-1.9)
1.0	0.728(7.1)	0.336(-50.6)	0.346(-49)
1.0	0.728(6.7)	0.336(-50.6)	0.346(-49)

* Values in brackets indicate percentage deviation.

% Deviation = (predicted - Expt'l)100/Expt'l

TABLE 17

Comparison of experimentally determined solubility of butadiene in styrene-heptane mixtures at 4 °C with those predicted using Equations 2.24 and 2.25

Mol.fr. of styrene	Equation2.24	Equation2.25	Equation2.25*
0.054	0.669(-1.5)[a]	0.642(-5.4)	0.674(-0.7)
0.100	0.669(-1.9)	0.623(-8.7)	0.679(-0.5)
0.144	0.670(-2.7)	0.607(-11.8)	0.683(-0.7)
0.196	0.671(-4.2)	0.591(-15.5)	0.688(-1.7)
0.259	0.671(-3.8)	0.576(-17.4)	0.692(-0.7)
0.315	0.672(-4.4)	0.566(-19.6)	0.696(-1.1)
0.486	0.675(-4.2)	0.552(-21.6)	0.702(-0.3)
0.541	0.675(-3.6)	0.554(-20.9)	0.702(0.4)
0.585	0.676(-2.6)	0.557(-19.8)	0.702(1.2)
0.680	0.677(-2.6)	0.569(-18.1)	0.701(0.8)
0.703	0.677(-4.2)	0.573(-18.8)	0.700(-0.9)
0.751	0.678(-2.9)	0.584(-16.3)	0.699(0.1)
0.879	0.680(-1.7)	0.624(-9.7)	0.691(0.0)
0.968	0.681(-0.3)	0.664(-2.7)	0.684(0.2)

*Binary interaction parameter empirically calculated as 0.17

[a]Value in brackets indicate percentage deviation

% Deviation = (Predicted - Expt'l)100/Expt'l

Appendix D

Diffusivity of butadiene in heptane

D.1 TREATMENT OF DATA FOR DIFFUSIVITY OF BUTADIENE

The mathematical analysis for measuring diffusivity by the steady state capillary cell method has been elaborated on earlier (81). Using Fick's first law of diffusion and assuming the mass density of the solute in the liquid approximately equal to that of the solvent, the following equation results:

$$D^{\circ}_{AB} = \frac{j_A \cdot \ell}{d} \left[\ell n\left(\frac{1+W_{Ao}}{1+W_{A\ell}}\right)\right]^{-1} \qquad (D.1)$$

Another equation similar to the one above can be derived assuming constant molar concentration along the diffusion path

$$D^{\circ}_{AB} = \frac{J_A \cdot \ell}{c} \left[\ell n\left(\frac{1+C_{Ao}}{1+C_{A\ell}}\right)\right]^{-1} \qquad (D.2)$$

For the calculation of the diffusivity of butadiene in heptane, Equation D.1 was used as the percent difference between the effective mass densities of solute and solvent was less than the effective molar volumes of solute and solvent.

TABLE 18

Diffusivity of butadiene in heptane

Temperature (°C)	Diffusivity $(cm^2.s^{-1})(10^5)$	Average diffusivity $(cm^2.s^{-1})(10^5)$
25	3.76	3.51
	3.48	
	3.22	
	3.57	
50	5.05	4.66
	4.26	
	4.68	

Appendix E

Calibration of Gel Permeation Chromatography

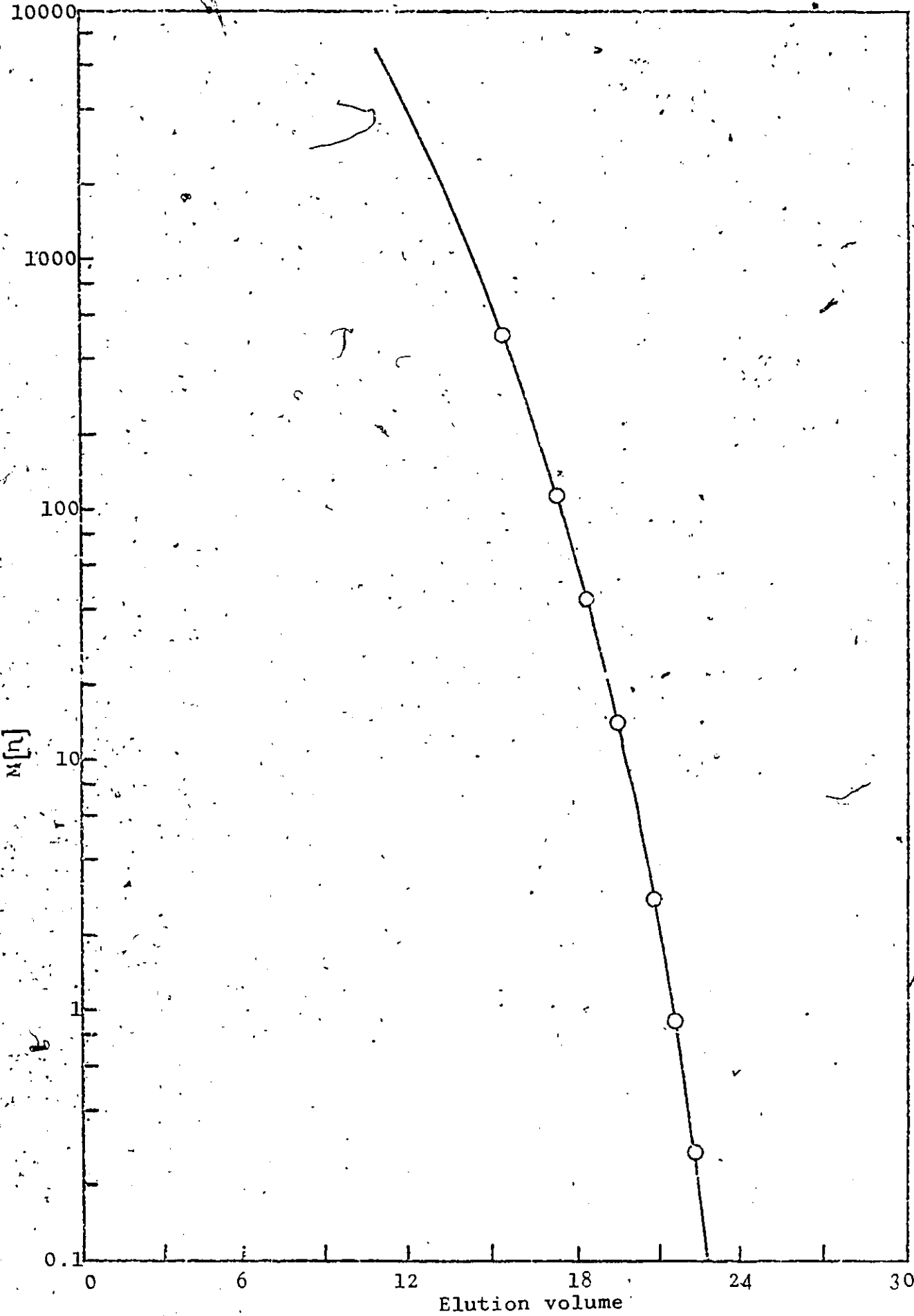

Figure 36 - Gel Permeation Chromatography calibration curve

E.1 CALCULATION OF $\bar{M}_n$ AND $\bar{M}_w$ FROM GPC CURVE

The retention volume and peak height for about fifteen equally spaced points along the GPC curve were measured. The molecular weights for the respective retention volumes were calculated utilizing the Mark-Houwink equation as discussed in Section 5.2.

$$[\eta] = \Omega M^{\omega} \tag{E.1}$$

$$M = \left[\frac{M[\eta]}{\Omega}\right]^{1/\omega+1} \tag{E.2}$$

The M $[\eta]$ values for the respective retention volumes obtained from the calibration curve are shown in Figure 36.

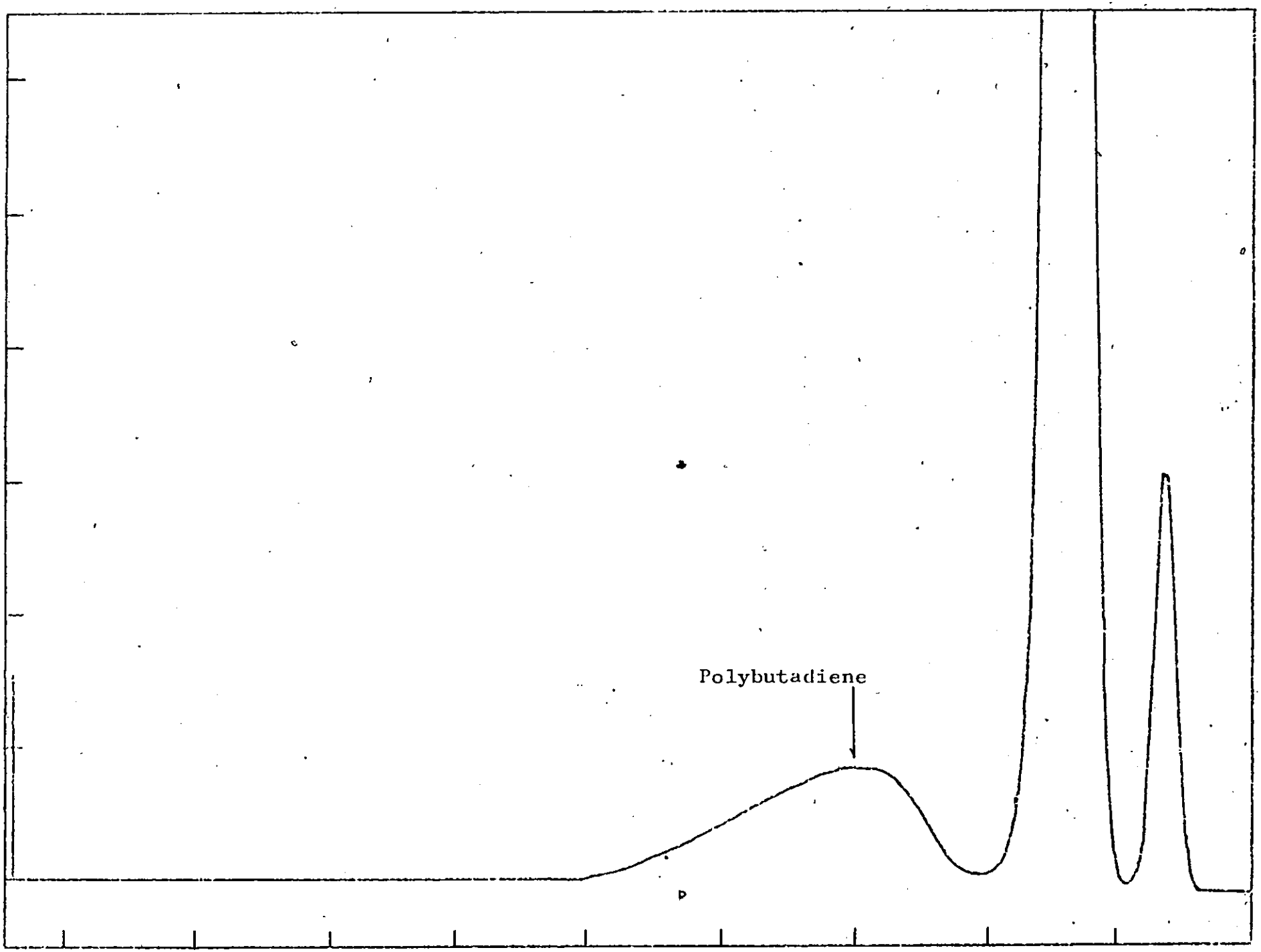

Figure 37 - Molecular weight distribution curve of a polybutadiene sample formed at 10°C

TABLE 19

Calculation of $\bar{M}_n$ and $\bar{M}_w$ from GPC curve

1	2	3	4	5	6
Retention vol.(cm^3)	Height (mm)	M [η]	Mol. Wt.	Col2/Col4	Col2xCol4
13.8	2.4	1450000	4.0092x10	5.9862x10	9.6221x10
14.4	4.4	1000000	3.2422x10	1.3571x10	1.4266x10
15.0	6.4	660000	2.5570x10	2.5029x10	1.6365x10
15.6	9.5	430000	2.0017x10	4.7460x10	1.9016x10
16.2	11.9	270000	1.5343x10	7.7560x10	1.8258x10
16.8	14.3	160000	1.1378x10	1.2568x10	1.6271x10
17.4	16.7	105000	8.9438x10	1.8672x10	1.4936x10
18.0	19.1	63000	6.6796x10	2.8595x10	1.2758x10
18.6	20.6	36000	4.8515x10	4.2461x10	9.9941x10
19.2	21.4	20000	3.4674x10	6.1718x10	7.4202x10
19.8	19.1	10000	2.3334x10	8.1855x10	4.4568x10
20.4	13.5	5000	1.5702x10	8.5876x10	2.1198x10
21.0	6.3	2300	1.0075x10	6.2531x10	6.3472x10
21.6	1.6	900	5.8940x10	2.7146x10	9.4304x10

$\bar{M}_n = \Sigma$col 2/ Σcol 5

$= 167.2/4.3848 \times 10^{-3}$

$= 38132$

$\bar{M}_w = \Sigma$col 6/ Σcol 2

$= 1.4621 \times 10^{7}/167.2$

$= 87446$

Appendix F

Effect of temperature on emulsion polymerization of butadiene

TABLE 20

Effect of heptane on conversion-time relationship for emulsion polymerization of butadiene

Temperature	4 °C
Butadiene	10.27 mol.dm^{-3} of water
Potassium laurate	0.1166 mol.dm^{-3} of water
Cumene hydroperoxide	0.00767 mol.dm^{-3} of water

Time (s)	Conversion (%)	Wt.ratio*
7740	18.4	0.0
10318	21.5	0.0
10318	23.1	0.0
13124	26.2	0.0
4403	7.5	0.85
7362	14.3	0.85
11024	16.2	0.85

* Weight ratio heptane to butadiene

TABLE 21

Effect of temperature on conversion-time relationship for emulsion polymerization of butadiene

Butadiene	10.27 $mol.dm^{-3}$ of water
Potassium laurate	0.1166 $mol.dm^{-3}$ of water
Cumene hydroperoxide	0.00767 $mol.dm^{-3}$ of water

Time (s)	Conversion (%)	Temperature (°C)
7740	18.4	4
10318	21.5	4
10318	23.1	4
13124	26.2	4
2400	13.1	10
5000	21.0	10
8042	28.0	10
15982	46.5	10

Appendix G

Effect of additives on emulsion polymerization of butadiene

TABLE 22

Effect of the concentration of heptane on the conversion-time relationship for emulsion polymerization of butadiene

Temperature	10 °C
Butadiene	10.27 $mol.dm^{-3}$ of water
Potassium laurate	0.1166 $mol.dm^{-3}$ of water
Cumene hydroperoxide	0.00767 $mol.dm^{-3}$ of water

Time (s)	Conversion (%)	Wt.ratio*
2400	13.1	0.0
5000	21.0	0.0
8042	28.0	0.0
15982	46.5	0.0
4125	11.5	0.85
8924	21.8	0.85
14900	28.8	0.85
18100	33.5	0.85
5334	11.5	1.32
8107	14.3	1.32
12126	20.0	1.32
17049	26.0	1.32
6100	8.3	2.22
10500	11.5	2.22
13078	12.8	2.22
17986	13.5	2.22

*Weight ratio of heptane to butadiene

TABLE 23

Effect of the concentration of cyclohexane on the conversion-time relationship for emulsion polymerization of butadiene

Temperature	10°C
Butadiene	10.27 $mol.dm^{-3}$ of water
Potassium laurate	0.1166 $mol.dm^{-3}$ of water
Cumene hydroperoxide	0.00767 $mol.dm^{-3}$ of water

Time (s)	Conversion (%)	Wt.ratio*
2400	13.1	0.0
5000	21.0	0.0
8042	28.0	0.0
15982	46.5	0.0
2994	12.1	0.85
5503	17.5	0.85
11470	27.5	0.85
19883	42.0	0.85
5132	11.0	1.32
8815	17.5	1.32
12126	20.5	1.32
18820	27.5	1.32
6126	9.9	2.22
14246	16.5	2.22

*Weight ratio of cyclohexane to butadiene

TABLE 24

Effect of the concentration of heptane and cyclohexane on the rate of polymerization

Temperature	10 °C
Butadiene	10.27 $mol.dm^{-3}$ of water
Potassium laurate	0.1166 $mol.dm^{-3}$ of water
Cumene hydroperoxide	0.00767 $mol.dm^{-3}$ of water

Solvent	Wt.ratio*	Mol.fr. of butadiene in oil phase	Polymerization rate (%conversion.h^{-1})
	0.0	1.0	9.0
Heptane	0.85	0.686	4.5
Heptane	1.32	0.584	3.6
Heptane	2.22	0.455	2.3
	0.0	1.0	9.0
Cyclohexane	0.85	0.647	5.0
Cyclohexane	1.32	0.541	3.8
Cyclohexane	2.22	0.412	2.4

*Weight ratio of solvent to butadiene

TABLE 25

Comparison of experimental rates of polymerization in the presence of heptane and cyclohexane with the predicted rate of polymerization

Temperature	10°C
Butadiene	10.27 $mol.dm^{-3}$ of water
Potassium laurate	0.1166 $mol.dm^{-3}$ of water
Cumene hydroperoxide	0.00767 $mol.dm^{-3}$ of water

Solvent	Mol.fr. of butadiene in oil phase	Polymerization rate(%conversion.h^{-1}) Experimental	Predicted
	1.0	9.0	9.0
Heptane	0.686	4.5	6.2(37.1)*
Heptane	0.584	3.6	5.3(46.1)
Heptane	0.455	2.3	4.1(78.3)
	1.0	9.0	9.0
Cyclohexane	0.647	5.0	5.8(16.0)
Cyclohexane	0.541	3.8	4.9(29.0)
Cyclohexane	0.412	2.4	3.7(54.2)

*Values in brackets indicate percentage deviation

%Deviation = (Predicted - Expt'l)100/Expt'l

TABLE 26

Effect of concentration of heptane and cyclohexane on molecular weight of polymerization

Temperature	10°C
Butadiene	10.27 $mol.dm^{-3}$ of water
Potassium laurate	0.1166 $mol.dm^{-3}$ of water
Cumene hydroperoxide	0.00767 $mol.dm^{-3}$ of water

Solvent	Wt.ratio*	mol.fr. of butadiene in oil phase	$\bar{M}_n(10^{-4})$	$\bar{M}_w(10^{-4})$
	0.0	1.0	4.1	17.0
Heptane	1.32	0.584	2.1	6.9
Heptane	2.22	0.455	0.9	2.1
	0.0	1.0	4.1	17.0
Cyclohexane	1.32	0.541	2.5	9.8
Cyclohexane	2.22	0.412	2.0	6.0

*Weight ratio of solvent to butadiene

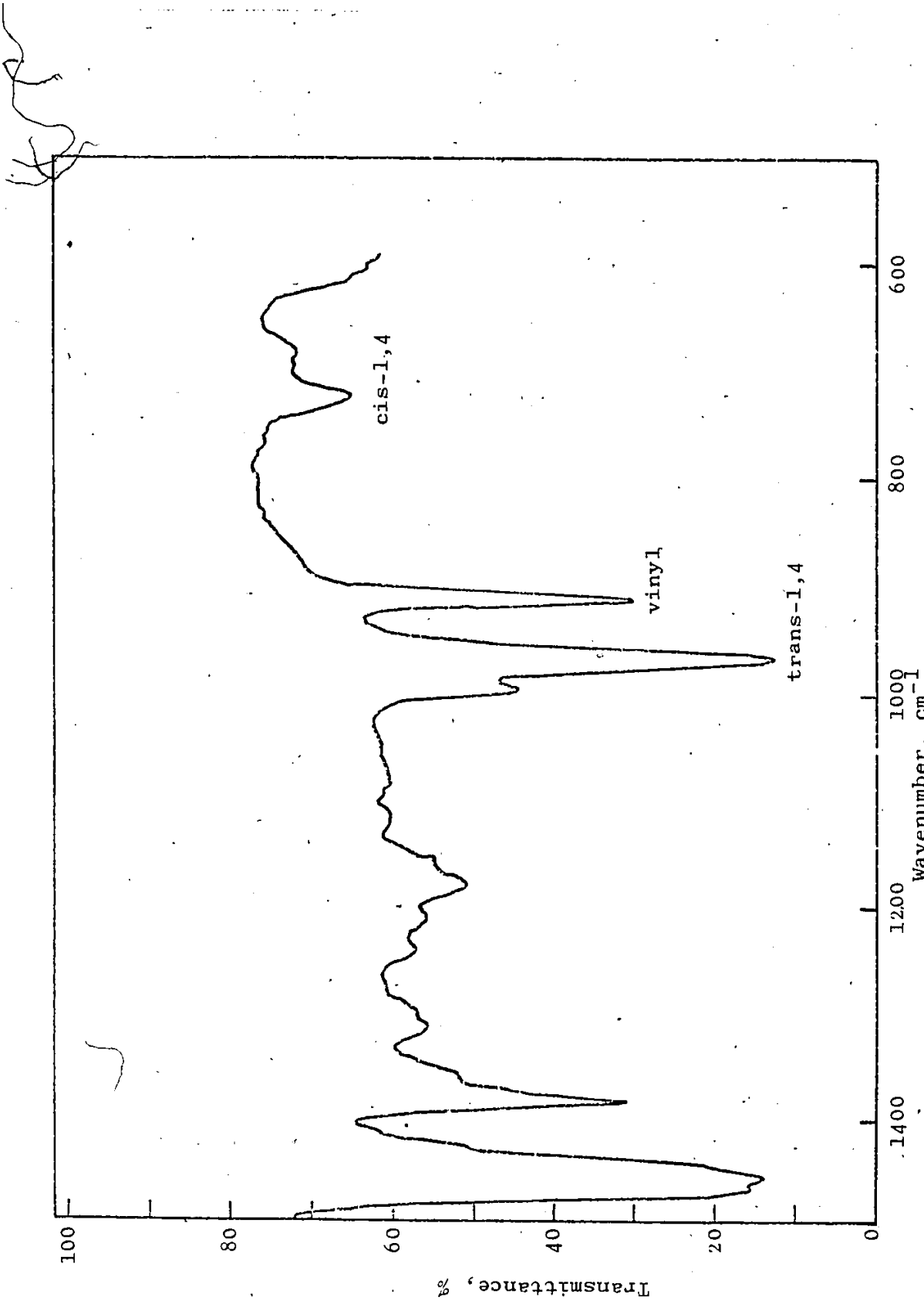

Figure 38 - Infrared spectrum of a polybutadiene sample formed at 4 °C

TABLE 27

Effect of concentration of heptane and cyclohexane on polybutadiene structures

Temperature	10°C
Butadiene	10.27 mol.dm^{-3} of water
Potassium laurate	0.1166 mol.dm^{-3} of water
Cumene hydroperoxide	0.00767 mol.dm^{-3} of water

Solvent	Wt.ratio*	Cis-1,4 (%)	Vinyl (%)	Trans-1,4 (%)
	0.0	19.8	34.7	45.5
Heptane	0.85	18.8	34.9	46.2
Heptane	1.32	18.0	36.5	45.6
Heptane	2.22	28.0	30.4	42.6
	0.0	19.8	34.7	45.5
Cyclohexane	0.85	20.5	35.8	43.7
Cyclohexane	1.32	16.8	33.9	49.2
Cyclohexane	2.22	18.7	35.3	46.0

*Weight ratio of solvent to butadiene

Appendix H

Effect of variation of potassium laurate concentration on emulsion polymerization of butadiene

TABLE 28

Effect of concentration of potassium laurate on conversion-time relationship for emulsion polymerization of butadiene

Temperature	10°C
Butadiene	10.27 $mol.dm^{-3}$ of water
Cumene hydroperoxide	0.00767 $mol.dm^{-3}$ of water

Potassium laurate ($mol.dm^{-3}$ of water)	Time (s)	Conversion (%)
0.042	6053	8.5
0.042	12040	16.5
0.1166	2400	13.1
0.1166	5000	21.0
0.1166	8042	28.0
0.1166	15982	46.5
0.21	6247	50.0
0.21	8650	59.3
0.21	12400	72.2

TABLE 29

Effect of concentration of potassium laurate on conversion-time relationship for emulsion polymerization of butadiene with heptane at heptane/butadiene weight ratio of 1.32

Temperature	10°C
Butadiene	10.27 $mol.dm^{-3}$ of water
Cumene hydroperoxide	0.00767 $mol.dm^{-3}$ of water

Potassium laurate ($mol.dm^{-3}$ of water)	Time (s)	Conversion (%)
0.042	12222	4.7
0.042	22922	7.5
0.1166	5334	11.5
0.1166	8107	14.3
0.1166	12126	20.0
0.1166	17049	26.0
0.21	6293	19.4
0.21	12400	31.2
0.21	15049	35.1
0.38	6135	40.9
0.38	10312	54.9
0.38	13303	62.8

TABLE 30

Effect of concentration of potassium laurate on rate of polymerization of butadiene with and without heptane

Temperature	10°C
Butadiene	10.27 $mol.dm^{-3}$ of water
Cumene hydroperoxide	0.00767 $mol.dm^{-3}$ of water

Wt.ratio*	Potassium laurate $mol.dm^{-3}$ of water	Polymerization rate (%Conversion.h^{-1})
0.0	0.042	4.8
0.0	0.1166	9.0
0.0	0.21	12.3
1.32	0.042	1.0
1.32	0.1166	3.6
1.32	0.21	7.0
1.32	0.38	11.6

*weight ratio of heptane to butadiene

TABLE 31

Effect of concentration of potassium laurate on molecular weight of polybutadiene with and without heptane

Temperature	10°C
Butadiene	10.27 $mol.dm^{-3}$ of water
Cumene hydroperoxide	0.00767 $mol.dm^{-3}$ of water

Wt.ratio*	Potassium laurate $mol.dm^{-3}$ of water	$\bar{M}_n(10^{-4})$	$\bar{M}_w(10^{-4})$
0.0	0.042	3.1	13.5
0.0	0.1166	4.1	17.0
0.0	0.21	7.0	38.0
1.32	0.042	0.9	2.4
1.32	0.1166	2.1	6.9
1.32	0.21	3.4	18.3
1.32	0.38	6.8	27.2

*Weight ratio of heptane to butadiene

TABLE 32

Effect of concentration of potassium laurate on polybutadiene structures with and without heptane

Temperature	10°C
Butadiene	10.27 $mol.dm^{-3}$ of water
Cumene hydroperoxide	0.00767 $mol.dm^{-3}$ of water

Wt.ratio*	Potassium laurate $mol.dm^{-3}$ of water	Cis-1,4 (%)	Vinyl (%)	Trans-1,4 (%)
0.0	0.042	17.3	37.3	45.3
0.0	0.1166	19.8	34.7	45.5
0.0	0.21	19.4	34.5	46.1
1.32	0.1166	18.0	36.5	45.6
1.32	0.21	17.7	35.8	46.5
1.32	0.38	19.3	37.3	43.5

*Weight ratio of heptane to butadiene

Appendix I

Effect of variation of initiator concentration on emulsion polymerization of butadiene

TABLE 33

Effect of concentration of cumenehydroperoxide on conversion-time relationship for emulsion polymerization of butadiene

Temperature	10°C
Butadiene	10.27 mol.dm^{-3} of water
Potassium laurate	0.1166 mol.dm^{-3} of water

Cumene hydroperoxide (mol.dm^{-3} of water)	Time (s)	Conversion (%)
0.00365	6224	24.9
0.00365	14500	44.9
0.00767	2400	13.0
0.00767	5000	21.0
0.00767	8042	28.0
0.00767	15982	46.5
0.01462	6104	29.0
0.01462	9123	36.3
0.01462	12191	43.0

The ratio of cumenehydroperoxide to tetraethylenepentamine was always kept constant as in the recipe given in Table 6

TABLE 34

Effect of concentration of cumenehydroperoxide on conversion-time relationship for emulsion polymerization of butadiene with heptane at heptane/butadiene weight ratio of 1.32

Temperature	10 °C
Butadiene	10.27 $mol.dm^{-3}$ of water
Potassium laurate	0.1166 $mol.dm^{-3}$ of water

Cumene hydroperoxide ($mol.dm^{-3}$ of water)	Time (s)	Conversion (%)
0.00767	5334	11.5
0.00767	8107	14.3
0.00767	12126	20.0
0.00767	17049	26.0
0.01462	6203	10.7
0.01462	13170	18.2
0.02924	6159	11.8
0.02924	9623	17.5
0.02924	13120	21.1

The ratio of cumenehydroperoxide to tetraethylenepentamine was always kept constant as in the recipe given in Table 6

TABLE 35

Effect of concentration of cumenehydroperoxide on rate of polymerization of butadiene with and without heptane

Temperature	10°C
Butadiene	10.27 $mol.dm^{-3}$ of water
Potassium laurate	0.1166 $mol.dm^{-3}$ of water

Wt.ratio*	Cumene hydroperoxide ($mol.dm^{-3}$ of water)	Polymerization rate (%conversion.h^{-1})
0.0	0.00365	8.1
0.0	0.00767	9.0
0.0	0.01462	8.9
1.32	0.00767	4.5
1.32	0.01462	3.9
1.32	0.02924	4.8

The ratio of cumenehydroperoxide to tetraethylenepentamine was kept constant as in the recipe given in Table 6

*Weight ratio of heptane to butadiene

TABLE 36

Effect of concentration of cumenehydroperoxide on molecular weight of polybutadiene with and without heptane

Temperature	10 °C
Butadiene	10.27 $mol.dm^{-3}$ of water
Potassium laurate	0.1166 $mol.dm^{-3}$ of water

Wt.ratio*	Cumene hydroperoxide ($mol.dm^{-3}$ of water)	$\bar{M}_n(10^{-4})$	$\bar{M}_w(10^{-4})$
0.0	0.00365	5.0	23.4
0.0	0.00767	4.1	17.0
0.0	0.01462	3.0	13.8
1.32	0.00767	2.1	6.9
1.32	0.01462	1.7	5.3
1.32	0.02924	0.9	2.7

The ratio of cumenehydroperoxide to tetraethylenepentamine was kept constant as in the recipe given in Table 6

*Weight ratio of heptane to butadiene

TABLE 37

Effect of concentration of cumenehydroperoxide on polybutadiene structures with and without heptane

Temperature	10°C
Butadiene	10.27 mol.dm^{-3} of water
Potassium laurate	0.1166 mol.dm^{-3} of water

Wt.ratio*	Cumene hydroperoxide (mol.dm^{-3} of water)	Cis-1,4 (%)	Vinyl (%)	Trans-1,4 (%)
0.0	0.00365	19.3	37.1	43.6
0.0	0.00767	19.8	34.7	45.5
0.0	0.01462	20.2	36.7	43.1
1.32	0.00767	18.0	36.5	45.6
1.32	0.01462	18.4	36.4	45.2
1.32	0.02924	21.5	33.6	44.9

The ratio of cumenehydroperoxide to tetraethylenepentamine was always kept constant as in the recipe given in Table 6

*Weight ratio of heptane to butadiene

Appendix J

Development of diffusivity correlations

J.1 STATISTICAL ANALYSIS OF THE CORRELATION FOR DIFFUSIVITY IN LIQUID SOLUTIONS OF NORMAL PARAFFINS

The correlation for diffusivity in liquid solutions of normal paraffins was developed using a nonlinear optimization technique. In performing the regression analysis for the development of Equation 6.17 certain assumptions about the error were made which included the usual assumptions that the errors are independent, have a zero mean, a constant variance and follow a normal distribution. If the above assumptions were correct, this would be confirmed by an analysis of the residuals. A residual plot shown in Figure 39 shows an essentially random distribution of points which indicates the adequacy of the model. For parameter precision analysis a 95% confidence region for the parameters was constructed by linearizing the nonlinear model about the least squares estimate parameters in the parameter space. The correlation and covariance matrices for the correlation indicated by Equation 6.17 were calculated. Correlation matrices indicate that the value of correlations at some point are high. The likely reason for this was that the data were taken from various sources and that different methods were employed to obtain them. In the case where the number of parameters are more than three, it became difficult to visualize a joint confidence region for the parameters. Therefore, the eigen value and the eigen vector analysis were done to identify the 10 (5 number of parametres) end points of the principal axes of the ellipsoidal region.

The sum of the squares was not the same at all points, indicating that the assumption of linearization was not justifiable. Since the data were from different sources, this was the best result which could be obtained. The covariance matrix, correlation matrix, 10 end points of the principal axes of the ellipsoidal region and the sum of squares at these points are listed below:

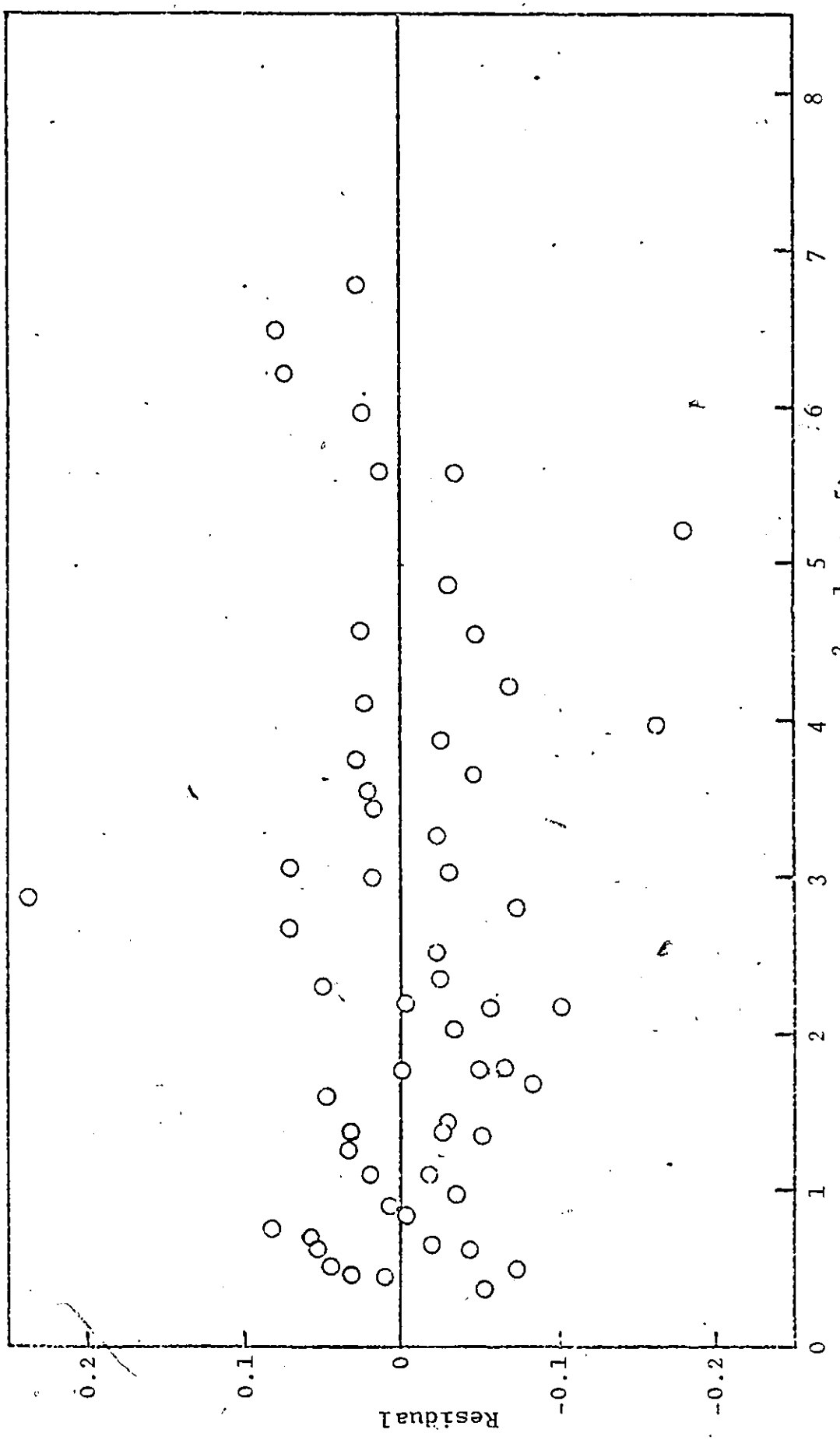

Figure 39 - Residual plot for the correlation for diffusivity in liquid solutions of normal paraffins

Covariance Matrix

0.2408E-04	-0.9695E-04	0.1831E-01	0.1386E-03	-0.2329E-03
-0.9695E-04	0.9493E-03	-0.1393	-0.8495E-03	0.4152E-03
0.1831E-01	-0.1393	26.602	0.1781	-0.1171
0.1386E-03	-0.8495E-03	0.1781	0.1364E-02	-0.1103E-02
-0.2329E-03	0.4153E-03	-0.1171	-0.1103E-02	0.2746E-02

Correlation Matrix

1.0	-0.64121	0.72338	0.764945	-0.90559
-0.64121	1.0	-0.87650	-0.746580	0.25722
0.723380	-0.8765	1.0	0.935085	-0.43319
0.764945	-0.746580	0.935085	1.0	-0.57011
-0.905590	0.2572	-0.43319	-0.570110	1.0

Five principal axes

1) (1.3181E-02, -0.7064, 10.2616, 0.7907, 1.4677,
1.3371E-02, -0.7063, 10.1324, 0.7906, 1.4667)

2) (0.0123, -0.7121, 8.8392, 0.8018, 1.4467,
0.0142, -0.7006, 11.5548, 0.7796, 1.4877)

3) (0.0160, -0.8654, 26.7533, 0.7085, 1.3790,
0.0106, -0.5473, -6.3593, 0.8728, 1.5555)

4) (0.0118, -0.6474, 18.6628, 0.7735, 1.3508,
0.0148, -0.7653, 1.7312, 0.8078, 1.5836)

5) (0.0084, -0.7052, 7.0746, 0.7470, 1.4655,
0.0181, -0.7075, 13.3194, 0.8343, 1.4689)

The sum of squares

Axes	One end	Other end
1	0.46	0.46
2	18.65	25.83
3	317.33	4422.17
4	111.65	340.86
5	85.55	96.78

TABLE 38

Comparison of various correlations developed for water

Number of data points - 237

Correlation	Average % absolute error
1. Equation (2.38)	10.303
2. $D^{\circ}_{AB} = 10.08(10^{-5})\eta_B^{1.16}V_A^{-0.52}$	10.207
3. $D^{\circ}_{AB} = 12.813(10^{-5})T^{-0.068}\eta_B^{-1.22}V_A^{-0.485}$	10.300
4. $D^{\circ}_{AB} = .0026(10^{-5})T^{1.46}\eta_B^{-0.934}V_A^{-0.24}P_B^{-0.25}$	10.188
5. $D^{\circ}_{AB} = 8.95(10^{-5})V_A^{-0.495}\eta_B^{(0.755/V_A-1.33)}$	10.762
6. $D^{\circ}_{AB} = (7.12 \cdot V_A^{-0.192} - 2.02)10^{-5}\ \eta_B^{(8.25/V_A-1.34)}$	9.653
7. $D^{\circ}_{AB} = 4.12(10^{-7})V_A^{-0.48}\eta_B^{(8.85/V_A-1.16)}T^{0.933}$	9.830
8. $D^{\circ}_{AB} = (12.15\ V_A^{-0.19} - 3.65)\eta_B^{(9.58\ V_A^{-1} - 1.12)}T^{1.52}(10^{-9})$	9.389

J.2 STATISTICAL ANALYSIS FOR THE GENERAL CORRELATION FOR DIFFUSIVITY PREDICTION

The correlation and covariance matrices for Equation 6.19 were developed. Eigen values were calculated and an eigen vector analysis was also performed to identify the 12 end points of the principal axes of the ellipsoidal region. The sum of squares at all of the end points are not the same and the reason for this is the same as that described earlier for the paraffin correlation. The covariance matrix, the correlation matrix, the principal axes and the sum of squares at the end point of these axes are listed below:

Covariance Matrix

0.5489E-06	-0.6226E-04	0.4398E-05	0.1817E-05	0.1492E-05	0.2267E-06
-0.6226E-04	-0.7462E-02	-0.5682E-03	-0.1347E092	-0.1511E-02	0.3650E-04
0.4398E-05	-0.5682E-03	0.1116E-03	0.2821E-03	0.3040E-03	0.2800E-06
0.1817E-05	-0.1347E-02	0.2821E-03	0.3782E-02	0.4369E-02	0.8062E-04
0.1492E-05	-0.1511E-02	0.3040E-03	0.4369E-02	0.5094E-02	-0.7681E-04
0.2267E-06	0.3650E-04	0.2800E-06	-0.8062E-04	-0.7681E-04	0.5969E-04

Correlation Matrix

1.0	-0.97285	0.56187	0.3988E-01	0.2823E-01	0.3961E-01
-0.9728	1.0	-0.62252	0.2535	-0.24514	0.5470E-01
0.5618	-0.62252	1.0	0.43414	0.40310	0.3430E-02
0.3988E-01	-0.25354	0.43414	1.0	0.99551	-0.1697E00
0.2823E-01	-0.24514	0.40310	0.99551	1.0	-0.1393E00
0.3961E-01	0.54700	0.3430E-02	-0.16969	-0.13930	1.0

Six principal axes

1) [0.0015, 1.2901, 0.9145, 0.2350, .5002, 0.4183,
0.0016, 1.2891, 0.9144, 0.2351, .5004, 0.4184]

2) [0.0098, 1.2978, 0.9137, 0.2484, .4890, 0.4183,
-0.0067, 1.2814, 0.9153, 0.2217, 0.5116, 0.4184]

3) [0.0082, 1.2819, 0.8937, 0.2388, 0.5054, 0.4210,
-0.0051, 1.2972, 0.9353, 0.2313, 0.4951, 0.4157]

5) [-0.0278, 1.3080, 0.9095, 0.2612, 0.5266, 0.4078,
0.0269, 1.2711, 0.9195, 0.2089, 0.4740, 0.4289]

6) [-0.0015, 1.2938, 0.9186, 0.2393, 0.5056, 0.4539,
0.0046, 1.2854, 0.9104, 0.2308, 0.4950, 0.3828]

The sum of squares

Axes	One end	Other end
1	123.756	91.671
2	64708.94	92160.12
3	42397.36	59272.7
4	1003807.0	629363.5
5	1062197.0	509824.0
6	10543.13	16302.73

TABLE 39

Comparison of correlations for liquid diffusivities at infinite dilution

	Average error	Number of data
A) General correlation for polar and non-polar substances:		
Wilke-Chang correlation (Γ=2.26 for water)	16.1	756
Tyn and Calus correlation	14.2	756
Equation 6.19	13.9	756
Equation 6.20	14.3	756
B) Correlations tested with data for non-polar solvents only		
Tyn and Calus correlation	14.1	254
Equation 6.19	13.4	254
Equation 6.20	13.4	254
Equation 6.21	13.4	254
C) Correlations tested for normal paraffin solvents and solutes		
Wilke-Chang correlation	13.3	58
Equation 6.19	12.7	58
Tyn and Calus correlation	12.5	58
Equation 6.17	3.4	58
D) Correlations tested for water as solvent:		
Wilke-Chang correlation (Γ=2.26)	10.4	237
Tyn and Calus correlation	13.3	237
Hayduk-Laudie corelation	10.3	237
Equation 6.18	9.4	237
Equation 6.19	12.8	237

TABLE 40

Comparison of experimental diffusivities with those predicted from various methods

	25°C $(cm^2.s^{-1})(10^5)$	50°C $(cm^2.s^{-1})(10^5)$
Experimental	3.51	4.66
Wilke-Chang correlation	3.97(13.1)	5.46(17.0)
Scheibel correlation	3.03(-13.5)	4.17(-10.6)
Reddy-Doraiswamy correlation	2.70(-22.9)	3.73(-20.3)
King, Hsueh, Mao correlation	4.47(-27.4)	6.14(31.8)
Equation 6.19	3.19(-8.9)	4.71(0.9)
Tyn and Calus correlation	4.21(19.9)	6.08(30.4)

*Values in brackets indicate percentge deviation

%Deviation = (Predicted - Expt'l)100/Expt'l